



Dear Editor,

please you find included the revised version of our work "**Lahar events in the last 2,000 years from Vesuvius eruptions. Part 1: Distribution and impact on densely-inhabited territory estimated from field data analysis**", which has been improved a lot thanks to the reviewers' comments. The revised version consists of a reply to the three reviewers, and it follows the marked version of the manuscript with all changes highlighted.

In particular, we have taken into account all reviewers' comments, as it can be seen in the marked version of the work. Also, all the general comments have been replied one-by-one in the reply letter, and the specific ones are reported and accordingly modified in the text. The whole work is indeed better now particularly thanks to all these comments.

We are available for any further information needed. Looking forward to hearing the submission results.

On behalf of all co-authors

Best regards

Dott. Mauro Antonio Di Vito

## Reply to the Reviewers

In the present letter, we report detailed responses one-by-one to the main reviewers' comments. All other comments that are annotated in the pdf documents attached by Reviewer 1 and Reviewer 2 are acknowledged and accepted in the revised version of the manuscript. In order to follow the full sequence for each of them (>250 annotated comments), we directly refer to the marked version of the manuscript, while here we reply to the main ones. With reference to these latter, they often coincide with the general comments.

### Reviewer 1

This is an interesting article based on an astonishing effort of field work. Congratulations. It is beyond doubt that a thorough re-appraisal of volcanic deposits is required for enhanced risk analysis.

We acknowledge very much this comment and the encouraging words, which are precious for us to further improving our work at this stage. Yes, it is important to focus the whole work on volcanic deposits, in particular these ones (pyroclastic and lahar deposits) that are quite dispersed around the volcano and in the plain; they acted as field constraints in evaluating the impact of the eruption and associated phenomena, and as inputs for the numerical modelling (companion papers part 2 and part 3).

I have attached an annotated pdf with many comments and change suggestions.

We acknowledge the detailed Reviewer's work as evident from the commented pdf attached. We have taken into account all corrections and suggestions, which can be better followed one-by-one directly on the marked version of the manuscript.

I have three main points:

1. Overall, I would like to see some restructuring of the manuscript as many figures in the Appendix would help the reader to better follow your reasoning. Please add several of them in the main body of the manuscript and not only the many maps with outcrop locations.

We acknowledge this comment, which we have taken into account considering the length of the whole manuscript. We have done our best to shorten some parts a little bit and favour some restructuring of the field description, including a table with the recognized lithofacies and one photo associated to

each of them; this is also a formal compromise to improve this part in the general context of the multidisciplinary work that we carried out.

2. Please add definitions to terms you are using that may be used in a subjective way (e.g. syn- and post-eruptive lahars) or numbers with units to statements that you are using in a poorly qualitative way (fine, finer...).

We acknowledge this comment very much, which has given us the chance to further check all definitions of lahars that we used in this work. This is aligned also with some comments by Reviewer 2. According to the concepts introduced by Sulpizio et al. (2006) and Iverson and Vallance (2015) and taking into account the field characteristics of the Pollena and 1631 lahar deposits around Somma-Vesuvius and in the Campanian Plain, we decided to reduce the number of lahar definitions from three to two, keeping in particular the syn-eruptive and post-eruptive ones. While the second definition applies to lahars occurred during long periods of volcanic quiescence (from several-to-tens of years to hundreds of years or more), the first one applies to those lahars occurred during or immediately after the eruptive activity. By immediate we mean even a few years because volcanic hazard (among the main goals of this work) can also occur due to lahars that are directly related to the volcanic activity. Of course, we could not exactly know when the studied lahars occurred in the past, which is why the two definitions are to be intended from the stratigraphic point of view (continuity, erosion, componentry, archeological evidence, etc...).

Besides, all details around the sedimentological part of the work have been double checked, in order to show results as quantitative and consistent as possible.

3. Being a non-native English speaker myself, I still feel that the manuscript could benefit from a language check.

We acknowledge this comment, which has given us the opportunity to double check all manuscript with the detail of single word. We think that now the manuscript is more fluent and more consistent among the various sections.

## **Reviewer 2**

The paper represents an interesting contribution; new stratigraphic data are presented here for the Pollena and the 1631 plinian eruptions and associated lahars, based on which a new impact area is defined, with important implications on hazard assessment.

We acknowledge this comment, which is important for us as motivation to further improve the whole work thanks in particular to the Reviewer's comments. The two studied eruptions are sub-Plinian and not Plinian, which we have double checked throughout the manuscript.

I think that authors should better describe their initial assumption and improve the description and interpretation, which are now quite poorly justified or vague. Below are some major points. It is an interesting paper, but it needs to be improved before its publication. Some figures need to be improved. The annotated PDF includes several suggestions.

We acknowledge this general comment and we acknowledge for all details included in the commented pdf, which we have taken into account comment-by-comment in the marked version of the manuscript. In particular, the description and interpretation, as well as the parts that get to the field-based volcanic hazard discussion are strengthened and better related to each other.

We have also worked on some figures and tables as shown in the marked version of the manuscript.

Terminology. I consider that authors should better define the terminology here used, especially for syn- post and inter-eruptive lahar. Post and inter-eruptive lahars do not necessarily point to similar events. Post-lahars can occur a few months or years after the eruption when the landscape is still responding to the hydrological and sedimentary-yield consequences of the eruption, and lahars are still remobilizing the primary pyroclastic deposits only. Inter-eruptive lahars occur without a direct volcanic influence. I have suggested some references to this point. I understand that authors refer to syn-eruptive lahar as those that originated from the primary pyroclastic deposits only, but the timing can be important for hazard assessment purposes.

We acknowledge this precious comment very much, which has helped us revising the full terminology, also in light of all the available literature. Lahars that are generated up to months to a few years after the eruption, especially when they are studied from the stratigraphic and archaeological points of view, can still be related to volcanic activity in a general sense, i.e. primary pyroclastic deposits can form then can be immediately remobilized triggering syn-eruptive lahars. We used this definition and meaning after Sulpizio et al. (2006) and Iverson and Vallance (2015), because we also wanted to stress the fact that even if the eruptive activity is over, the formation of

lahars due to a specific volcanic activity cannot be excluded in terms of volcanic hazard. Instead, what we defined as post-eruptive lahars enters more appropriately in the context of hydrogeological hazard, which can occur during long periods of volcanic quiescence; all of this is clearer now throughout the manuscript. Finally, we have removed the definition of inter-eruptive, as we did not use it in this work.

Lahar deposit textures are poorly described, please add a figure illustrating the main facies here described (line 377). En-masse deposition here described for lahars is poorly justified and contrasts with several recent studies. Water escape features are not evidence of en-masse deposition. A few descriptions and pictures are included in the appendix; I consider more useful for the reader to add some figures in the main text, is quite annoying to go to the appendix to understand the main text. I suggest including a simple table with a picture of each facies here described and a resume of their main characteristics.

We acknowledge this comment. We have added a table summarizing all recognized lithofacies, also taking into account some of the comments by Reviewer 1. In this way, we have taken the chance to reconsider the appendix on the field description (Appendix C), by strengthening the main body of the manuscript with more field details and figures.

With reference to the depositional mechanisms, we have clarified that the entire vertical sequences from lahars can form by rapid progressive aggradation, while each depositional layer forms en masse. These are impulsive and dense mass flows, which can be fed by multiple pulses. Each pulse gives rise to a variably-thick massive layer through a high depositional rate, while we agree that the vertical “sum” of the layers forms over time, i.e. by progressive aggradation. This is clearer now in the text. Indeed, the large-scale multiphase experiments by Roche (2012, 2015) confirm that the two end member depositional mechanisms are not in competition to each other, and that the mutual interplay between transport and deposition in lateral mass flows (vs. vertical fallout) makes the speed of local deposition higher or lower depending on relationships between single flow pulse, feeding time and local topography. Furthermore, the recognized water escape features for us are evidence of rapid aggradation of single units in a sequence crossed by these features during its contraction.

Authors should better describe the componentry of both Pollena and 1631 eruptions, their differences, and how they were used to discriminate syn-eruptive lahars from each one of these eruptions or if stratigraphic relationships were the main criteria. Right now is written as the reader perfectly knows the stratigraphy of the Somma-Vesuvius area.

We acknowledge this comment, which we have taken into account by specifying sedimentological details in the Materials and Methods section, and also throughout the manuscript wherever those features are presented. In particular, the stratigraphic methods and the archaeological pieces of evidence were used to discriminate the various lahar deposits, and besides a new paragraph on the eruptive history of Somma-Vesuvius has been added to help the reader following the sequence of the reconstructed volcanic events.

I suggest authors avoid mixing descriptions with interpretations.

We acknowledge this comment, which we have kept in mind during the revision process, by acting wherever that could have been confused or overlapped.

Figure 7 is not a distribution map; is a map that shows the outcrops where lahars from Pollena eruption are outcropping. This map does not allow the reader to understand the source area of lahars nor how the volume of these lahar deposits was estimated. I suggest at least including as a layer the drainage system. And what does the 0 value mean in the thickness scale? In the map, there are several points (white dots) with this value. The same observations for the figure of the lahars associated with the 1631 eruption.

We acknowledge this comment. The mentioned figure refers to the geospatial dataset, in which all studied stratigraphic sections are reported; the figure shows those locations with the associated deposit thicknesses. In the section of presentation of the results, we have clarified, also after paleomagnetic considerations, about the provenance of the volcanoclastic material, etc..., by making clearer that the lahar volume calculations are referred to the numerical modelling companion papers (part 2 and part 3, the first of the two in particular). The drainage system is regulated by the slopes of the main valleys, also we have added arrows to show the material provenance following the sedimentological characteristics of the deposits and their lateral continuity. The main flow directions and provenance are now represented with comprehensive arrows as shown in the primary deposit distribution maps. The 0-m value refers to the locations in which no lahar deposits were observed, which as absence of presence gives some evidence of absence of the lahar deposits. The volume evaluation has been carried out with the GIS database, defining cells characterized by homogeneous thickness and morphology and using the average thickness within them.

It is not completely clear to me as syn-eruptive and “post(inter)” eruptive lahars from Pollena eruption are discriminated. One of the main parameters is that post-eruptive events crop on top of the humified surface or soil layers with evidence of anthropic use, while syn-eruptive lahar deposits lay directly

on top of the primary deposits (line 405). Can authors better explain this point as, for example, for the Avella area, were both syn-eruptive and post-eruptive lahars of the Pollena eruptions are described? Also, it is not clear how the outcrops in the SW area (white dots in figure 6) are interpreted as syn-eruptive if primary deposits from Pollena are not mapped here (based on Figure 5).

We acknowledge this comment and the suggestion to clarify the difference (from the stratigraphic viewpoint) between the two types of lahar deposits throughout the manuscript. Indeed, such difference is based on stratigraphic relationships between primary and secondary deposits, which we do think is clearer now (see previous reply).

Where the white dots with the 0-m value are present, it means that no secondary deposits are present, which is coherent with the absence of primary deposits occurring in some of the studied stratigraphic sections.

Line 422. Why post-eruptive (here consider as inter-eruptive) lahar are still associated with the Pollena eruption and defined as post only because they contain or are overlaid by fragments from Mercato and Avellino eruptions? Just as an example, at Colima volcano, all syn-eruptive, post or inter-eruptive lahars from recent activity contain pumice fragments from the 1913 plinian eruption. Syn-eruptive lahars can erode the substratum during their emplacement. Finally, why are post(inter)-eruptive lahars associated with a specific eruption? Still unclear how is the timing between a syn-eruptive and a post(inter)-eruptive lahar here considered if the post-eruptive events are still correlated to an eruption. Authors can solve this problem by changing the terminology here used and distinguishing between post and inter-eruptive.

Please see the response above about the syn-eruptive and post-eruptive features for the studied lahars and their deposits. In particular, the lahars defined as post-eruptive were defined on the basis of their stratigraphic position and to be related to one eruption but characterized by the presence of features typical of long time after the eruption (anthropogenic use of the territory, presence of paleosols, etc...).

Some lahars from the Valle de Avella and Somma-Vesuvius area show up to 50% of the mud fractions, it could be interesting to define the % of silt and clay, as inter-eruptive lahars could also be discriminated based on their granulometry.

We acknowledge this comment. Distributing the fine fraction ( $>5 \phi$ ) is something that was done by extrapolation modelling for inputs into the numerical modelling companion paper (part 2). This has

been clarified in the Material and Methods section. In particular, the high presence of ash and fine ash in the deposits of this area did not help us to discriminate between various type of lahars based on grain-size only.

Authors should better explain how the lahar volume is here estimated as the map distribution only shows their outcrops. And if the distribution of fall and PDC deposits from Pollena and 1631 eruptions are here redefined, it could be interesting if authors can estimate the new volume.

We acknowledge this comment, which we have taken into account by a GIS calculation of the volumes, as reported in the marked version of the manuscript. With reference to the lahar deposits, their volumes were calculated using GIS tassellation, by weighting each cell with its average deposit thickness, then multiplying the average value by the cell surface. With reference to the primary deposits, their dispersal has been assessed by calculating the areas of the 10-cm isopachs, then comparing the new values with the literature ones. However, we are still working on the volume estimation for both studied eruptions, but this is the subject of another paper in preparation.

### **Reviewer 3**

The Manuscript contains a lot of information about occurrence of volcanoclastic flows/lahars in the Vesuvian area (Italy). The work is potentially of interest for an international audience, but, at present, it is too confused and in some part not consistent with current models and physics to be recommended for publication as it is.

We acknowledge this general comment. We have taken the chance in the revised version to improve our work taking into account these Reviewer's general comments.

The paper is very long and in some part very hard to read due to the long description of data that may be better organised in Tables. I refer in particular to the stratigraphic description and sedimentological analysis, which are not well organised. In particular, I found not appropriate for a paper dealing with stratigraphic analysis not to present photos of the most significant outcrops in the main text. Also, the lithofaces analysis is poorly significant as it is. This is because the lithofaces codes are introduced without any explanation and they are not summarised in a table (shortening the description).

We acknowledge this comment. We agree that in particular the stratigraphic part was not so clear, which we have improved now, as it can be seen in the marked version of the manuscript. Such improvement has also been possible thanks to the comments from the annotated pdf documents of Reviewer 1 and Reviewer 2. We have added a table summarizing the recognized lithofacies, by also including one photo for each of them, in order to optimize the spaces in this multidisciplinary work.



The grain size data of figure 11 are poorly descriptive if the finest part is not analysed. Also, some of the statistical parameters of Table 1 are not significant, being the distributions very far from gaussian-like.

We acknowledge this comment. We have clarified in the marked version of the manuscript that the finest part ( $>5 \phi$ ) was defined in the numerical modelling companion paper (part 2); it has also been clarified in the Materials and Methods section. We agree that the table of the parameters should have been checked and reconsidered, which we have done in the revised version of the work.

A lot of inconsistencies are present throughout the manuscript (i.e. Somma-Vesuvius vs. Vesuvius, volcanoclastic flows vs lahars). They need to be accurately checked and corrected.

Checked and corrected. Thanks.

The calculation of the velocity and dynamic pressure is basically wrong, in absence of a detailed determination of the flow behaviour. The Authors assume the clasts are transported within the flow, but it may be not the case depending on flow conditions. Lahars can transport boulders as large as meters as passive load, solely due to the pore pressure within the underlying flow. On the other hand, it is not possible to derive the velocity of the flow from the deposit as it is presented, because simply it was zero at time of deposition. So, it is not possible to associate a dynamic parameter with a deposit location as in Figure 17.

We acknowledge this comment. We have clarified that this relatively simple method is not the key point to assess lahar volcanic hazard in the Campanian Plain. It is a simplified method that helps constraining the numerical modelling results just as orders of magnitude and results are used relying on their representativeness and uncertainty, as explained in the companion papers in Part. 2 and 3. However, the approximation here is that the calculated velocities and pressures are referred to the point locations upstream, meaning that those parameters should have been close to the calculated values in the areas nearby the boulder findings. The flow must have entrained and transported those clasts, and in order to do that the velocity and pressure must have been at least close to the values that we report (see Roche et al., 2013; Roche, 2015; Martí et al., 2019, and references therein for details on this approach).

1 **Lahar events in the last 2,000 years from Vesuvius eruptions. Part 1: Distribution and impact**  
2 **on densely-inhabited territory estimated from field data analysis**

3 Mauro A. Di Vito (1,\*), Ilaria Rucco (2), Sandro de Vita (1), Domenico M. Doronzo (1), Marina Bisson (3), Mattia de'  
4 Michieli Vitturi (3), Mauro Rosi (4), Laura Sandri (5), Giovanni Zanchetta (4), Elena Zanella (6), Antonio Costa (5)

5 (1) Istituto Nazionale di Geofisica e Vulcanologia - Sezione di Napoli Osservatorio Vesuviano, Napoli, Italy

6 (2) Heriot-Watt University, School of Engineering and Physical Sciences, Edinburgh, United Kingdom

7 (3) Istituto Nazionale di Geofisica e Vulcanologia - Sezione di Pisa, Pisa Italy

8 (4) Università di Pisa, Dipartimento di Scienze della Terra, Pisa, Italy

9 (5) Istituto Nazionale di Geofisica e Vulcanologia - Sezione di Bologna, Bologna, Italy

10 (6) Università di Torino, Dipartimento di Scienze della Terra, Torino, Italy

11 \*Corresponding author: Mauro A. Di Vito (mauro.divito@ingv.it)

12

13 **Abstract**

14 Lahars represent some of the most dangerous phenomena in volcanic areas for their destructive  
15 power, causing dramatic changes in the landscape with no premonitory signs and impacting on  
16 population and infrastructures. In this regard, the Campanian Plain turns out to be very prone to the  
17 development of these phenomena, since the slopes of the Somma-Vesuvius and Campi Flegrei  
18 volcanoes, along with the Apennine reliefs are mantled by pyroclastic deposits that can be easily  
19 ~~remobilised~~[remobilized](#), especially after intense and/or prolonged rainfall.

20 This study focuses on the analysis of the pyroclastic fall and flow deposits and of the syn- and post-  
21 eruptive lahar deposits related to two sub-Plinian eruptions of Vesuvius, 472 ~~AD~~[CE](#) (Pollena) and  
22 1631. To begin with, historical and field data from the existing literature and from hundreds of  
23 outcrops were collected and organized into a database, which was integrated with several new pieces

24 of data. In particular, stratigraphic, sedimentological (facies analysis and laboratory) and  
25 archaeological analyses were carried out, in addition to rock magnetic investigations and impact  
26 parameter calculations. The new data are ~~mainly~~also referred to the finding of ash beds in more distal  
27 areas, which ~~was~~were included into new isopach maps for the two sub-Plinian eruptions.

28 The results show that for both the eruptions the distribution of the primary deposits is wider than ~~the~~  
29 ~~one~~ previously known. A consequence of these results is that a wider areal impact should be expected  
30 in terms of civil protection, as the sub-Plinian scenario is the reference one for a future large eruption  
31 of Vesuvius. Such distribution of the pyroclastic deposits directly affects the one of the lahar deposits,  
32 also because a significant remobilization took place during and after the studied eruptions, which  
33 involved the distal phreatomagmatic ash. From these integrated analyses, it was possible to constrain  
34 the timing of the deposition and the kind of deposits remobilized (pyroclastic fall vs. flow), as well  
35 as was possible to calculate the velocities and dynamic pressures of the lahars, and ultimately- infer  
36 the lahar transport and emplacement mechanisms.

37 The multidisciplinary approach adopted in this work shows how it is crucial to assess the impact of  
38 lahars in densely populated areas even at distances of several to tens of km from active volcanoes.  
39 This especially applies to large parts of the densely populated areas around Somma-Vesuvius up to  
40 the nearby Apennine valleys.

41 Keywords: Somma-Vesuvius; Apennine valleys; pyroclastic deposits; lahars; areal distribution; local  
42 impact.

43

## 44 **1. Introduction**

45 The ~~emplacement~~movement of volcanoclastic mass flows, and the consequent damage along the  
46 flanks of active volcanoes and perivolcanic plains, represent a constant threat to inhabited areas and  
47 populations (e.g., Waite et al., 1983; Lowe et al., 1986; Pierson, 1985; Newhall and Punongbayan,

48 1996). ~~These phenomena~~Such systems are variably-fluidized, gravity-driven flows that consist of a  
49 mixture of pyroclastic sediment and water. ~~are~~They can be triggered by various mechanisms, among  
50 which the most common are intense or prolonged atmospheric precipitations (Arguden and Rodolfo,  
51 1990; Rodolfo and Arguden, 1991; Pareschi et al., 2000; Rodolfo, 2000; Scott et al., 2001; Vallance  
52 and Iverson, 2015). Such precipitations or water runoff, especially during and/or ~~immediately~~ after  
53 the eruptions, can cause the ~~detachment of landslides that can evolve into lahars~~ remobilization of  
54 pyroclastic deposits evolving into water-saturated multiphase systems called lahars (e.g., White et al.,  
55 1997; Sheridan et al., 1999; Scott et al., 2001; Baumann et al., 2020). The last century was affected  
56 by a significant number of highly-impacting lahar events associated to well-studied explosive  
57 volcanic eruptions worldwide, such as for example at Colima (Mexico) in 1913 (Rodriguez-Sedano  
58 et al., 2022), Nevado del Ruiz (Colombia) in 1985 (Voight, 1990), Ruapehu (New Zealand) in 2007  
59 (Lube et al., 2012), and Merapi (Indonesia) in 2011 (Jenkins et al., 2015).

60 According to Rodolfo (2000), Sulpizio et al. (2006), and Vallance and Iverson (2015), volcaniclastic  
61 mass flows can be generated at variably ~~long~~ time ~~intervals~~, spanning from eruptive ~~on~~ to post-  
62 eruptive phases of tens to hundreds of years. In case ~~these~~ flows are directly related to volcanic  
63 eruptions ~~(i.e., that is occurring during or shortly after the eruptive event)~~, lahars are defined as syn-  
64 eruptive, and can represent an important multihazard factor in the short ~~to~~ ~~middle~~ term for  
65 perivolcanic areas (Rodolfo, 2000; Sulpizio et al., 2006). ~~On the other hand~~ Instead, in case they are  
66 unrelated to any eruption dynamics, ~~so~~ that is occurring during long periods of volcanic quiescence,  
67 they are defined as post ~~or inter~~ eruptive (Vallance and Iverson, 2015), and can represent a long-  
68 term hazard factor (e.g., Siebe et al., 1999; Pareschi et al., 2002; Zanchetta et al., 2004a, 2004b;  
69 Sulpizio et al., 2006). Usually, ~~these latter~~ post-eruptive lahars are not accounted for ~~in the~~  
70 assessment of volcanic hazard, although their study is important for hydrogeological hazard  
71 assessment and long-term territorial planning.

72 In this sense, ~~i.e.~~ that is from the hazard assessment point of view, one of the priorities concerns the  
73 assessment of those areas potentially exposed to such a threat, taking into account the temporal

74 recurrences of the phenomena (~~during~~ over days to months after an eruption, or years to decades after)  
75 and ~~the~~ physical features of the volcanoclastic mass flows (volume, thickness, velocity, dynamic  
76 pressure, concentration, and invasion areas). We stress the fact that the definition of syn-eruptive  
77 lahars (Sulpizio et al., 2006; Vallance and Iverson, 2015) adopted in the present work is important  
78 when accounting for the multihazard of explosive eruptions, which in areas like Vesuvius and  
79 surroundings should not be neglected for its assessment and mapping purposes (de' Michieli Vitturi  
80 et al., this issue; Sandri et al., this issue). The methodology used in this work is geological (see Section  
81 3.2), and the syn-eruptive definition of lahars is necessary to avoid underestimations of the volcanic  
82 hazard from sub-Plinian eruptions at Vesuvius.

83 A lot of the existing literature analyzed the hazard related with volcanoclastic mass flows on the flanks  
84 of active volcanoes, through the reconstruction of historical and prehistoric events (e.g., Scott, 1989;  
85 Scott et al., 1995; Vallance and Scott, 1997; [Zaragoza et al., 2020](#)), by using empirical relationships  
86 or physical models (e.g., Macedonio and Pareschi, 1992; Costa, 1997; Iverson et al., 2000; [Walsh et](#)  
87 [al., 2020](#)). However, the areas affected by these phenomena can be extended well beyond the  
88 boundaries of the volcanic complex, also including the surrounding plains and the downwind-lying  
89 mountainous areas, which are subjected to tephra fallout sometimes even at great distances from the  
90 volcano (e.g., Siebe et al., 1999; Pareschi et al., 2000, 2002; Zanchetta et al., 2004a, 2004b; Di  
91 Crescenzo and Santo, 2005). In these areas, volcanoclastic mass flows may cause victims and  
92 damages, even where considered safe or scarcely affected by other volcanic hazards.

93 In this paper, we present the results of a multidisciplinary study, including geomorphological,  
94 stratigraphic, sedimentological and rock magnetic investigations, as well as impact parameter  
95 calculations by reverse engineering from the deposits. These investigations followed several  
96 surveying campaigns carried out in natural exposures, archaeological excavations, and trenches dug  
97 specifically for this purpose in the plain surrounding the Vesuvius edifice and along the Apennine  
98 valleys (Fig. 1). One of the goals of the study is to show the presence of lahar deposits even in areas  
99 very far from both the Apennine hills and the valleys of Somma-Vesuvius, demonstrating the high

100 mobility of these flows. ~~Technically, the ones descending on the Apennine flanks should be termed~~  
101 ~~as volcanielastic debris flows; here we merge into an only one term, lahars, to indicate secondary~~  
102 ~~mass flows strictly related to specific eruptions.~~ The study of the past lahar deposits has been useful  
103 for the understanding of the feeding drainage basins ~~for different types of volcanielastic mass flows,~~  
104 their extent and facies variations with distance from the source area, and their associated  
105 ~~environmental~~ impact on landscape. As already pointed out by Di Vito et al. (2013, 2019), in the past  
106 4.5 ka repeated lahar and flooding episodes related to the main eruptions of Somma-Vesuvius and  
107 Campi Flegrei volcanoes strongly stroke the Campanian Plain and its human settlements, influencing  
108 their abandonment or evidencing attempts of resettlement. In particular, for the areas around  
109 Vesuvius, these phenomena included: i) large volume and high energy lahars, originated from the  
110 volcanic edifice, which affected the volcanic apron; ii) large flooding phenomena, i.e. overflowing of  
111 water affecting the Campanian plain; iii) lahars originated from the perivolcanic mountains that  
112 affected the Apennine valleys, and invaded the areas of the plain at their mouths. All of these  
113 phenomena differed to each other in terms of amount and grain-size of the involved sediment. The  
114 data and pieces of information described here were the basis for validating a new model for lahar  
115 transport (de' Michieli Vitturi et al., submitted this issue), which was applied for assessing the related  
116 hazard at Vesuvius and Campanian Plain (Sandri et al., submitted this issue).

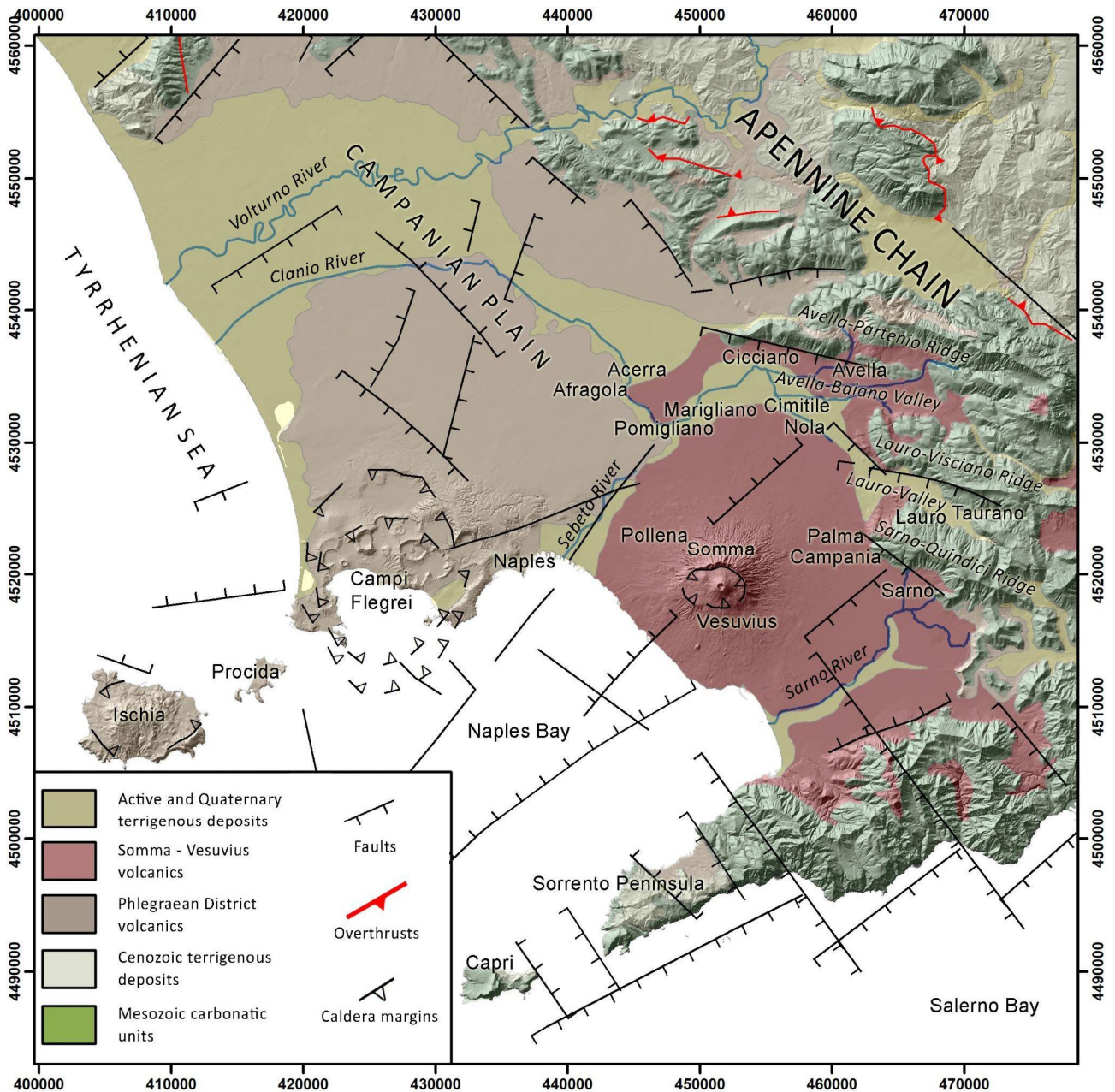
117 The structure of the work consists of an integrated geological, geomorphological, stratigraphic and  
118 sedimentological ~~integrated~~ study, a paleomagnetic and sediment-mechanic impact assessment  
119 calculation, and a comprehensive discussion on the lahar problem in the Campanian Plain.

120

## 121 **2. Geological setting**

122 The study area is part of the Campanian Plain, which includes the lowlands surrounding Mount  
123 Vesuvius volcano and the nearby Apennine ridges and valleys (Fig. 1). The orography of the area is  
124 characterized by three WNW-ESE trending mountain ridges that border eastward the plain, with an

125 elevation ranging from 500 to 1600 m a.s.l., and slope angles from 30 to 60°. From north to south,  
 126 the Avella-Partenio, Lauro-Visciano and Sarno-Quindici mountain ridges are separated by two  
 127 depressions: the Avella-Baiano Valley, in which the alluvial plain of the Clanio river occurs, and  
 128 the Lauro valley. Both are narrow valleys that widen toward north-west, among the cities of Cicciano,  
 129 Nola and Palma Campania (Fig. 1). The reliefs are characterized by a high drainage density,  
 130 associated with a poorly developed and torrential hydrographic network, which over time has favored  
 131 the incision and dismantling of the pyroclastic cover on the ridges, and the development of numerous  
 132 detrital conoids that connect with the main valley floor (Di Vito et al., 1998).



133

134 Fig. 1. Geological and structural sketch of the Campania Region on a Shaded Relief derived from TINITALY DEM. The  
135 coordinates are expressed in WGS 84 UTM N33 (modified after Orsi- et al., 1996).

136

137 Vesuvius, or more properly Mt. Somma-Vesuvius, is a composite central volcano less than 39,000  
138 years old, composed of the remnant of the oldest Mt. Somma edifice, dismantled by repeated episodes  
139 of caldera collapse, and the more recent Mt. Vesuvius, grown inside it. Its volcanic history is  
140 characterized by an initial phase, dominated by low-energy effusive and explosive eruptions, which  
141 ended at around 22,000 years ago. Since then, the volcano generated four Plinian eruptions with VEI  
142 5-6, each preceded by long periods of quiescence and all accompanied by a summit caldera collapse  
143 (Somma caldera; Cioni et al., 1999). The last Plinian eruption occurred in 79 CE and once again  
144 modified the Somma caldera, inside which the recent cone has subsequently grown due to an  
145 alternation of periods of open conduit, persistent Strombolian and effusive activity, and long periods  
146 of quiescence with obstructed conduit, interrupted by high-energy sub-Plinian eruptions. In historical  
147 times, the other more energetic events were the sub-Plinian ‘Pollena’ (472 CE) and 1631 eruptions  
148 (Santacroce et al., 2008). The last eruption occurred in 1944 and caused the return to obstructed  
149 conduit conditions, which characterize the current quiescent phase of the volcano. The rocks  
150 composition varies from slightly silica-undersaturated (K-basalt to K-trachyte) to highly silica-  
151 undersaturated (K-tephrite to K-phonolite). The Somma-Vesuvius complex is characterized by  
152 ~~Mount Vesuvius is a composite central volcano with~~ a well-developed radial drainage network, which  
153 feeds an extensive volcanoclastic apron that morphologically connects the edifice with the  
154 surrounding plain (Santacroce et al., 2003). It represents the active southern termination of the Plio-  
155 Quaternary volcanic chain that borders the eastern Tyrrhenian margin (Peccerillo, 2003). Volcanism  
156 in this margin is related to the extensional tectonic phases that accompanied the anticlockwise rotation  
157 of the Italian peninsula, during the complex interaction between the Africa and Eurasian plates, which  
158 generated the Apennine thrust-and-fold belt (Ippolito et al., 1973; D’Argenio et al., 1973; Finetti and  
159 Morelli, 1974; Bartole, 1984; Piochi et al., 2004; Patacca and Scandone, 2007; Vitale and Ciarcia,



160 2018). The extension along the Tyrrhenian margin of the Apennine chain was accommodated by the  
161 activation of NW-SE normal faults and NE-SW normal to strike-slip transfer fault systems, which  
162 dismembered the chain in horst and graben structures, and allowed magmas to reach the surface and  
163 feed the volcanism (Mariani and Prato, 1988; Faccenna et al., 1994; Acocella and Funiciello, 2006).  
164 The Campanian Plain is one of these grabens that hosts the Neapolitan volcanic area. It is a NW-SE  
165 elongated structural depression, filled by a thick sequence of marine and continental sedimentary  
166 deposits, and volcanic-volcaniclastic successions that compensated its subsidence, leading to a  
167 complete emersion at around 39 ka (Brocchini et al., 2001; De Vivo et al., 2001; Santangelo et al.,  
168 2017). This graben is bordered toward NW, NE and SE by the Meso-Cenozoic carbonate and  
169 terrigenous successions of the Apennine chain, and is subdivided in minor NE-SW oriented horst-  
170 and-graben structures (Carrara et al., 1973; Finetti and Morelli, 1974; Fedi and Rapolla, 1987;  
171 Brancaccio et al., 1991). Neapolitan volcanoes lie on these second-order structural highs (Marotta et  
172 al., 2022 and reference therein), and the products of their most powerful eruptions blanketed the  
173 Apennine reliefs and filled their valleys with several meter-thick covers of ~~loose~~ pyroclastic fall  
174 deposits, composed ~~of by~~ of pumice lapilli and ash layers separated by paleosoils (Pareschi et al.,  
175 2002; Bisson et al., 2007; Cinque and Robustelli, 2009; [Gurioli et al., 2010](#)).  
176 In terms of water drainage ~~of the water~~, the pyroclastic cover has peculiar geotechnical characteristics,  
177 such as a positive correlation between grain-size and permeability, which enabled the development  
178 of lahars in the area. In particular, coarser pumice layers are characterized by interconnected  
179 ~~inner~~ inter-clast void spaces that control water accumulation, instead ash layers, soils and paleosoils  
180 by a high water retention capacity (Andosol-like soils), so that the differential behavior can regulate  
181 equilibrium among deposits stability vs. remobilization (Fiorillo and Wilson, 2004).  
182 Regarding the volcanic activity of Vesuvius in the last 2,000 years, the largest eruptions after the 79  
183 CE Plinian one were two sub-Plinian eruptions, the 472 CE Pollena and 1631 ones, but several other  
184 effusive and explosive events ~~frequently~~ occurred in historical times. In the Campanian Plain, lahar  
185 deposits related to these two eruptions are quite abundant due to past heavy rains (Fiorillo and Wilson,

186 [2004; Zanchetta et al., 2004b; Stanzione et al., 2023](#)), also the sub-Plinian scenario is of interest for  
187 civil protection purposes, which is why in the present work we focus on these [reference explosive](#)  
188 [CE Pollena and 1631](#) eruptions. ~~Throughout the work, a~~ particular attention is ~~put given on to the~~  
189 distribution of the primary pyroclastic deposits and ~~the~~-related syn-eruptive lahars, which are mass  
190 flow events ~~strictly directly~~ related to specific eruptions, even if the condition is not necessarily that  
191 of an event contemporaneous to the eruption. ~~Those~~ deposits are mainly composed ~~by of~~ >90%  
192 fragments from the parental eruption, ~~while the remaining fragments pertain to other eruptions mixed~~  
193 ~~by volcanoclastic colluvium~~ (Sulpizio et al., 2006). The syn-eruptive feature is thus related to the  
194 ~~involvement remobilization~~ of pyroclastic deposits more than to the exact timing of [lahar](#)  
195 emplacement, the latter being of the order of max a few years (before ~~significant~~-humification  
196 processes ~~or significant human activities~~ can occur). ~~Such a feature distinction is important because~~  
197 ~~directly related to volcanic hazard.~~

198

### 199 **3. Materials and methods**

#### 200 **3.1. Evidence from historical sources**

201 We collected data from historical sources, maps, documents, and newspapers to supplement the  
202 geological data, gathered directly or indirectly, for the definition of the areal distribution of the syn-  
203 eruptive and post-eruptive lahar deposits at Vesuvius and in the surrounding region. Such collection  
204 concerned the phenomena that took place starting from the sixteenth century CE to 2005. This time  
205 span has been chosen depending on data availability, and to show the high recurrence of events over  
206 time in the area. The data were collected and grouped not only by years but also by the municipal  
207 areas existing at those times. It should be noted that the distribution of the data can be affected by the  
208 different urbanization over time, and by the presence of damage to people, ~~things~~[infrastructures and](#)  
209 [goods](#), economic activities and settlements. In the absence of local ~~instrumental~~  
210 ~~meteorological weather data~~ series, ~~corresponding to over~~ the analyzed period, we assumed that the

211 phenomena of remobilization of the pyroclastic deposits, and the consequent generation of large  
 212 ~~alluvial flooding~~ events and volcaniclastic mass flows, coincided with extreme weather events often  
 213 described and reported in the analyzed sources. ~~The reports reach a quite significant number,~~  
 214 ~~approximately 500, and concern 97 municipalities~~We identified about 500 individual reports,  
 215 covering events between the sixteenth century CE and 2005 that took place in 97 different  
 216 municipalities.- The data were organized in a geospatial database, so that it was possible to define  
 217 different areas affected by frequent syn-eruptive floods and lahars, concomitant/related with the sub-  
 218 Plinian eruption of 1631, to be used as benchmark for the main geological analyses. ~~With reference~~  
 219 ~~to~~We could not add the Pollena eruption to this historical data set, as there are no ~~historical~~available  
 220 sources for similar occurrences other than documents deriving from archaeological excavations  
 221 ~~activities~~-(see next sections).

222 The municipalities with the highest number of reports are: Sarno (43), Salerno (32), Siano (26), Vietri  
 223 sul Mare (22), Bracigliano (21), Nocera Inferiore (20), Maiori (19), Quindici (17) (Fig. 1). The events  
 224 of greatest intensity, which affected more than five municipal territories at the same time, are 19;~~they~~  
 225 ~~likely were multiple soil slip debris flows~~. Some of these occurrences result closely connected with  
 226 the volcanic events of Vesuvius, such as those that occurred in 1631, 1823, 1910, 1949 and 1954,  
 227 simultaneously or within months to a few years after the Vesuvius eruptions of 1631, 1822, 1906 and  
 228 1944.

<u>Eruption</u>	<u>Lahar/Intense Alluvial Event</u>	<u>Municipalities affected</u>
<u>December 1631</u>	<u>16/12/1631</u>	<u>Sant'Anastasia, San Giorgio a Cremano, Massa di Somma, Somma, Ottaviano, San Sebastiano, Trocchia, Torre del Greco, Portici, Pugliano, Madonna dell'Arco, Palma, Nola Arpaia, Arienzo, Cicciano, Marigliano, Benevento, Avellino</u>
<u>October 1822</u>	<u>24/01/1823</u>	<u>Amalfi, Bracigliano, Cava de' Tirreni, Cetara, Minori, Nocera Inferiore, Pagani, Salerno, Sant'Egidio del Monte Albino, Tramonti, Vietri sul Mare</u>
	<u>12/02/1823</u>	<u>Maiori</u>

	<a href="#">12/04/1823</a>	<a href="#">Sarno</a>
	<a href="#">18/10/1823</a>	<a href="#">Corbara, Praiano, Sant'Egidio del Monte Albino, Sarno, Siano</a>
	<a href="#">15/11/1823</a>	<a href="#">Salerno</a>
<a href="#">April 1906</a>	<a href="#">24/10/1910</a>	<a href="#">Amalfi, Boscotrecase, Cercola, Cetara, Ercolano, Giffoni Valle Piana, Maiori, Marano di Napoli, Minori, Napoli, Pollena Trocchia, Torre del Greco, Vico Equense, Vietri sul Mare, Sant'Anastasia, San Giorgio a Cremano, Sarno, Scala, Pomigliano d'Arco, Portici, Ravello, Salerno</a>
<a href="#">March 1944</a>	<a href="#">02/10/1949</a>	<a href="#">Lauro, Maiori, Minori Nocera Inferiore, Sarno, Vietri sul Mare</a>
	<a href="#">25/10/1954</a>	<a href="#">Cava de' Tirreni, Maiori, Minori, Nocera Inferiore, Salerno, Tramonti, Vietri sul Mare</a>

229 [Tab. 1. Historical archive of lahar and alluvial events related to the four most significant Vesuvius eruption in the last](#)  
230 [four centuries, and municipalities affected by such events.](#)

231 The absence of information in the Lauro and Avella-Baiano [y](#)Valleys is likely due to the absence of  
232 detailed descriptions of alluvial events, or most likely to the position of the inhabited areas generally  
233 located on the hills thus far from the lower part of the valleys.

234

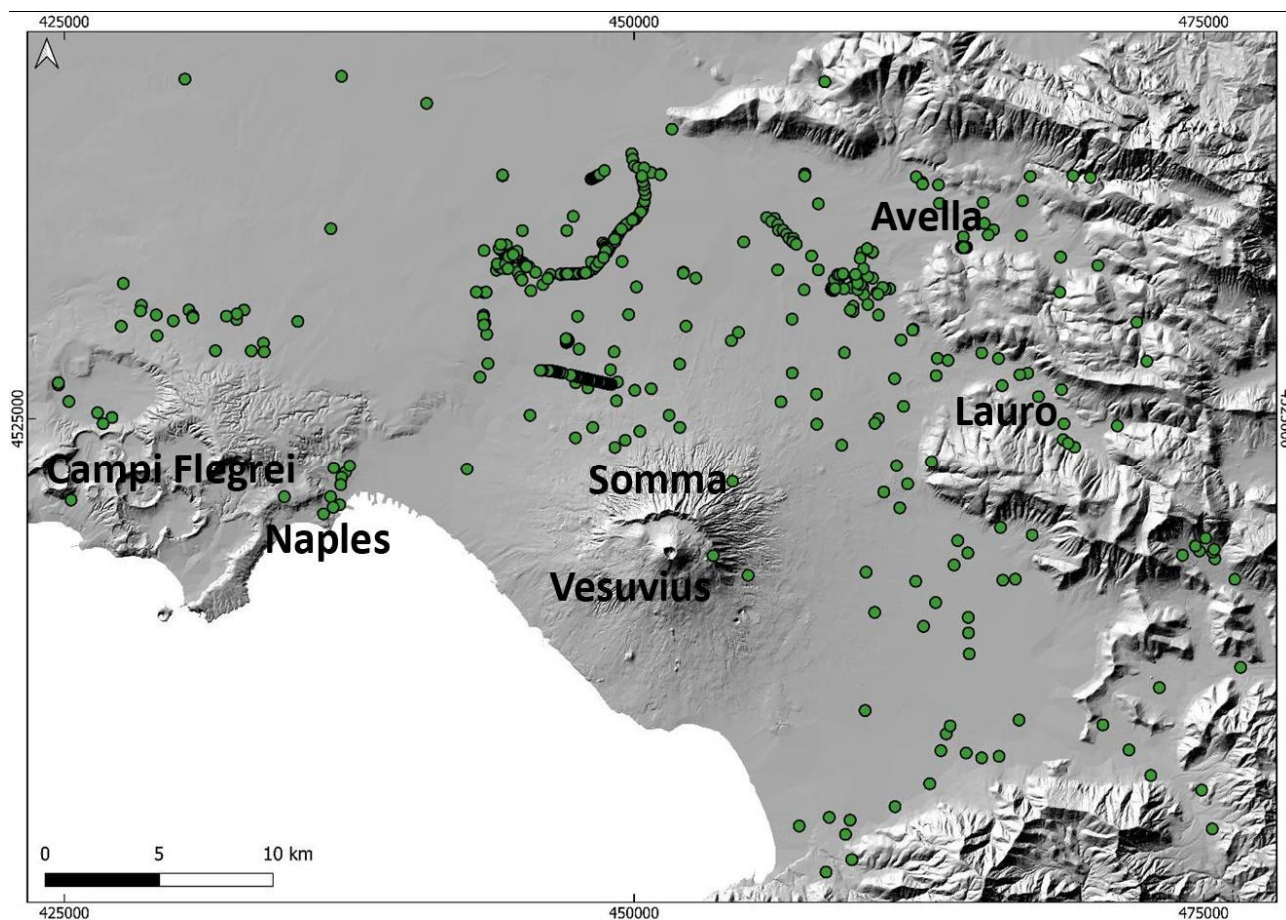
### 235 **3.2. Field and archaeological investigations**

236 We used a set of geological, stratigraphical, sedimentological, archaeological, and pedological  
237 information for the reconstruction of the type of events, their emplacement mechanisms, timing, and  
238 impact on pre-existing structures/environment. Such an approach enabled us to cross-check  
239 geological and archaeological evidence allowing us to accurately fix the age of events. Conversely,  
240 the presence of well-dated primary pyroclastic deposits can define the age of human traces otherwise  
241 not easily datable. Furthermore, the identification of the “primary” (fallout and pyroclastic current,  
242 along with the archeological findings) can give the absolute age (*ante* or *post quem*) of a given deposit.  
243 The definition of isochronic paleosurfaces can also contribute to the reconstruction of the paleo-  
244 environments affected by the deposition, and of the variations that occurred during depositional  
245 processes. For this purpose, particular attention was paid to the basal contacts between the deposits.

246 In some areas like Nola, the lahar deposits directly overlie the primary pyroclastic deposits ~~(of (both~~  
247 ~~for the 472 CE Pollena ~~or and~~ 1631 eruption))~~, while in other ~~cases~~ areas some pyroclastic units or  
248 the whole primary deposits are missing (eroded) or lacking. Only the correlation with the nearby areas  
249 ~~P~~permitted to define whether the emplacement of the ~~secondary deposits~~ lahars eroded partly or  
250 ~~entirely significantly~~ the underlain primary deposits, vice versa the complete absence in the  
251 emplacement areas ~~was could also be “simply”~~ due to their distribution of these latter. The analysis  
252 of the internal structure marked by sharp changes in grain sizes, color, presence of ~~erosive~~ erosional  
253 unconformities, or interposition of lenses of coarser material also permitted the identification of one  
254 or more flow units within the same individual deposit package. The macroscopic characteristics of  
255 the sequences permitted some inferences on the transport and depositional mechanisms, while the  
256 grain-size and componentry ~~analysis~~ analyses provided information ~~of on~~ the source deposits that  
257 were remobilized. This brings to another important definition, that is syn-eruptive vs. post-eruptive  
258 lahars, according to the definition of Sulpizio et al. (2006) and Iverson and Vallance (2015), which  
259 applies during or respectively soon after the eruption vs. several years to centuries after the eruption  
260 ended, respectively. The macroscopic analysis allowed us to distinguish between the syn-eruptive  
261 and post-eruptive deposits, ~~which. The first ones~~ are defined by the occurrence of pyroclastic  
262 components with ~~homogeneous~~ a lithology, similar to the one of the primary deposits, ~~and the post-~~  
263 ~~(or inter-) eruptive deposits.~~ The second ones are characterized by some evidence of depositional  
264 stasis, ~~such as like~~ humified paleosurfaces, ~~evidence~~ below the lahar deposits or of anthropic  
265 anthropogenic activities, or ~~also through deposits that contain~~ by the presence of humified material  
266 and/or fragments of older eruptions in the deposits ~~following the progressive erosion within the~~  
267 feeding slopes and valleys. All these characteristics allowed the correlation between the various  
268 volcanoclastic units for the whole set of the studied sequences, marking the differences needed to  
269 hypothesize on the source and invasion areas.

270 We reviewed all the volcanological and archaeological data collected during the last 20 years from  
271 drill cores, outcrops, archaeological excavations, and from the existing literature, in collaboration

272 with colleagues of the Archaeological Superintendence of Campania region. The preliminary  
273 collection and analysis of the existing data permitted to plan a hundred of new stratigraphic trenches  
274 (Fig. 2), with the aim of collecting stratigraphic, ~~stratimetric~~, sedimentological, lithological and  
275 chronological data on the ~~sequences both of~~ primary pyroclastic and secondary (lahar) deposits.  
276 Particular attention was also paid to the ~~primary pyroclastic deposits and to syn and post-eruptive~~  
277 ~~lahars, and to their~~ geometric relations of these deposits with the paleotopography and ~~the~~ preexisting  
278 ~~anthropic-anthropogenic~~ structures.



279  
280 Fig. 2. Shaded relief of the studied area and location of all the sites where stratigraphic analyses were carried out.

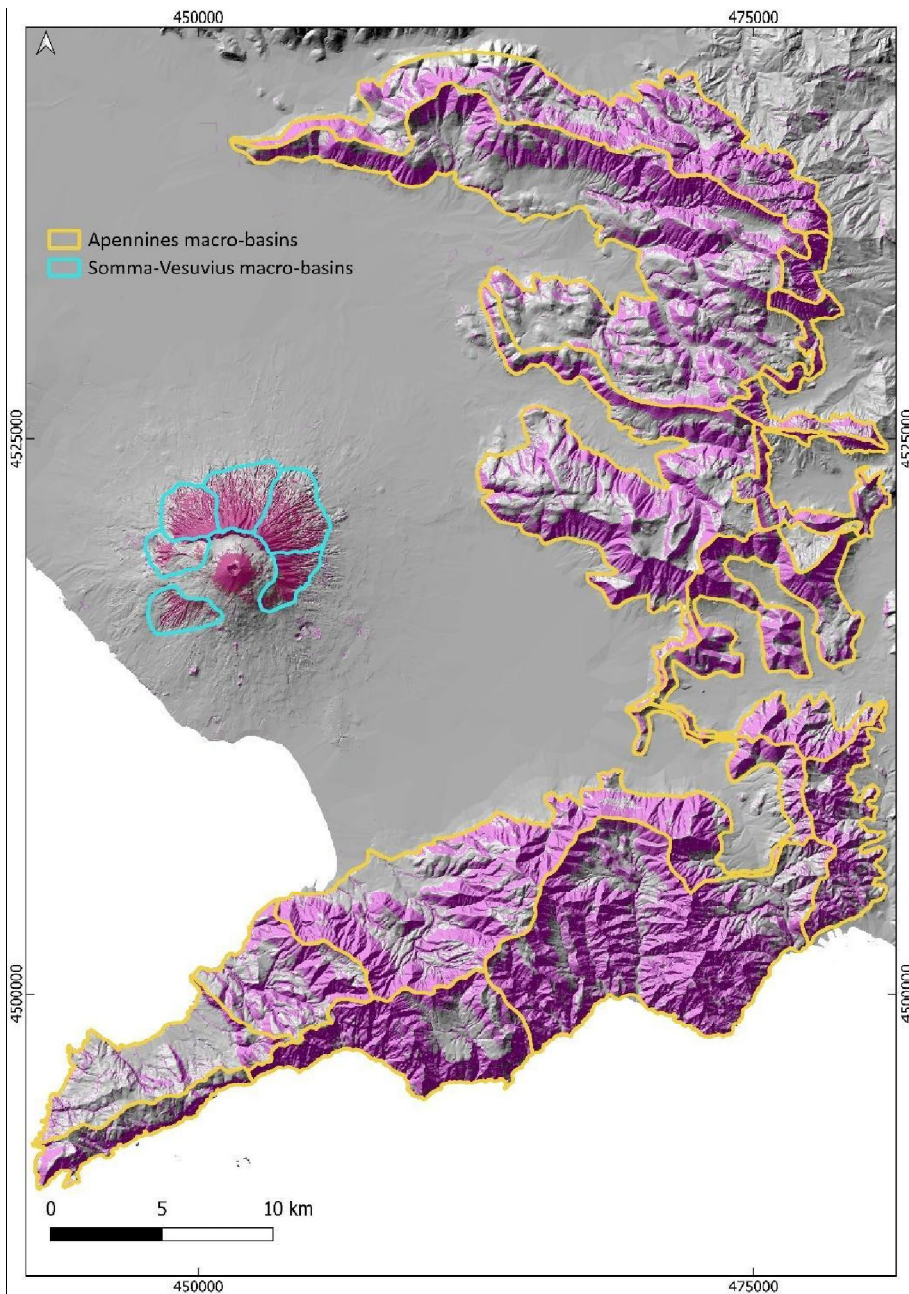
281  
282 The collected data were organized into a geospatial database (QGIS Platform), in which each point  
283 represents an investigated site linked to a series of information, such as the precise location, ~~the~~  
284 kindtype of volcanic sequence, and ~~the stratimetriestratigraphic~~ features (primary and secondary  
285 units, thickness, type of deposit, etc...). The data were visualized using a Digital Elevation Model

286 (DEM) of the Campanian Plain as reference topography and the UTM WGS 84 – Zone 33N reference  
287 projection.

288

### 289 **3.3. Geomorphological analysis**

290 This analysis is aimed at identifying the macro-basins that fed the lahars in the study area after the  
291 two sub-Plinian eruptions (Pollena and 1631). The analysis was carried out on the basis of the slopes  
292 distribution and the watersheds extracted from a Digital Elevation Model (DEM). The DEM was  
293 derived from a LiDAR flight of 2012 ~~and stored with~~ (cell size of 10 m). In particular, six macro-  
294 basins characterized by slopes  $> 20^\circ$  were identified in the Somma-Vesuvius area, whereas fifteen  
295 macro-basins with slopes  $> 25^\circ$  were identified in the Apennines to the East of the volcano (Fig. 3).  
296 The different slopes thresholds are defined starting from previous studies (Pareschi et al., 2000, 2002;  
297 see also Bisson et al., 2013, 2014), and on the basis of a better analysis of the physical characteristics  
298 of the remobilized material, in turns related to the various types of deposits. In fact, ~~along the slopes~~  
299 ~~ofon the steep slopes and in the valleys of~~ Somma-Vesuvius, ~~they~~ deposits are ~~mainly~~ mainly ash-  
300 rich pyroclastic current deposits and subordinately lapilli fallout deposits, while ~~for on~~ the  
301 ~~Apennines~~ Apennines they are ash and lapilli fallout deposits ~~emplaced along the variably deep~~  
302 slopes. Each basin was considered as a single feeding unit for the lahars generation, and this is an  
303 input for the modeling of possible future lahars in the companion papers (de' Michieli Vitturi et al.,  
304 ~~submitted~~ this issue; Sandri et al., ~~submitted~~ this issue).



305

306 Fig. 3. The macro-basins defined on the basis of their geomorphological features to study the areas of possible  
 307 accumulation and mobilization of deposits, which are used in modeling lahar generation of future events.

308

### 309 3.4. Laboratory and analytical work

#### 310 3.4.1. Grain-size

311 In ~~several the selected studied sites among all the studied ones reported in~~ (Fig. 4), macroscopic  
 312 ~~analysis-analyses~~ of the stratigraphic sequences ~~was-were first~~ carried out in the field to first identify

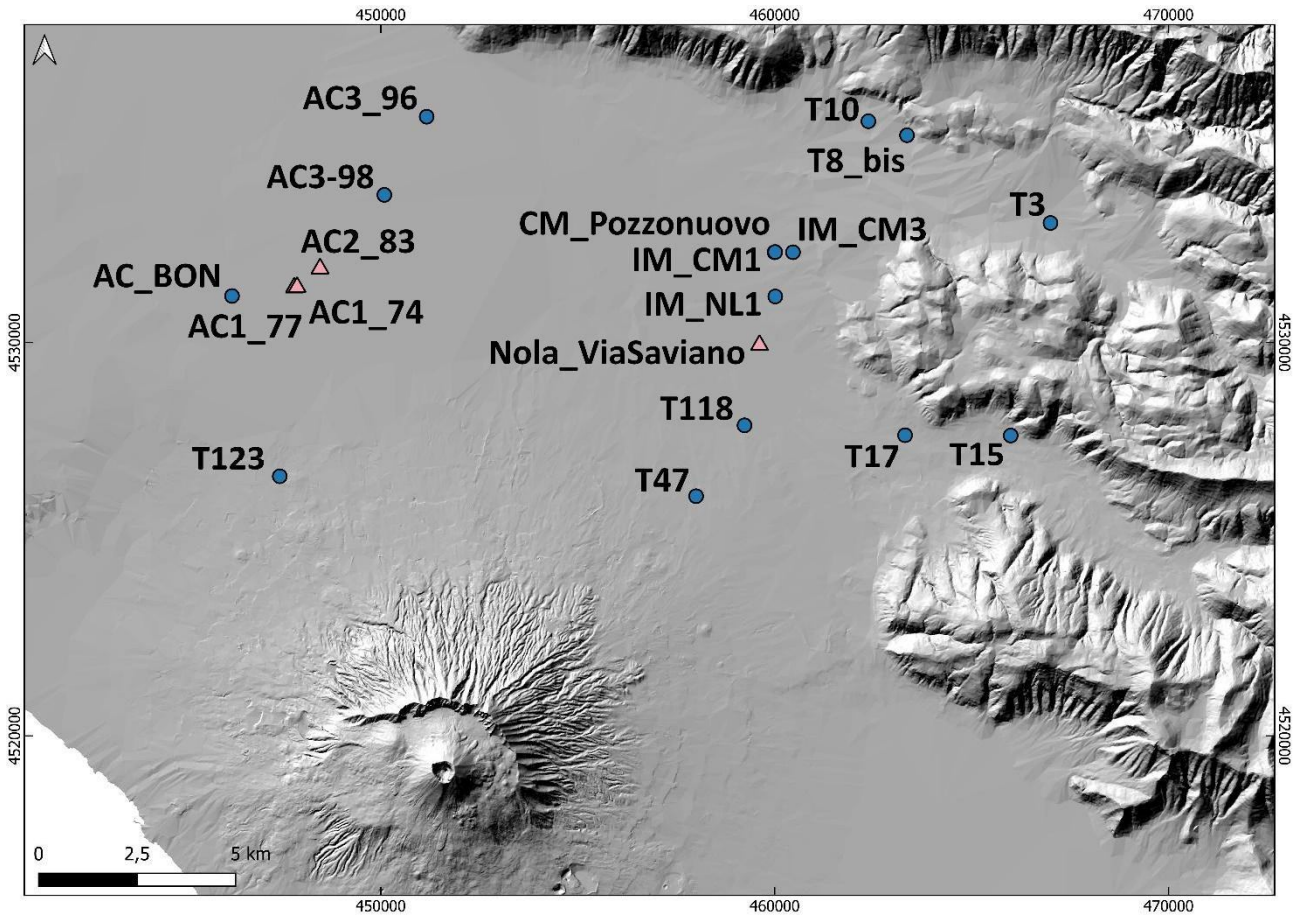


313 any homogeneities or similarities between the juvenile fraction of the primary and secondary deposits,  
314 and [then](#) recognize the various volcanoclastic units. This was followed by sampling the deposits and  
315 carrying out the laboratory analyses.

316 In particular, the sampling was mostly made on the syn-eruptive lahar deposits, but also on the post-  
317 eruptive and, in a few cases, on the primary pyroclastic deposits. All lab analyses were performed in  
318 the laboratories of sedimentology and optical microscopy at the Istituto Nazionale di Geofisica e  
319 Vulcanologia, Sezione di Napoli Osservatorio Vesuviano (INGV – OV). The material samples were  
320 pre-heated at a temperature of 60-70 °C to eliminate any fraction of humidity, then were quartered  
321 and sieved. To avoid any breaking of fragile clasts like pumices, the dry sieving of the grain-size  
322 classes between -4 (a coarse limit variable depending on the sample) and 0 phi was made manually,  
323 while for the classes between 0.5 and 5 phi a mechanical sieving apparatus was used.

324 [In particular, ~~The the~~ fine ash-rich deposit samples with a high degree of cohesion \(\[with a significant\]\(#\)](#)  
325 [amount >0 phi](#)) were ~~first combined with~~[diluted in](#) distilled water ~~and thus, then~~ boiled to remove all  
326 ~~the~~ ash aggregates, before being analyzed for ~~granulometry grain-sizes~~ following a wet procedure,  
327 [and finally dried and weighted by classes. The cumulative class >5 phi was further separated by](#)  
328 [interpolation modelling \(de' Michieli Vitturi et al., this issue\)](#). In the post-processing of the data, the  
329 GRADISTAT excel package by Blott and Pye (2001) was used to determine the main statistical  
330 parameters. On selected samples, a microscopic componentry analysis was performed, consisting of  
331 recognizing and separating the various lithotypes that compose the volcanoclastic deposits, that is  
332 juvenile, lithic and crystal clasts. The clasts recognition was made manually for the coarser fractions,  
333 while for the finest fractions it was necessary the use of a reflected-light binocular microscope.

334



336

337 Fig. 4. Location of sites in which the sampling was carried out for sedimentological and paleomagnetic analyses. The  
 338 pink triangles represent the sites for which a paleomagnetic study was carried out ([AC1\\_74](#), [AC1\\_77](#), [AC2\\_83](#), and  
 339 [Nola\\_Via\\_Saviano](#)). [In several sites, multiple samples were taken at different stratigraphic heights; samples labeled with](#)  
 340 [US were taken at CM\\_Pozzonuovo site \(see results\).](#)

341

### 342 3.4.2. Input for impact parameters

343 A significant number of large clasts and boulders was also found embedded in the [ash matrix of the](#)  
 344 lahar deposits at different locations. These clasts have dimensions from several centimeters to several  
 345 tens of centimeters in diameter, and their nature is variable, that is limestone, ceramic, brick, tephra,  
 346 lava, sandstone, iron (in order of abundance). Most of the clasts are fragments of artifacts from  
 347 buildings, structures, and other archaeological finds of the Roman period, and their shape can be  
 348 approximated in the field to ellipsoid. All these features suggest that they were entrained from  
 349 substrate into the lahars to ultimately be deposited together with the [ash main finer solid load of the](#)

350 [lahars](#). In the dynamics of volcanoclastic mass flows like lahars and pyroclastic currents, the  
351 occurrence of boulder entrainment by flow dynamic pressure is recognized as a ~~it is~~ quite common  
352 feature (e.g., Zanchetta et al., 2004a; Pittari et al., 2007; Duller et al., 2008; Toyos et al., 2008; Cas  
353 et al., 2011; Carling, 2013; Doronzo, 2013; Jenkins et al., 2015; Roche, 2015; Martí et al., 2019;  
354 Guzman et al., 2020). The capability of a flow to entrain a clast is a function of flow properties  
355 (velocity, density) and clast properties (dimension, density, shape), and dynamic pressure well  
356 syntheses and quantifies such capability also in terms of flow hazard (Toyos et al., 2008; Zuccaro and  
357 De Gregorio, 2013; Jenkins et al., 2015). In Appendix [1A](#), a theoretical scheme is presented to invert  
358 these field features for calculation of the impact parameters at local scale.

359

### 360 **3.4.3. Rock magnetism**

361 The lahar deposits related to the Pollena eruption were analyzed by rock magnetism ~~at two~~  
362 ~~localities, in the municipalities of~~ Acerra and Nola ~~at four localities~~ (Fig. 4), where the lahars  
363 ~~interacted with anthropogenic structures. At each locality, we collected oriented samples, then~~  
364 ~~measured about 200 specimens.~~ We sampled both the deposit matrix and some potsherds embedded  
365 along three trenches (74, 77 and 83) and in the “Nola-Via Saviano” excavation (~~Fig. 4~~). The purpose  
366 of the magnetic measurements was threefold: i) evaluating the magnetic fabric of the deposits to infer  
367 the local to regional flow directions of the lahars and possibly their origin, whether ~~from the~~  
368 Apennines or ~~from~~ Vesuvius. ~~The magnetic fabric in this type of deposits records the main flow~~  
369 ~~direction (local/regional) followed during the emplacement processes;~~ ii) estimating the deposition  
370 temperature ( $T_{dep}$ ) of the deposits, to understand whether the lahar was triggered soon after the  
371 eruption or at later times. ~~The hypothesis is that the temperature is higher in case of syn-eruptive~~  
372 ~~lahars deriving from hot (pyroclastic current) deposits, and lower in all other cases of post-eruptive~~  
373 ~~ones;~~ iii) testing the relative sequence (contemporaneity) of the lahars emplacement with respect to  
374 the Pollena eruption. All hand-samples were oriented *in-situ* with magnetic and solar compasses and

375 reduced to standard sizes at the CIMaN-ALP laboratory (Peveragno, Italy), where all the magnetic  
376 measurements were made. In Appendix [2B](#), the adopted paleomagnetic techniques [and nomenclature](#)  
377 are described.

378

## 379 **4. Results**

### 380 **4.1. Field stratigraphy and sedimentological features**

381 In this study, data of about 500 sites were collected, covering an area of >1000 km<sup>2</sup> from the plain  
382 around the volcanic edifice to the Apennine valleys to the north and east (Fig. 2).

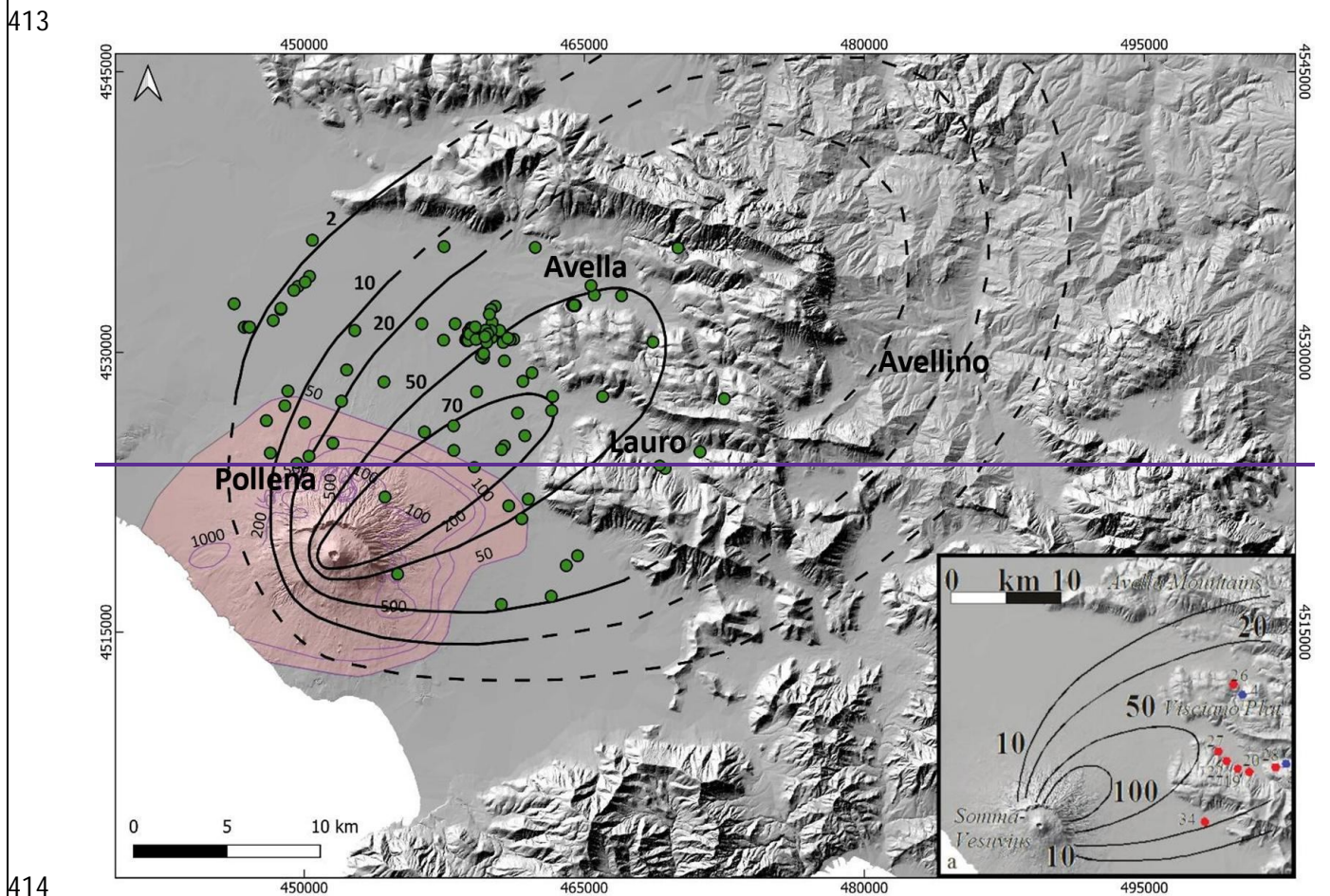
383

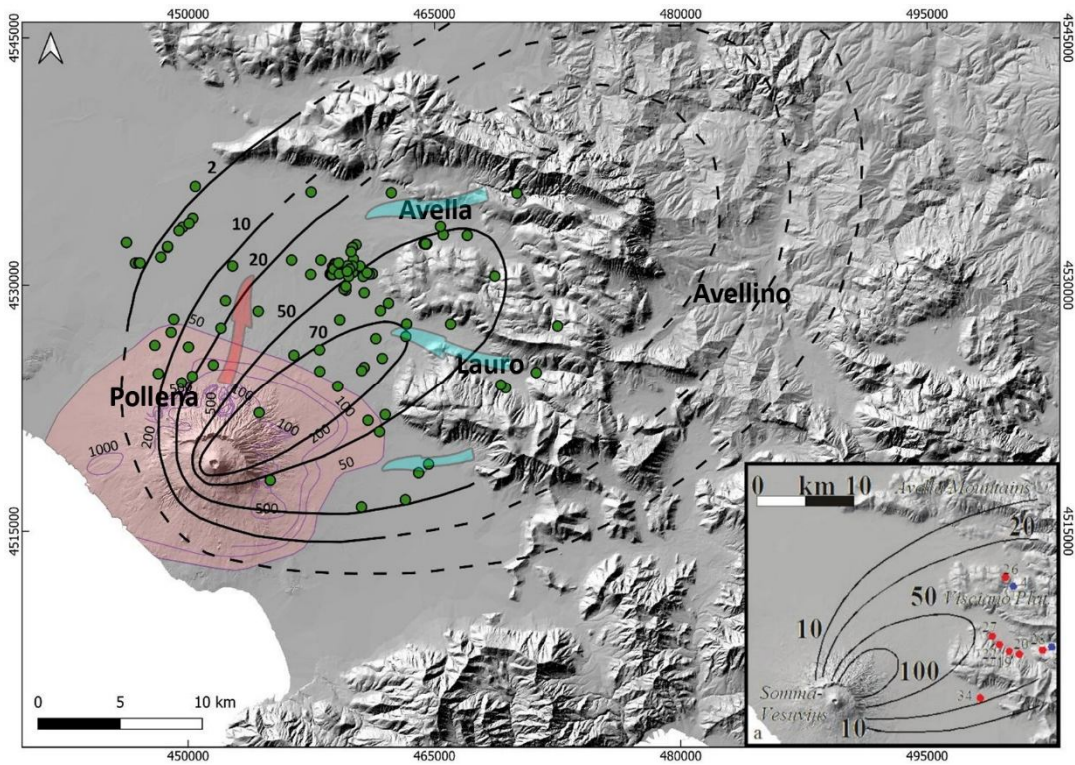
#### 384 **4.1.1. Pyroclastic deposits: ~~eruptions of Pollena and 1631~~ [eruptions](#)**

385 The integration of the collected data with the existing ones (Rosi and Santacroce, 1983; Rosi et al.,  
386 1993; Rolandi et al., 2004; Sulpizio et al., 2005; Perrotta et al., 2006; Bisson et al., 2007; Santacroce  
387 et al., 2008; Gurioli et al., 2010; De Simone et al., 2011) allowed the reconstruction of the distribution  
388 maps for both the fallout and pyroclastic current deposits. In particular, the spatial distribution  
389 highlights that for both the Pollena and 1631 primary deposits, thick fine ash deposits are widely  
390 distributed and cover the coarse fallout sequence or directly the ground, modifying the isopachs  
391 reconstructed by previous authors (Sulpizio et al., 2006 and references therein; Figs. 5 and 6). This  
392 enlargement of the area affected can have important implications on the hazard evaluation in terms  
393 of possible damages on a densely inhabited territory.

394 The area covered by the comprehensive isopach maps (including both ~~the lapilli fallout~~ and ash  
395 fallout) turns out to be wider than ~~the one~~ previously known, above all because we ~~also~~ took into  
396 account for the ash ~~deposited by~~ fallout [occurred](#) during [the](#) final [phreatomagmatic](#) stages of the  
397 eruptions, ~~mostly dominated by phreatomagmatic explosions~~ (Rosi and Santacroce, 1983; Sulpizio et  
398 al. 2005). The great ~~distribution and~~ availability [and distribution](#) of these ash deposits could explain  
399 the wide generation and distribution of the syn-eruptive lahars in the area. This has important

400 implications ~~in-on~~ the evaluation of the source area and ~~of the~~ material available for ~~the~~ lahars  
 401 accompanying and following ~~this-these~~ eruptions. ~~In particular~~ Interestingly, there is an increase of  
 402 the areas covered by pyroclastic deposits ~~and the calculated volume of the emitted products~~. For  
 403 example, the area covered by the pyroclastic current deposits ~~thus results in~~ is of about 200 km<sup>2</sup> for  
 404 the Pollena eruption, and 120 km<sup>2</sup> for the 1631 eruption, while. More significantly, ~~tThe QGIS~~  
 405 ~~recalculated 10-cm isopach area for covered by~~ the fallout deposits ~~it is of~~ 433-837.35 km<sup>2</sup> (Pollena  
 406 eruption) and 427-5287.51 km<sup>2</sup> (1631 eruption), respectively which compared to the lower values of  
 407 569 km<sup>2</sup> (Pollena eruption) and 158 km<sup>2</sup> (1631 eruption) after Sulpizio et al. (2006) give an extra  
 408 surface of about 47% and 230%, respectively. Geotechnically, ~~A~~ another implication is that the wide  
 409 presence of fine and cohesive ash, ~~not only~~ on top of the coarse fallout sequences ~~and, in general but~~  
 410 ~~also~~ on the ground, ~~reduces the permeability of the substrate~~, preventing ~~the water~~ infiltration of the  
 411 ~~water and~~, favoring ~~the stream formations~~ surficial runoff and creating sliding surfaces (Baumann et  
 412 al., 2020). ~~They can also enhance the mobility of the flows by creating sliding surfaces.~~





415

416

417

418

419

420

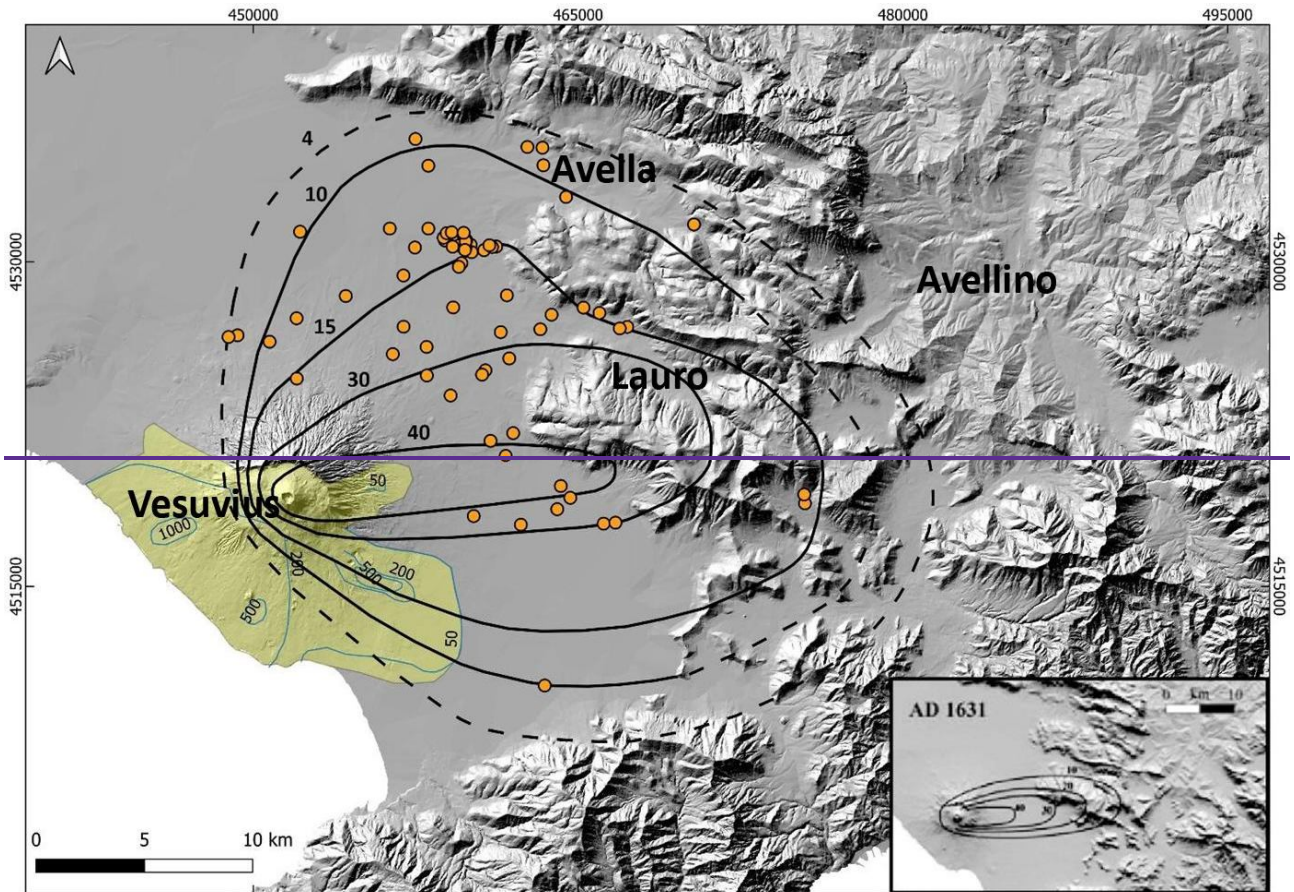
421

422

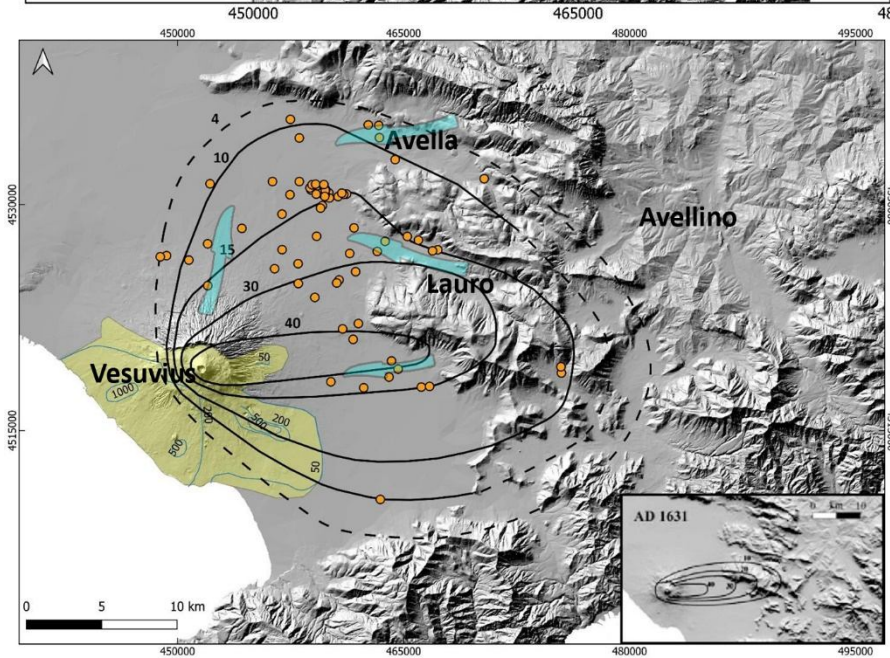
423

Fig. 5. Pollena eruption: the black lines represent the isopachs (in cm) of the fallout deposits modified after Sulpizio et al.; (2006) (in the insert) on the basis of the new collected data (green dots), while in pink is colored the area affected by PDC the pyroclastic current deposits (isopachs in cm, purple lines); modified after Gurioli et al. (2010) (purple lines). The dotted parts of the isopachs represent some uncertainty related to the absence of new further data are extrapolated. The light blue arrows represent the general remobilization of the pyroclastic fallout deposits and lahar propagation from the Apennine slopes, while the pink one represents the combined remobilization of the pyroclastic current and fallout deposits and lahar propagation from Somma-Vesuvius.

424



425



426

427 Fig. 6. 1631 eruption: the black lines represent the isopachs (in cm) of the fallout deposits, modified after Santacroce et  
 428 al., (2008) (in the inset) on the basis of the new collected data (orange dots), while in yellow is colored the area affected  
 429 by PDC-pyroclastic current deposits (isopachs in cm, light blue lines). The light blue lines represent the inferred  
 430 distribution on the basis of an integration between field data and fountschronicles, modified after Gurioli et al. (2010). The  
 431 dotted parts of the isopachs represent some uncertainty related to the absence of new further data are extrapolated. The

432 light blue arrows represent the general remobilization of the pyroclastic fallout deposits and lahar propagation from the  
433 Apennine slopes and Somma-Vesuvius.

434

435 The ~~significant widening of the~~ area affected by accumulation of the 1631 eruption tephra-fallout  
436 deposits is wider than previously known, particularly towards the north ~~for the 1631 eruption, which~~  
437 follows the inclusion of the final ash deposits into the new isopachs. Interestingly, such widening of  
438 the area agrees with the ~~wide~~ occurrence of lahars in the plain north of Vesuvius, as documented in  
439 the ~~chronicles and historical~~ sources (Rolandi et al., 1993; Rosi et al., 1993, and references therein),  
440 and as follows.

441

#### 442 **4.1.2. Lahar deposits**

443 The lithological and sedimentological analyses carried out in the field allowed the macroscopic  
444 definition of the primary pyroclastic deposits ~~involved in~~ affected by the remobilization, and of the  
445 lahar deposits. In many cases, the archaeological findings permitted to define the local  
446 paleoenvironment and ~~the related~~ land use, ~~and also to~~ then permitted to constrain the age and timing  
447 of the deposition.

448 We grouped all deposit descriptions into representative lithofacies to more directly characterize both  
449 the primary pyroclastic and lahar deposits (Tab. 2 and Fig. 7). Given the amount of data and  
450 description of the studied areas, we used these lithofacies to characterize a number of macro-areas  
451 between the Somma-Vesuvius sector and the nearby Apennine valleys (Appendix C). The lithofacies  
452 mostly recognized are P to indicate paleosoil and humified surface, mL and mA (massive lapilli and  
453 massive ash, respectively) to indicate the primary deposits, while the lahar deposits usually belong to  
454 the facies Gms and mM, which indicate massive, matrix-supported gravel deposits and massive lahar  
455 deposits, respectively. Other recognized lithofacies are Sh, Ss and fM. Sh indicates hyper-  
456 concentrated flow deposits, and consists of an alternation of coarse and fine beds. Ss includes scour

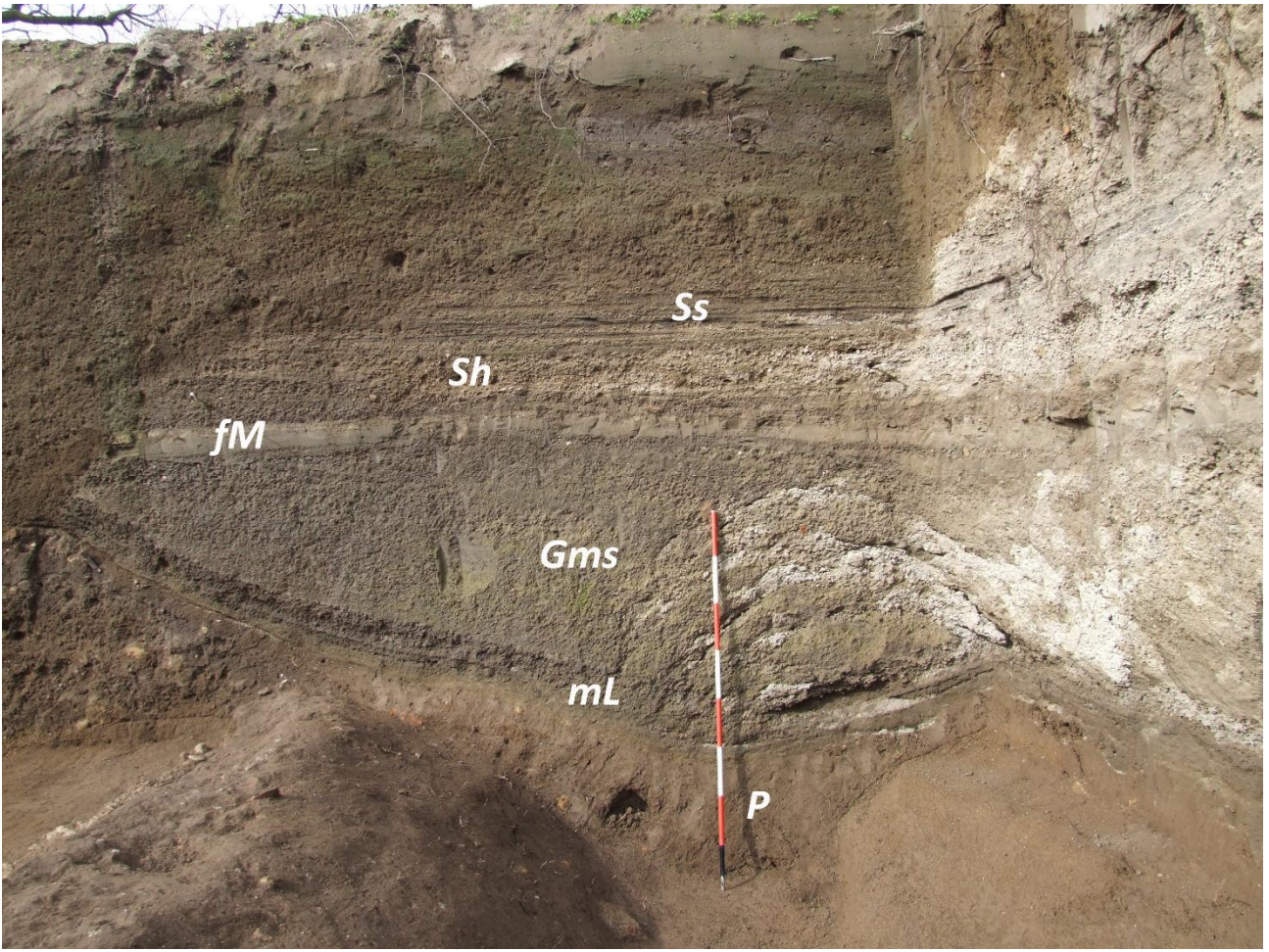


457 ~~and fill structures, and consists of an erosive, concave upwards basal surface and a planar/convex~~  
 458 ~~top. fM is fine mud, and indicates the decantation deposit formed when the flow loses its energy.~~

<u>Symbol</u>	<u>Lithofacies</u>
<u>P</u>	<u>Paleosol and humified surface, massive and composed of fine sand and silt from brown to dark brown, with several percentages of clay and organic matter. It indicates a stasis in the depositional processes.</u>
<u>mL</u>	<u>Alternation of <del>M</del> massive lapilli layers. Pyroclastic fall deposit, <del>massive and</del> composed of pumices and scoria lapilli with sparse accidental lithics.</u>
<u>mA</u>	<u>Massive ash. Pyroclastic fall deposit, <del>massive and</del> composed of fine to coarse ash with sparse pumice fragments, scoriae and accidental lithics.</u>
<u>Gms</u>	<u>Massive gravel and sand deposit, matrix-supported and poorly-sorted. The matrix is composed of fine to coarse sand, while the gravel clasts comprise scoriae and pumice clasts from the pyroclastic fall deposits. The massive feature of the single layers suggests a rapid emplacement from a highly-concentrated lahar.</u>
<u>mM</u>	<u>Massive mud deposit composed of fine sand, silt and clay, sometimes with sparse pumice and lithic clasts. It is generated from a mud-dominated lahar.</u>
<u>Sh</u>	<u>Horizontal lamination and bedding features in sands. The deposit is composed of an alternation of fine to coarse sand and gravel, which can be gradual or <del>net</del>sharp. It comes from an hyper-concentrated lahar (less dense than the Gms one).</u>
<u>Ss</u>	<u>Scour and fill structures composed of fine to coarse sand, generally with a normal grading. A single structure consists of an erosive, concave upwards basal surface and a planar/convex top.</u>
<u>fM</u>	<u>Fine mud deposit composed of fine sand, silt and clay. It is generated when the lahar loses its energy and the fine grains settle gently.</u>

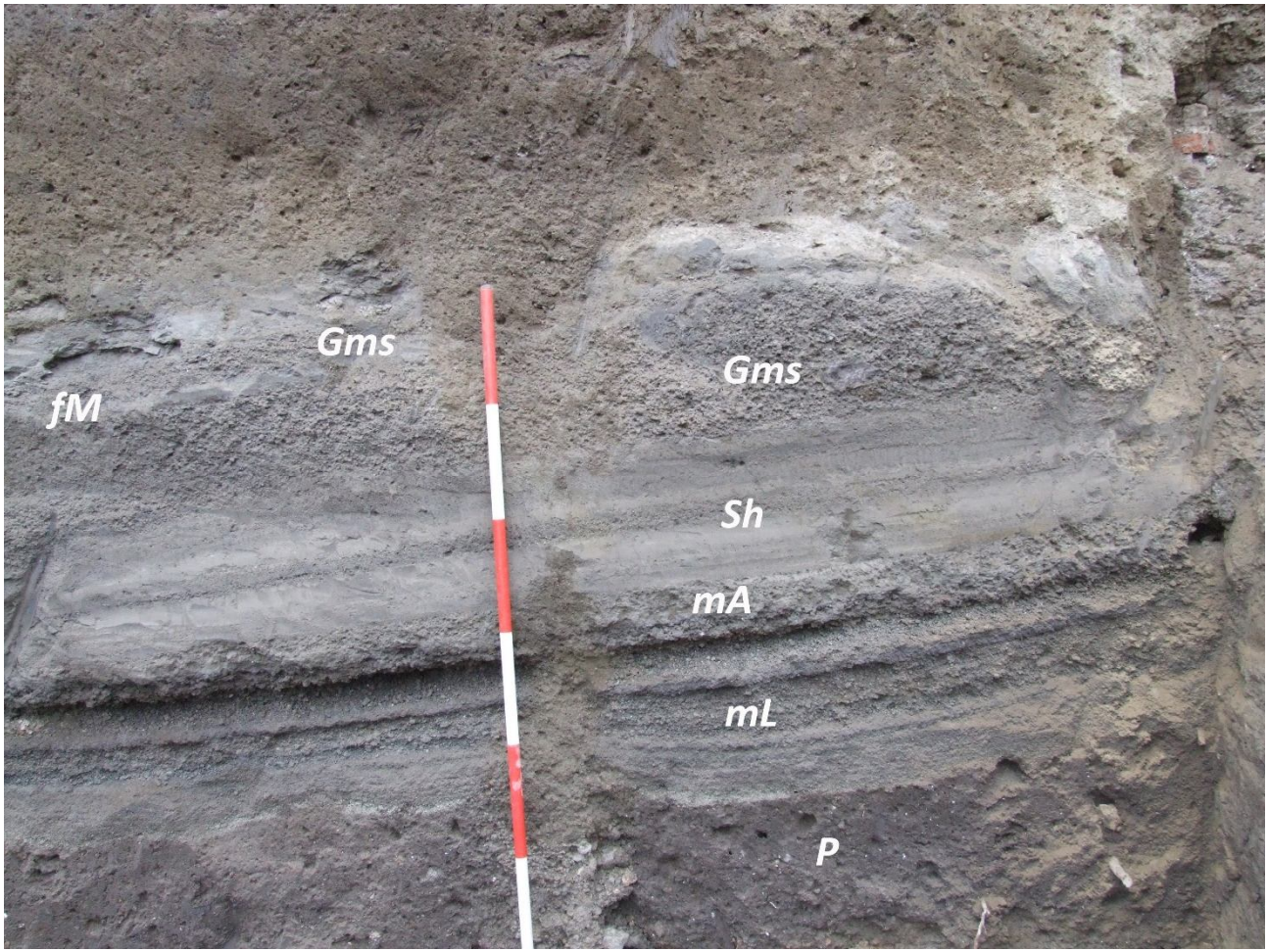
459 Tab. 2. Symbol and description of the recognized lithofacies, and photos representative of each of them.

460



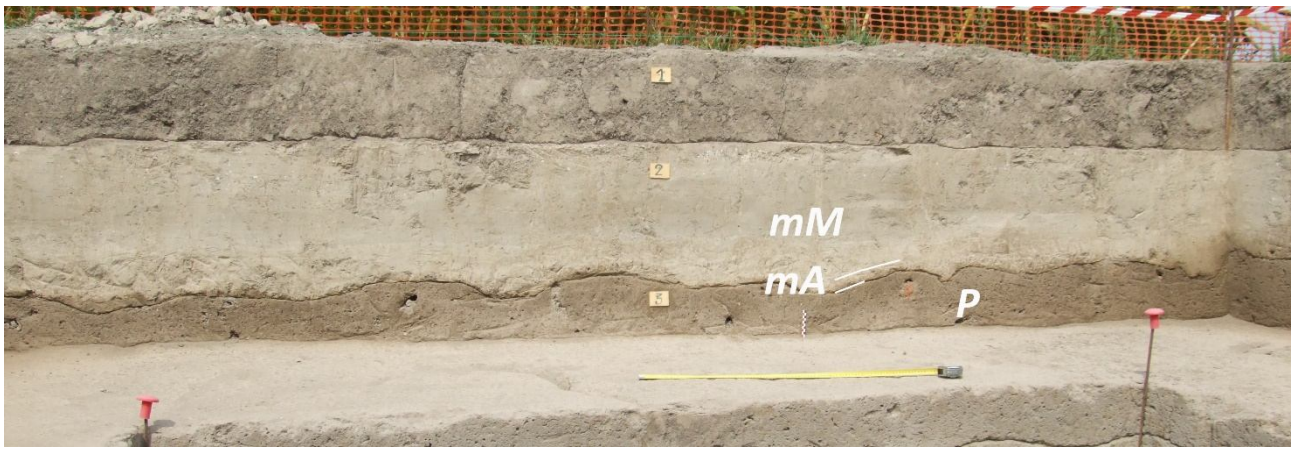
461

462 [a\)](#)



463

464 [b\)](#)



465

466 [c\)](#)

467 [Fig. 7. In these three photos of archaeological excavations \(a-b, Nola; c, Acerra\), the main lithofacies recognized in the](#)  
 468 [field are shown, including paleosols, pyroclastic deposits, and lahar deposits; the corresponding lithofacies descriptions](#)  
 469 [are reported in Tab. 2.](#)

470

471 Usually, the syn-eruptive lahar deposits directly overlie the primary pyroclastic deposits, sometimes  
472 eroding them. They have a matrix-supported texture and are composed of fine to very fine cohesive  
473 ~~cohesive~~ ash, and contain ~~scattered and~~ more or less abundant mm- to cm-sized pumices and lithic  
474 fragments. ~~In general, These deposits are generally composed of~~ consist of multiple depositional  
475 flow units, each one resulting from single-pulse “en masse” ~~transport~~ emplacement, the piling of  
476 which resulting from rapid progressive aggradation through multiple flow pulses, in analogy with  
477 dense pyroclastic currents (Sulpizio et al., 2006; Doronzo, 2012; Roche, 2012, 2015; Breard and  
478 Lube, 2017; Smith et al., 2018; Guzman et al., 2020; see Sulpizio et al., 2014, p. 56) and similarly to  
479 lahar events occurred for example at Ischia (Italy) in 2022 (De Faleo et al., 2023). For  
480 ~~this~~ Consequently, the studied lahars were modelled using a shallow layer approach (de’Michieli  
481 Vitturi et al., this issue). The different depositional flow units in the same deposit are distinguishable  
482 (still in continuity) from each other based on vertical granulometric changes, sparse pumice  
483 alignments, ~~internal lamination~~ deposit layering and/or unconformities. ~~Compared, f~~ For example,  
484 compared with to ~~channeled~~ channeled pyroclastic currents, dense water flows and floods, such  
485 depositional units (layers) could have been repeatedly emplaced, from bottom to top, under  
486 accumulation rates ~~of several~~ of a few tens to ~~a few~~ hundreds kg/m<sup>2</sup>s (Lowe, 1988; Russell and  
487 Knudsen, 1999; Whipple et al., 2000; Girolami et al., 2010; Roche, 2015; Marti et al., 2019; Guzman  
488 et al., 2020). In various areas, ~~the “en masse” transports~~ such rapid sequential emplacement is  
489 suggested by the presence of water escape structures through the whole deposit ~~and~~ by crossing the  
490 sequence of several units. These are vertical structures consisting of small ~~vertical~~ “pipes” filled ~~by~~  
491 with fine mud, transported by the escaping water, and formed soon after the emplacement of the lahar  
492 units. The ~~lithological~~ textural characteristics are variable even within the same site, but in general  
493 the deposits are ~~generally~~ massive, and contain vesicles, from circular to flattened ~~and,~~ coated by fine  
494 ash that adhered into the voids after water evaporation loss. For the syn-eruptive lahar deposits, the  
495 pumice fragments are those of the primary deposits, ~~while.~~ On the other hand, in the upper parts of  
496 the sequences it is not uncommon to find units that contain pumices fragments related to previous

497 eruptions, ~~in particular the~~ (9.0 ka B.P. "Mercato" and ~~the~~ 3.9 ka B.P. "Avellino" Plinian eruptions),  
498 recognizable based on pumice texture and crystal content (Santacroce et al., 2008). In this second  
499 case, these lahar deposits are considered as post-eruptive, meaning that the pyroclastic deposits older  
500 than the two studied sub-Plinian eruptions were progressively involved in an advanced erosion of the  
501 slopes and valleys exposed to weathering for some time, and then were deeply remobilized. Also,  
502 ~~the presence in the sequences~~ of slightly humified surfaces below the lahar deposits or the evidence  
503 trace of human artifacts, such as for example excavations, ~~plowing~~ ploughing, etc.,... are considered  
504 as ~~constraints evidence for of~~ a long period non-without deposition, ~~and; also in this case, the~~ lahars  
505 ~~generation is are~~ considered as post-eruptive. In other words, the similar componentry of the  
506 ~~secondary lahar deposits vs. and primary~~ pyroclastic deposits ~~for related to the two sub-Plinian~~  
507 ~~eruptions, as well as, and the evidence of short-term exposure between these two vertical continuity~~  
508 ~~between the fallout and lahar deposits directly lying on the fallout deposits~~, are strong indicators of  
509 the syn-eruptive occurrence of the lahar events. Instead, the absence of such features is more  
510 indicative of a post-eruptive origin, ~~with i.e.~~ lahars events ~~also~~ more spaced in time from the  
511 corresponding eruption.

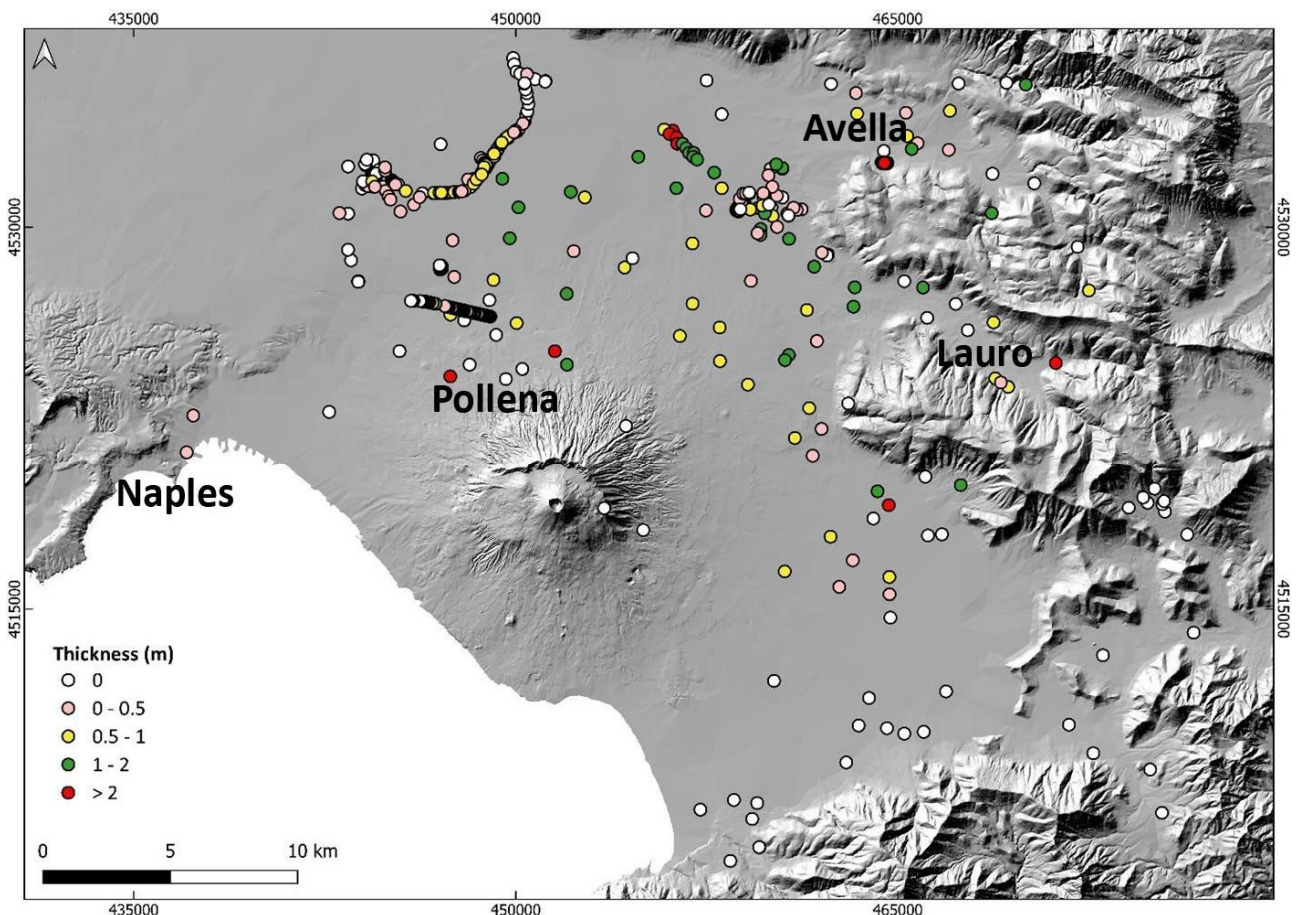
512 In Appendix 3C, a description is reported for some of the most representative sequences, which were  
513 sampled in different areas throughout the plain (Figs. 2 and 4).

514

#### 515 **4.1.3. Distribution maps of the lahar deposits**

516 Here we present ~~the~~ distribution maps for the lahar deposits of the ~~eruption of~~ Pollena and 1631  
517 eruptions (Figs. ~~87-110~~). The maps show the distribution of all thicknesses detected in the studied  
518 sites. In particular, the syn-eruptive Pollena lahar deposits are distributed in the NW quadrants of the  
519 volcano and in the Avella, Lauro and Sarno valleys (see Fig. 1), with a thickness exceeding 1 m in  
520 the Vesuvius apron and in the plain between Nola and Cimitile (see Figs. 1 and 87). A volume  
521 estimation of the remobilized deposits is of the order of  $73 \times 10^6 \text{ m}^3$  for the northern Vesuvius area,

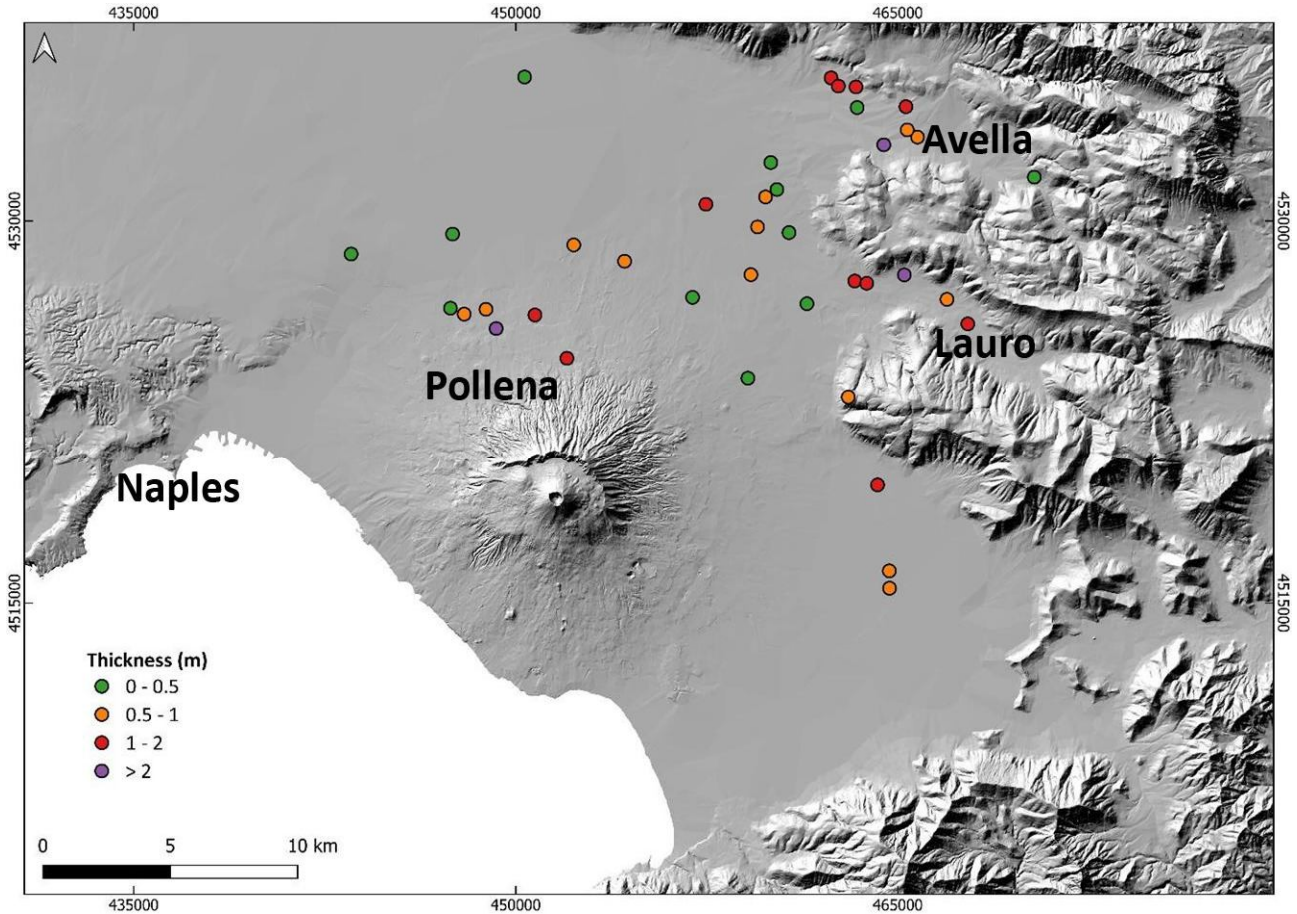
522 and  $42 \times 10^6 \text{ m}^3$  for the Lauro Valley. [Such volumes are referred to the depositional areas, and not to](#)  
 523 [the detachment ones; for the latter see de' Michieli Vitturi et al. \(this issue\) and Sandri et al. \(this](#)  
 524 [issue\). The provenance of the material in each site was inferred by sedimentological recognition and](#)  
 525 [magnetic reconstruction. Then, the covered areas were subdivided into polygons in the geospatial](#)  
 526 [database, in order to weight the local deposit thicknesses and estimate the volumes with a lower](#)  
 527 [approximation.](#)  
 528



529 Fig. 87. Distribution of the syn-eruptive lahar deposits related to the Pollena eruption. [The 0 m points represent the studied](#)  
 530 [sites where the lahar deposits were absent, and in some cases even the primary pyroclastic deposits below were absent;](#)  
 531 [they are reported anyway, as their absence might have not necessarily occurred by no deposition \(local erosion\).](#)  
 532  
 533

534 The post-eruptive [lahar](#) deposits of the Pollena eruption are more ~~concentrated~~ [distributed](#) in the  
 535 Avella and Lauro valleys, and in the plain north of the volcano close to the apron area (low-angle  
 536 edifice outer slopes) (Figs. 1 and 98). Their deposits contain both fragments from the Pollena eruption  
 537 and from preceding eruptions, suggesting that pyroclastic deposits of the older sequences were

538 progressively eroded and involved in remobilization processes over time. As an example, ~~in~~ on Figs.  
539 ~~A3a-d C1-4~~ it is ~~possible to recognize~~ remark that whitish pumice fragments from the Pomici di  
540 Avellino and Mercato eruptions were identified on top of the Pollena lahar deposits.  
541



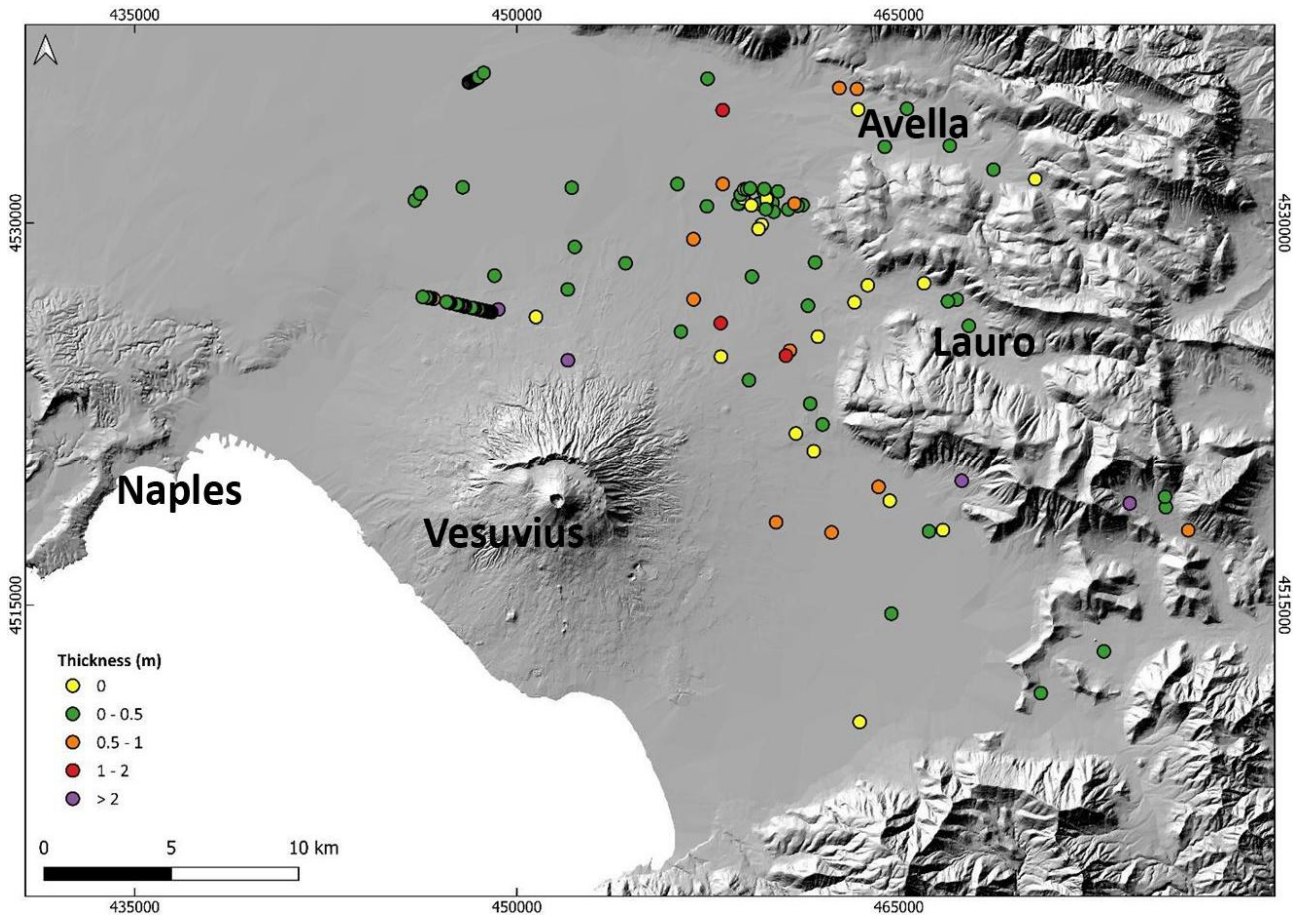
542  
543 Fig. 98. Distribution of the post-eruptive lahar deposits related to the Pollena eruption.

544  
545 The distribution of the syn- and post-eruptive Pollena lahar deposits is related to the primary  
546 pyroclasts deposition: the dense distribution of the lahar deposits north of Somma-Vesuvius depends  
547 on the presence of thick pyroclastic current deposits that were remobilized from the northern slopes  
548 of the volcano, while the distribution in the Apennine valleys is related to the fallout deposits that are  
549 thicker along the major Pollena dispersal axis (Fig. 5).

550 Above the Pollena ~~primary and secondary~~pyroclastic and lahar deposits ~~(meaning after the~~  
551 ~~emplacement of the Pollena lahars)~~ (both syn- and post-eruptive), the studied sequences in almost all  
552 the sites show the presence of a well-developed soil bed with many traces of cultivation, as well as

553 of ~~the presence of~~ inhabited areas and buildings (Figs. ~~A3a-d~~ C1-4). These traces and the presence of  
554 ~~a well-developed~~ the soil bed are evidence of a progressive geomorphological stabilization of the  
555 territory. The occurrence of the 1631 sub-Plinian event determined a new phase of marked  
556 geomorphological instability for a large territory surrounding the volcano. In Fig. 109, it is shown the  
557 distribution of the syn-eruptive lahar deposits for the 1631 eruption in all the studied areas ~~with,~~  
558 having a variable thickness, generally <50 cm. ~~They~~ Such distribution affected mostly the areas of  
559 Acerra-Nola, Sarno, the Vesuvius apron and the Apennine valleys (Figs. 1 and 109). Rosi et al. (1993)  
560 and Sulpizio et al. (2006) reported that floods and lahars heavily impacted (also with injuries and  
561 victims) the N and NE quadrants of Somma-Vesuvius soon after the eruption with a timescale of days  
562 (Rosi et al., 1993; see also the historical chronicles of Braccini, 1632), corroborating the syn-eruptive  
563 behavior of such lahars. ~~Furthermore s~~ Some lahar deposits are ~~also~~ intercalated within the primary  
564 pyroclastic deposits, ~~while but in~~ generally they directly stand ~~in continuity~~ on top of the primary  
565 pyroclastic deposits (Rosi et al., 1993); both cases unequivocally constrain the syn-eruptive behavior  
566 of the 1631 eruption lahars.





568

569

570

571

572

573

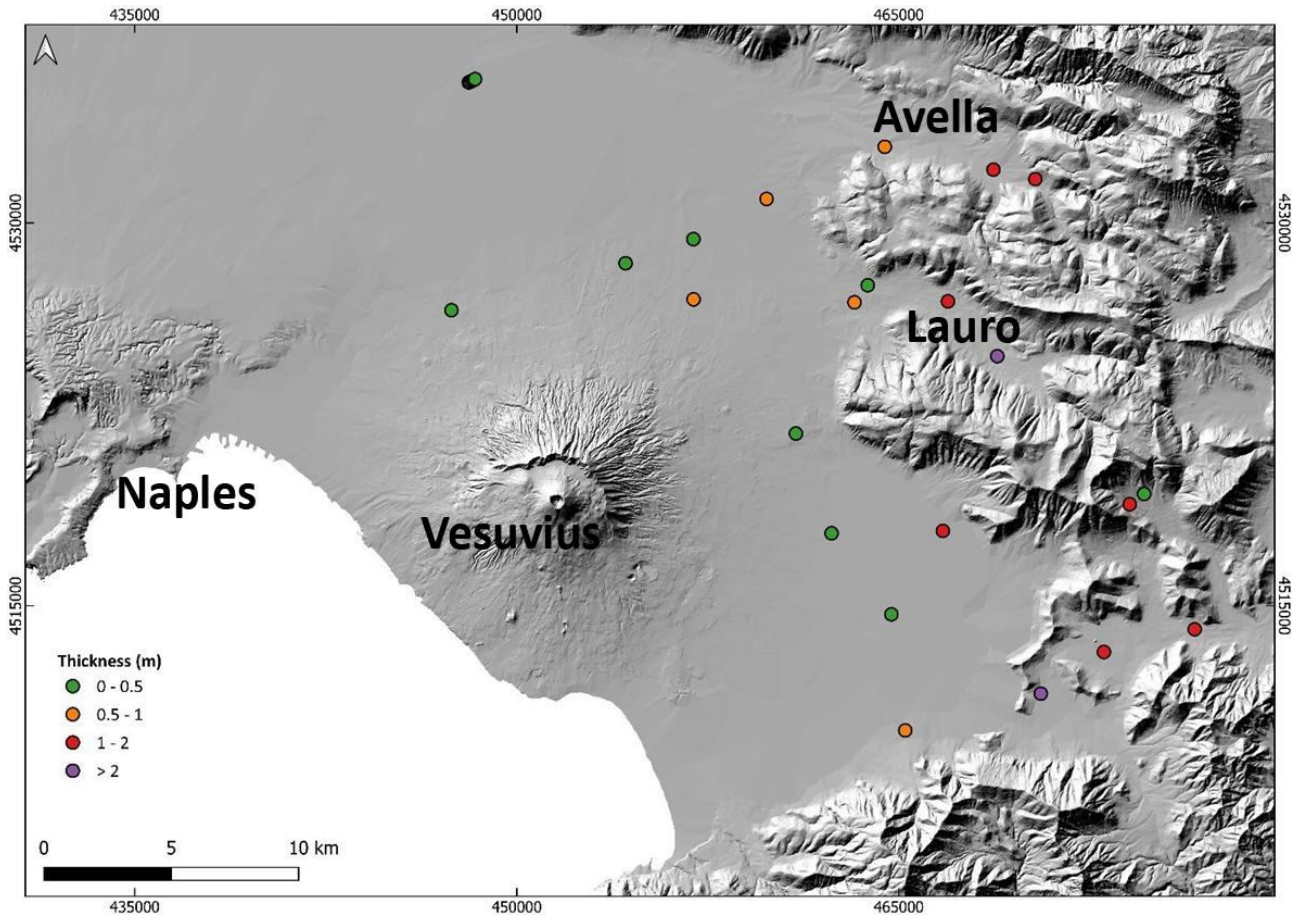
574

575

576

Fig. 109. Distribution of the syn-eruptive lahar deposits related to the 1631 eruption. [The 0 m points represent the studied sites where the lahar deposits were absent, and in some cases even the primary pyroclastic deposits below were absent; they are reported anyway, as their absence might have not necessarily occurred by no deposition \(local erosion\).](#)

[In Fig. 110, M](#)minor post-eruptive lahar deposits of the 1631 eruption are reported [in Fig. 10](#), with a preferential distribution to the E quadrants of the volcano from N to S, both in the plain and the valleys. These deposits are still significant, with a thickness of around half a meter to a meter or more in a few points.



578  
579 Fig. 110. Distribution of the post-eruptive lahar deposits related to the 1631 eruption.

580

581 The distribution of the syn- and post-eruptive 1631 lahar deposits mainly reflects the major dispersal  
 582 axis affecting the fallout deposits distribution, while the pyroclastic current deposits were minorly  
 583 remobilized as exposed on the gentler slopes of southwestern Vesuvius (Fig. 6).

584

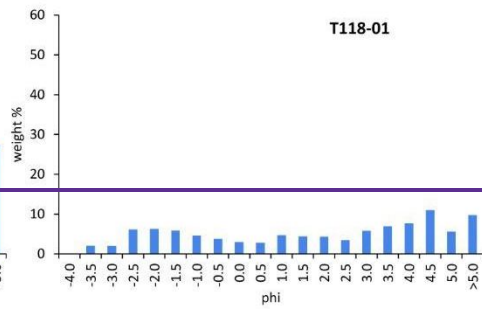
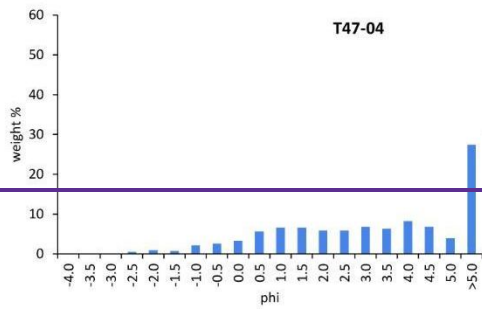
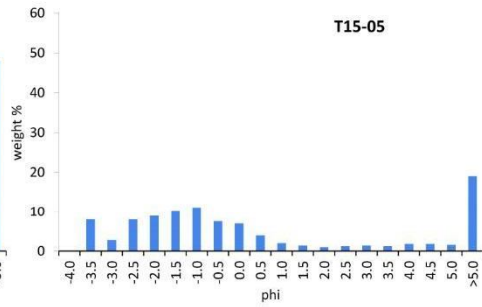
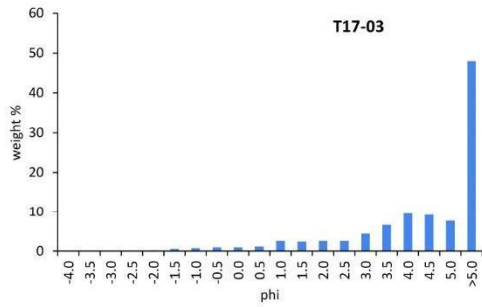
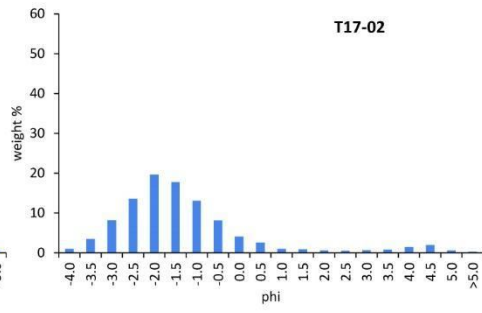
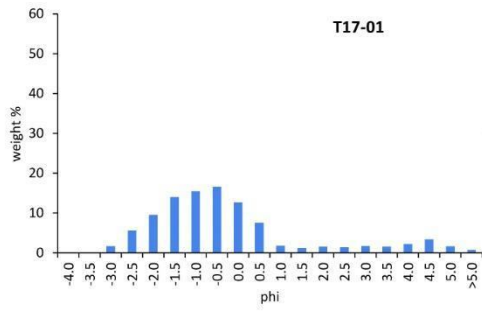
#### 585 4.1.4. Sedimentological characteristics of the Pollena lahar deposits

586 The field analysis was carried out ~~on-in~~ about 500 ~~studied-different~~ sites for the construction of the  
 587 database and maps, and-while the laboratory analysis ~~carried-out~~ was carried out on 30 ~~selected~~  
 588 representative samples representative of the different areas-contribute; ~~both analyses contributed to~~  
 589 ~~the distinction between syn- and post-eruptive lahars in the area.~~ The results of the grain-size analyses  
 590 in the form of (histograms-cumulative curves and statistical parameters) are presented in Fig. 121 and

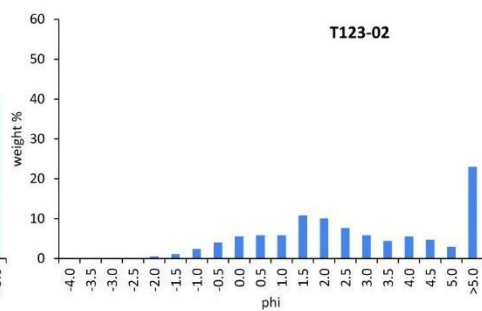
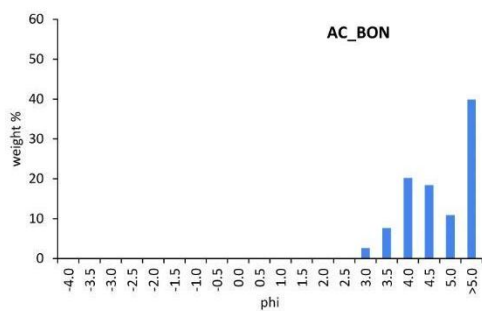
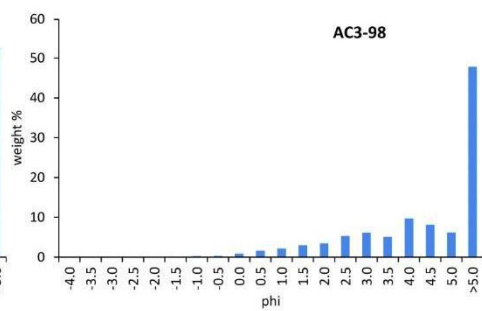
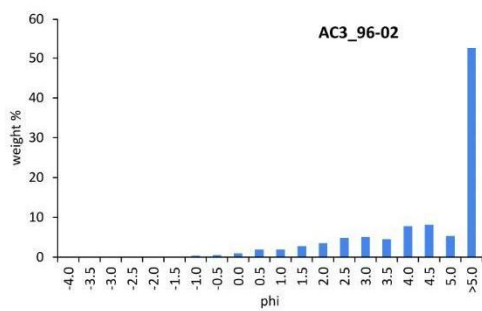
591 Tab. 1.

592 Petrological analysis on the syn-eruptive lahar deposits have not been performed because the  
593 lithology (colour, texture, mineral content) of the components is the same as the juvenile material of  
594 the primary deposits (more details can be found described in Sulpizio et al., (2005). The loose crystals  
595 consist of sanidine, leucite, biotite and pyroxene fragments. Based on the results of the grain-size  
596 analyses-distributions of the samples, the coarser classes are defined from -4 to -1 phi, the medium  
597 ones-are from -0.5 to 2.5 phi, and the finest one-are from 3 phi. The juvenile pumice clasts are an  
598 ubiquitous component of the lahar deposits (both syn- and post-eruptive), but they decrease with  
599 distance toward-for the finer grain-size classes, while the crystal content increases in-with the same  
600 progression. The lithic clasts are abundant in-for the coarser classes, they decrease with distance in  
601 for the middle-medium grain-size classes, and increase again in-for the finer classes.

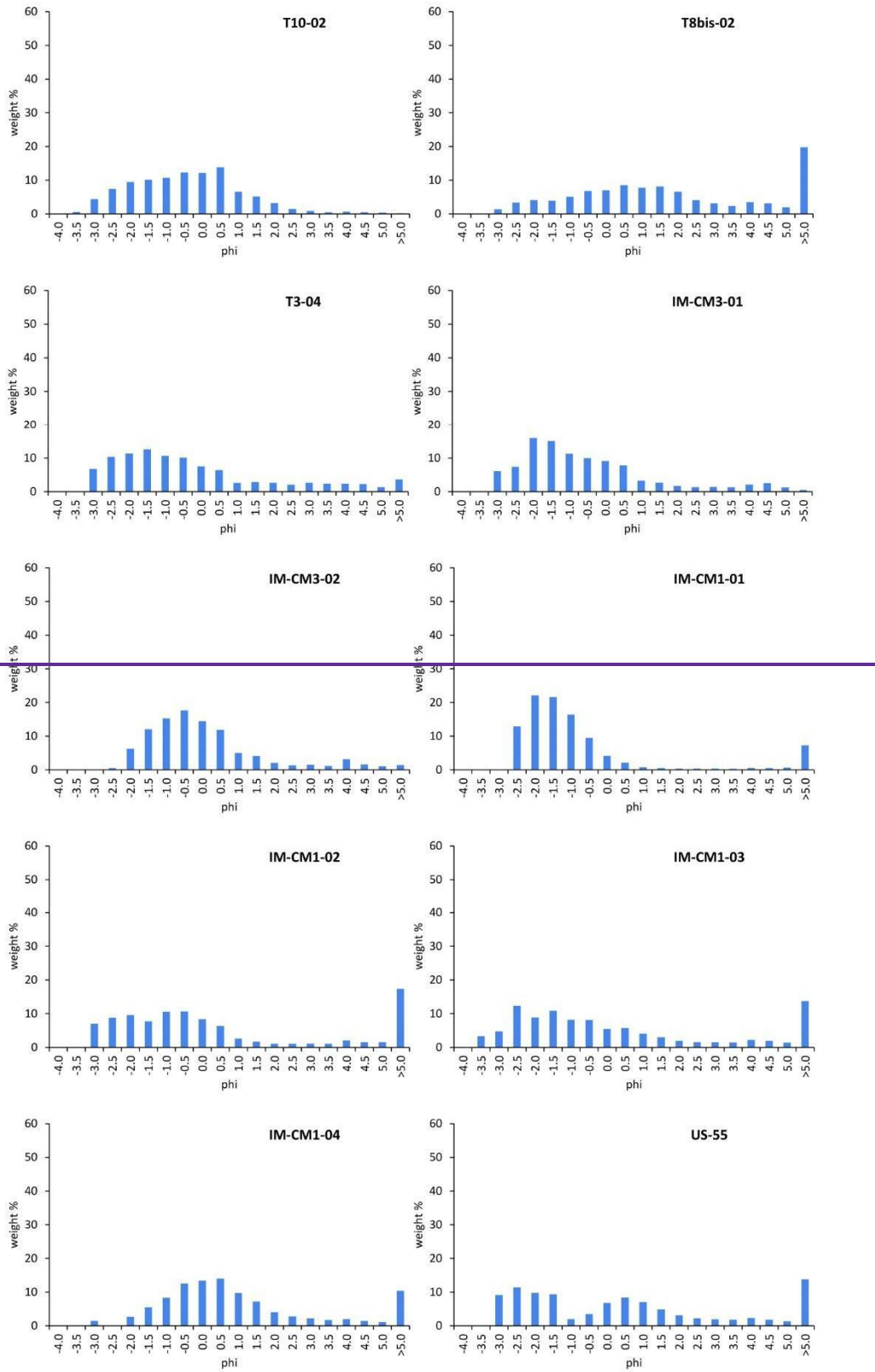
## Vallo di Lauro



## Somma-Vesuvius



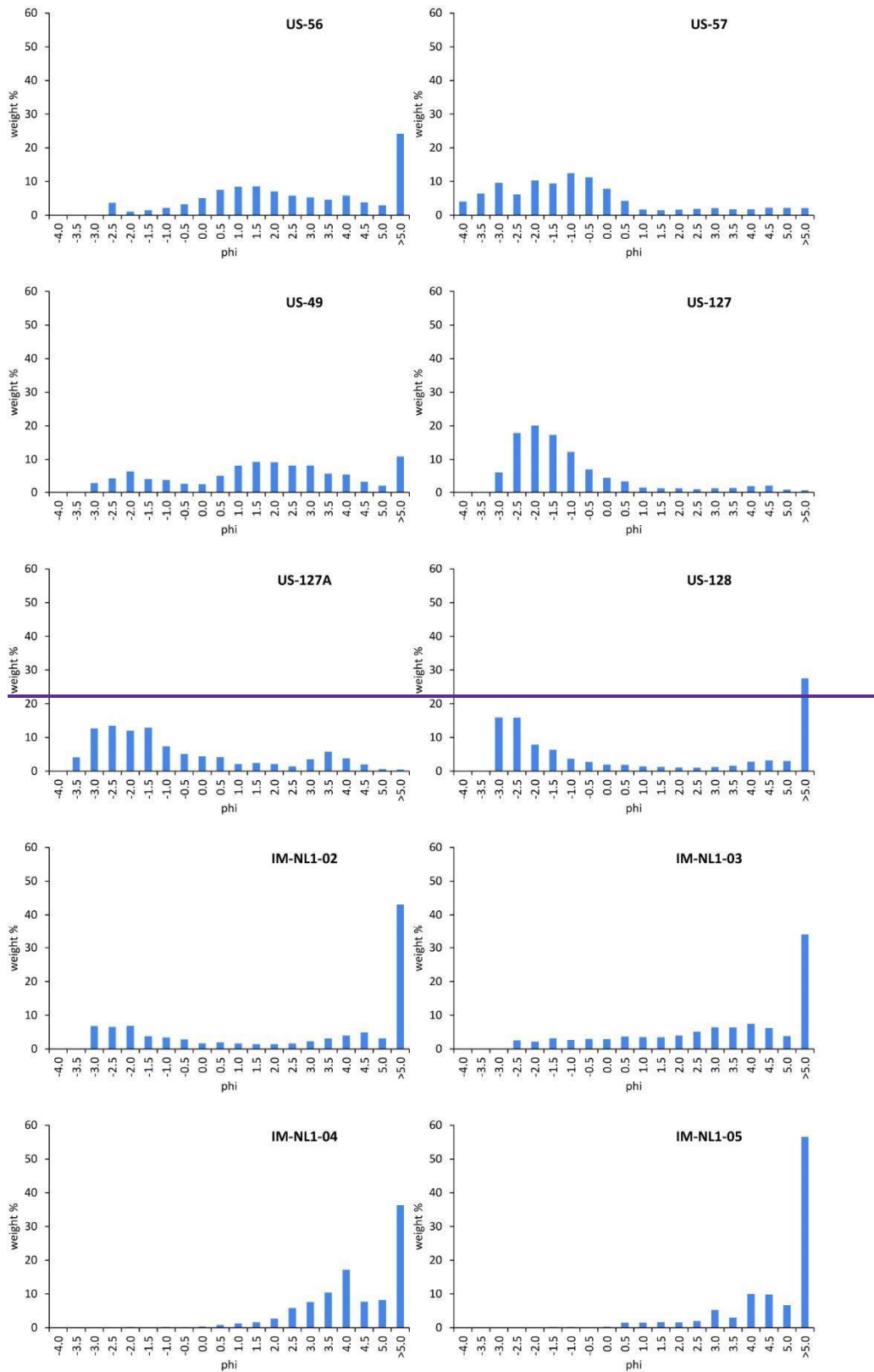
# Valle di Avella



603

604

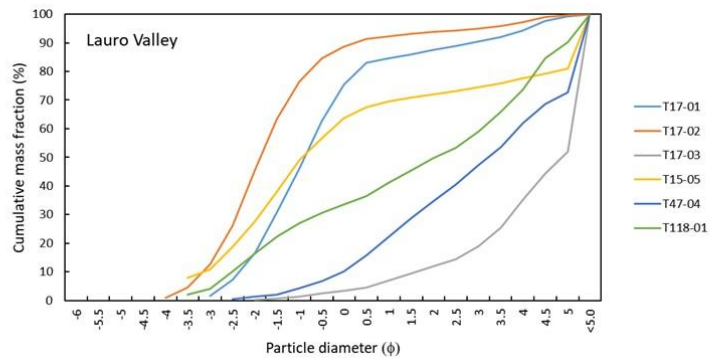
605



606

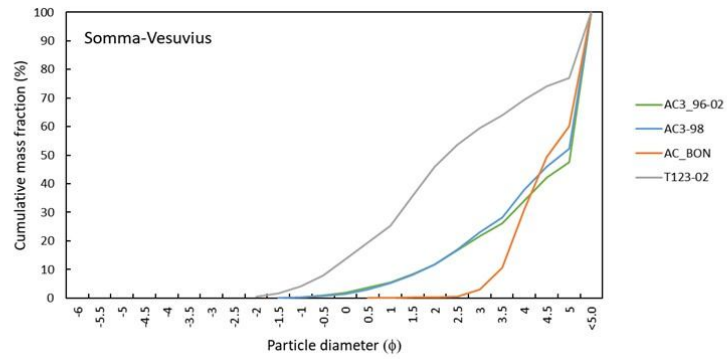
607

Fig. 11. Histograms of the grain-size analysis on selected samples for the locations reported in Fig. 4.



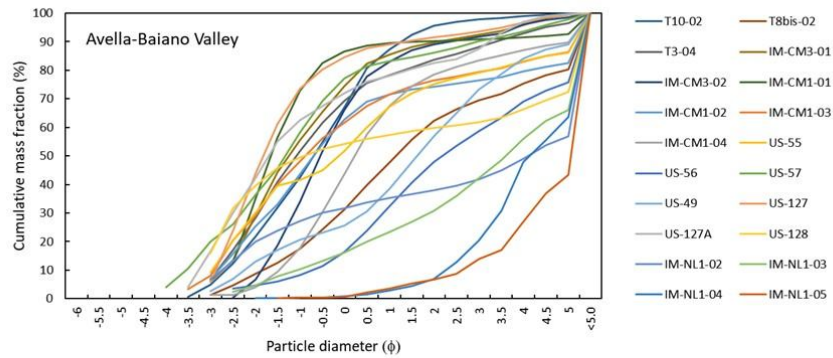
608

---



609

---



610

611 Fig. 12. Cumulative curves of the grain-size analysis on the samples taken at the locations reported in Fig. 4, and  
 612 subdivided in three sectors: Lauro Valley (top), Somma-Vesuvius (middle), and Avella-Baiano Valley (bottom).

613

<u>Site</u>	<u>Distance from Mt. Somma rim</u>
<u>T17</u>	<u>12.8 km</u>
<u>T15</u>	<u>15 km</u>
<u>T47</u>	<u>7.6 km</u>
<u>T118</u>	<u>9.9 km</u>
<u>AC3_96</u>	<u>15 km</u>
<u>AC3_98</u>	<u>13 km</u>
<u>AC_BON</u>	<u>11.5 km</u>
<u>T123</u>	<u>6.5 km</u>
<u>T10</u>	<u>18 km</u>
<u>T8bis</u>	<u>18.4 km</u>
<u>T3</u>	<u>19.1 km</u>



614

<a href="#"><u>IM-CM3</u></a>	<a href="#"><u>14.3 km</u></a>
<a href="#"><u>IM-CM1</u></a>	<a href="#"><u>14 km</u></a>
<a href="#"><u>US-55</u></a>	<a href="#"><u>13.6 km</u></a>
<a href="#"><u>US-128</u></a>	<a href="#"><u>13.6 km</u></a>
<a href="#"><u>IM-NL1</u></a>	<a href="#"><u>13 km</u></a>

SAMPLE	MODE 1	MODE 2	MODE 3	SKEWNESS	SORTING	FACIES
<b>Lauro Valley</b>						
T17-01	-0.743			1.179	1.464	Gms
T17-02	-2.243			1.532	1.404	Gms
T17-03	0.747	3.731		-1.054	1.481	Sh
T15-05	-3.743	-1.243	3.731	0.890	1.752	Gms
T47-04	1.247	3.731		-0.447	1.579	Mm
T118-01	-2.243	0.747	3.731	-0.049	2.352	Gms
<b>Avella-Baiano Valley</b>						
T10-02	0.247			0.274	1.457	Sh
T8bis-02	-2.243	0.247	1.247	-0.009	1.742	Sh
T3-04	-1.743	1.247	3.237	0.881	1.789	Gms
IM-CM3-01	-2.243			1.015	1.587	Gms
IM-CM3-02	-0.743	3.731		1.134	1.379	Gms
IM-CM1-01	-2.243			1.954	1.010	Gms
IM-CM1-02	-2.243	-1.243	3.731	0.932	1.633	Gms
IM-CM1-03	-2.743	-1.743	0.247	0.810	1.809	Gms
IM-CM1-04	0.247			0.406	1.394	Fm
US-55	-2.743	0.247	3.731	0.495	1.941	Gms
US-56	-2.743	1.247	3.731	-0.402	1.700	Sh
US-57	-3.243	-2.243	-1.243	0.756	1.860	Gms
US-49	-2.243	1.247		-0.460	2.012	Gms
US-127	-2.243			1.686	1.507	Gms
US-127A	-2.743	-1.743	3.237	0.914	2.167	Gms
US-128	-3.243	3.731		1.434	1.990	Gms
IM-NL1-02	-3.243	-2.243	3.731	0.609	2.378	Gms
IM-NL1-03	-1.743	0.247	3.731	-0.458	1.996	Gms
IM-NL1-04	3.731			-1.698	0.995	Mm
IM-NL1-05	1.247	2.737	3.731	-1.137	1.224	Mm
<b>Somma-Vesuvius</b>						
AC3_96-02	0.247	2.237	3.731	-0.734	1.245	Mm
AC3-98	2.737	3.731		-0.838	1.197	Mm
AC_BON	3.731			-3.026	0.425	Mm
T123-02	0.247	1.247	3.731	-0.228	1.420	Mm

615

<u>Sample</u>	<u>Mean (<math>\phi</math>)</u>	<u>Sorting (<math>\phi</math>)</u>	<u>Lithofacies</u>
<u>Lauro Valley</u>			
<u>T17-01</u>	<u>-0.93</u>	<u>1.41</u>	<u>Gms</u>
<u>T17-02</u>	<u>-1.83</u>	<u>1.23</u>	<u>Gms</u>
<u>T17-03</u>	<u>2.42</u>	<u>1.46</u>	<u>Sh</u>

<u>T15-05</u>	<u>-1.39</u>	<u>1.74</u>	<u>Gms</u>
<u>T47-04</u>	<u>1.67</u>	<u>1.61</u>	<u>Mm</u>
<u>T118-01</u>	<u>1.13</u>	<u>2.7</u>	<u>Gms</u>
<b><u>Avella-Baiano Valley</u></b>			
<u>T10-02</u>	<u>-0.78</u>	<u>1.47</u>	<u>Sh</u>
<u>T8bis-02</u>	<u>0.31</u>	<u>1.83</u>	<u>Sh</u>
<u>T3-04</u>	<u>-0.95</u>	<u>1.83</u>	<u>Gms</u>
<u>IM-CM3-01</u>	<u>-1.13</u>	<u>1.54</u>	<u>Gms</u>
<u>IM-CM3-02</u>	<u>-0.48</u>	<u>1.35</u>	<u>Gms</u>
<u>IM-CM1-01</u>	<u>-1.66</u>	<u>0.86</u>	<u>Gms</u>
<u>IM-CM1-02</u>	<u>-1.17</u>	<u>1.62</u>	<u>Gms</u>
<u>IM-CM1-03</u>	<u>-1.13</u>	<u>1.83</u>	<u>Gms</u>
<u>IM-CM1-04</u>	<u>0.06</u>	<u>1.39</u>	<u>Fm</u>
<u>US-55</u>	<u>-0.84</u>	<u>1.97</u>	<u>Gms</u>
<u>US-56</u>	<u>1.17</u>	<u>1.8</u>	<u>Sh</u>
<u>US-57</u>	<u>-1.51</u>	<u>1.86</u>	<u>Gms</u>
<u>US-49</u>	<u>0.69</u>	<u>2.16</u>	<u>Gms</u>
<u>US-127</u>	<u>-1.66</u>	<u>1.39</u>	<u>Gms</u>
<u>US-127A</u>	<u>-1.02</u>	<u>2.23</u>	<u>Gms</u>
<u>US-128</u>	<u>-1.72</u>	<u>1.91</u>	<u>Gms</u>
<u>IM-NL1-02</u>	<u>-0.5</u>	<u>2.49</u>	<u>Gms</u>
<u>IM-NL1-03</u>	<u>1.25</u>	<u>2.1</u>	<u>Gms</u>
<u>IM-NL1-04</u>	<u>2.99</u>	<u>0.89</u>	<u>fM</u>
<u>IM-NL1-05</u>	<u>2.64</u>	<u>1.20</u>	<u>fM</u>
<b><u>Somma-Vesuvius</u></b>			
<u>AC3_96-02</u>	<u>2.37</u>	<u>1.26</u>	<u>mM</u>
<u>AC3-98</u>	<u>2.48</u>	<u>1.2</u>	<u>mM</u>
<u>AC BON</u>	<u>3.52</u>	<u>0.38</u>	<u>mM</u>
<u>T123-02</u>	<u>1.37</u>	<u>1.5</u>	<u>mM</u>

616

617 Tab. 34. Statistical parameters (mean and sorting) extracted from the grain-size analyses, and reference lithofacies (see  
618 Tab. 2 for descriptions). ~~Mode 1, 2 and 3 indicate the coarsest, medium and fine modes, respectively. Mode 1, 2 and 3~~  
619 ~~represent the most frequently occurring grain size classes.~~

620

621 Field observations and ~~statistical granulometric grain-size parameters analyses~~(modes, skewness,  
622 ~~sorting~~), highlight significant differences between the sectors of Lauro Valley, Avella-Baiano Valley,  
623 and Somma-Vesuvius. A common feature between the three sectors is that the lahar deposit samples  
624 are mostly massive, poorly-sorted and ~~polimodal~~polymodal; only a few samples are moderately-  
625 sorted and unimodal (~~more than one grain size are present but one prevails~~sorting <1.5 phi). On the

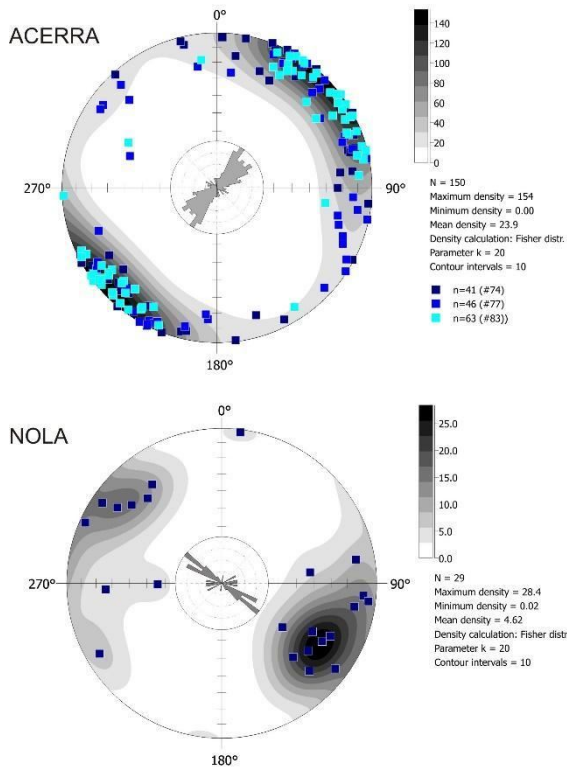
626 other hand, the grain-size modes ~~extracted-found~~ show some interesting differences (in Fig. 12 the  
627 cumulative curves are shown). The coarse modes for Lauro Valley and Avella-Baiano Valley span  
628 from fine/medium lapilli to coarse ash, while for Somma-Vesuvius span from coarse to fine ash. The  
629 medium modes for Lauro Valley and Avella-Baiano Valley span from coarse to medium ash, while  
630 for Somma-Vesuvius span from medium to fine ash. The fine modes for Lauro Valley and Avella-  
631 Baiano Valley, and for Somma-Vesuvius span from medium to fine ash. ~~Also, the skewness values~~  
632 ~~for Lauro Valley and Avella-Baiano Valley show a fine to coarse mode while for Somma-Vesuvius~~  
633 ~~show a coarse code.~~ All these differences basically depend on the origin of the primary pyroclastic  
634 deposits, fallout vs. pyroclastic currents, which were remobilized from different sectors, Apennines  
635 and Somma-Vesuvius. The grain-size analysis ~~of the above described granulometry~~ is used ~~to~~  
636 informs an input information for the ~~model of~~ lahar transport model (de' Michieli Vitturi et al.,  
637 submitted this issue) aimed at assessing the related hazard (Sandri et al., submitted this issue).

638

#### 639 **4.2. Magnetic results**

640 Both Acerra and Nola localities show a well-defined magnetic fabric for the (Pollena syn-eruptive  
641 lahar deposits, irrespective of being syn- or post-eruptive). Principal susceptibility axes ( $K_1 > K_2 > K_3$ )  
642 are clustered, Magnetic lineation ( $K_1$ ) and magnetic foliation ( $K_3$ , pole of the plane) are mostly sub-  
643 horizontal or gently emblicated, and (The magnetic The anisotropy degree  $P_j$  ( $K_1/K_3$ ) is mostly lower  
644 than 1.060, but can reach high values ( $P = \text{like } 1.200$ )). At Acerra, the magnetic foliation is always  
645 dominant, and the fabric is oblate. The  $P_j$  is linearly correlated to the mean susceptibility ( $k_m$ ). In  
646 Appendix B, the full nomenclature is defined for completeness. The magnetic fabric has a horizontal  
647 magnetic foliation and a clustered magnetic lineation, whose mean direction is NE-SW. Considering  
648 the chaotic nature of the lahar deposits, the high  $P_j$  and the clustered susceptibility axes can highlight  
649 a channelized flow (Fig. 132). At Nola, instead, the fabric is both prolate/oblate, and  $P_j$  is lower than  
650 1.040. The susceptibility axes are more dispersed than Acerra, but mean magnetic lineation clearly

651 shows a NW-SE direction. If one considers the oblate specimens only, the magnetic foliation is sub-  
 652 horizontal, on the contrary, the magnetic foliation of the prolate specimens is steeply dipping ( $65^\circ$ )  
 653 toward SE. At Nola, the flow direction inferred by AMS is consistent and parallel to the invasion  
 654 basin.

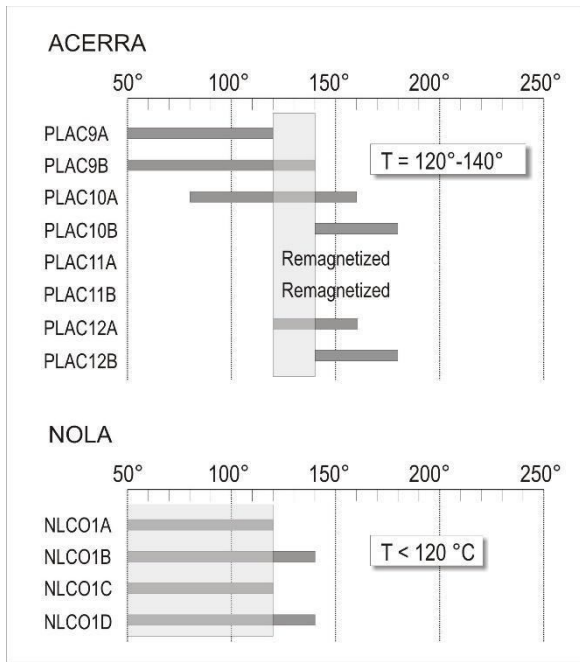


655

656 Fig. 132. Equal area projection and Rose diagram of the  $K_1$  directions at Acerra and Nola.

657

658 ~~The deposition temperature is low at both deposits.~~ At Acerra the  $T_{\text{dep}}$  interval is 120-140 °C, while  
 659 for Nola  $T_{\text{dep}}$  is lower than 120 °C (Fig. 143). In the Nola case, a low temperature magnetization  
 660 component lower than 120 °C cannot be directly considered as a TRM. In fact, the low  $T_b$  Earth's  
 661 field component of magnetization can also be produced by a viscous remanent magnetization (VRM),  
 662 acquired during exposure to weak fields (Bardot and McClelland, 2000). The acquisition of the VRM  
 663 depends on the duration of the exposure. For age around that of the Pollena eruption, the minimum  
 664  $T_{\text{dep}}$  which can be distinguished is ca. 120 °C. For this reason, we considered the Nola lahar to be  
 665 emplaced at low temperature.



666

667 Fig. 143. Deposition temperature at Acerra and Nola. The site  $T_{\text{dep}}$  is estimated from the overlapping reheating  
 668 temperature ranges for all lithic clasts sampled.

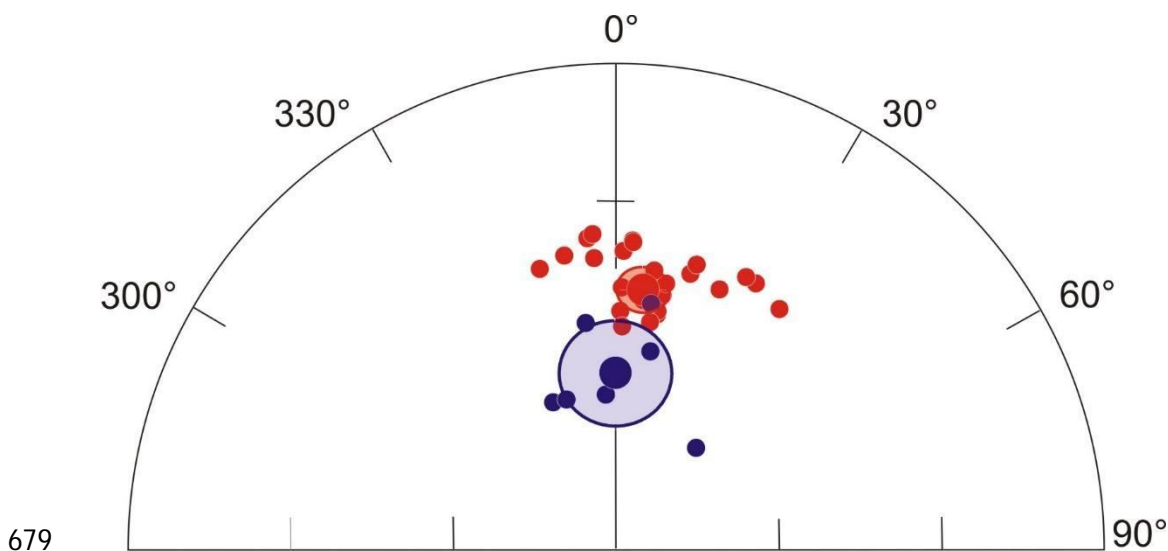
669

670 The mean paleomagnetic direction for each locality, calculated using Fisher's statistics, is well-  
 671 defined, and its directional value and confidence limits do not overlap (Fig. 154). Thus, the two  
 672 directions-and-is-are statistically distinguishable at the 95% confidence limits (Fig. 14). Since a  
 673 paleomagnetic direction is a record of the Earth's magnetic field acting during the emplacement, it  
 674 follows that-Therefore, the lahar deposits of-at these two localities are not synchronous.

675 Overall, all magnetic measurements just discussed show distinctly different characters between  
 676 Acerra and Nola, clearly indicating two distinct events of emplacement.

677

678



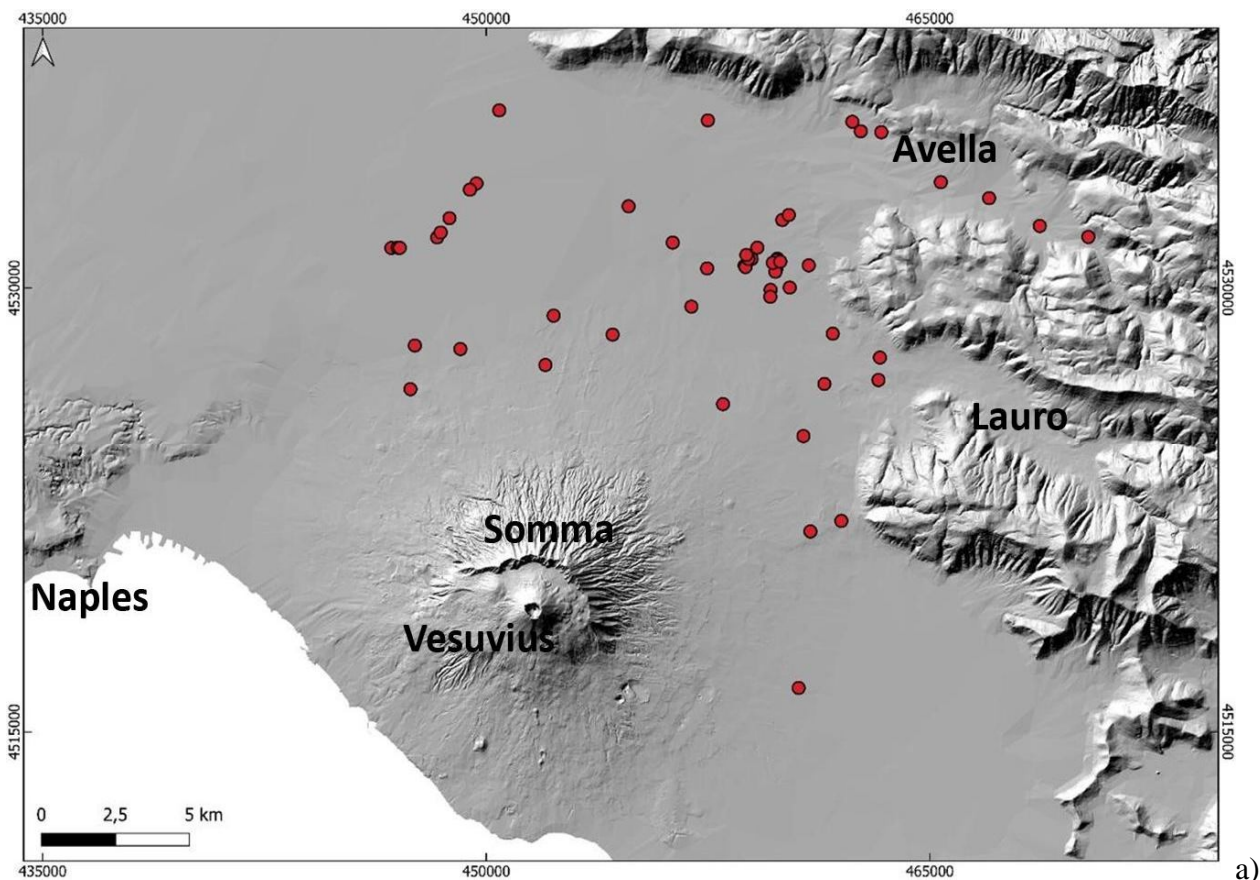
679  
 680 Fig. 154. Equal-area projection of the characteristic remanent magnetization directions, and their mean value with  
 681 associated confidence limit, from Acerra (red dots, mean value:  $n=26$   $D=7.5^\circ$ ,  $I=43.4^\circ$ ,  $\alpha_{95}=3.5^\circ$ ), and Nola (blue  
 682 dots, mean value:  $n=7$ ,  $D=0.8^\circ$ ,  $I=60.2^\circ$ ,  $\alpha_{95}=9.0^\circ$ ).

683

### 684 4.3. Lahar dynamics

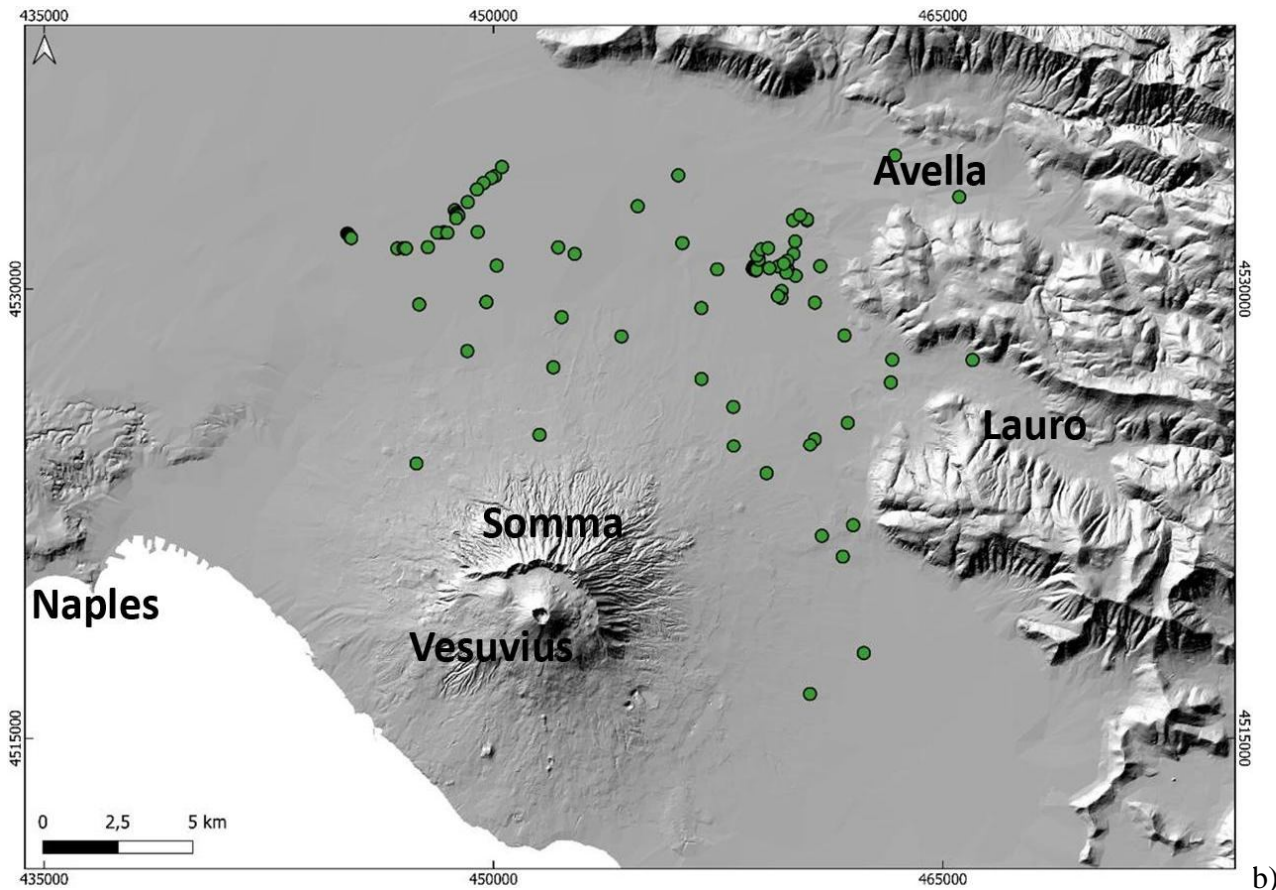
685 By inverting the field evidence and data, it is possible to reconstruct the macroscopic flow dynamics  
 686 that occurred in the lahar invasion, which are particularly interesting to understand the impact that  
 687 those lahars had on the Vesuvius territory. As already described, the lahar deposits show thicknesses  
 688 that are variable from several centimeters to a few meters, and this can depend on multiple local  
 689 factors: i) topography; ii) distance from source; iii) erosion; iv) source area and type of remobilized  
 690 sediment (variably sized fallout vs. flow deposits). In particular, thicker deposits are found near the  
 691 mouth of the valleys and in the flat alluvial plain, as shown in the deposit distribution maps. On the  
 692 other hand, the deposits show ~~on the whole~~ a general tabular-like shape (Fig. 7), ~~and the~~ with an  
 693 average thickness ~~is~~ of the order of 0.5-1 m recurrent for several studied sites, which is the first  
 694 evidence of the lahars impact and mass flow emplacement in the area. In terms of runout distance,  
 695 the lahars travelled for 10 to 15 km from sources (Somma-Vesuvius and Apennine detachment areas),  
 696 ~~measured directly on the deposit distribution maps~~ based on the geospatial database that includes all  
 697 studied sites. It was possible to infer the source areas based on the common sedimentological features

698 of the lahar deposits between nearby sites. On the other hand, distant sites with sedimentologically  
699 different deposits were fed from different source areas. These important ~~quantitative~~ constraints are  
700 used to validate and inform lahar numerical models (de' Michieli Vitturi et al., submittedthis issue)  
701 and simulations (Sandri et al., submittedthis issue) using a shallow layer approach for hazard  
702 assessment. We cannot rule out that lahar pulses from different source areas (Somma-Vesuvius vs.  
703 Apennines) might have overlapped and further aggraded in the open plain.  
704 At several locations, we found ~~erosive-erosional~~ unconformities ~~between~~ (Fig. 165a) between the  
705 lower and upper flow units (Fig. 165b), as well as between ~~primary-the~~ pyroclastic ~~deposits~~ and lahar  
706 ~~unitsdeposits~~. Erosion is an important factor for the entrainment of pre-existing material and objects,  
707 which ~~includeing~~ large-size clasts external to the remobilized pyroclastic material. Size and density  
708 of the largest clasts embedded in the deposits can give an idea of the carrying capacity of the lahars.  
709



710





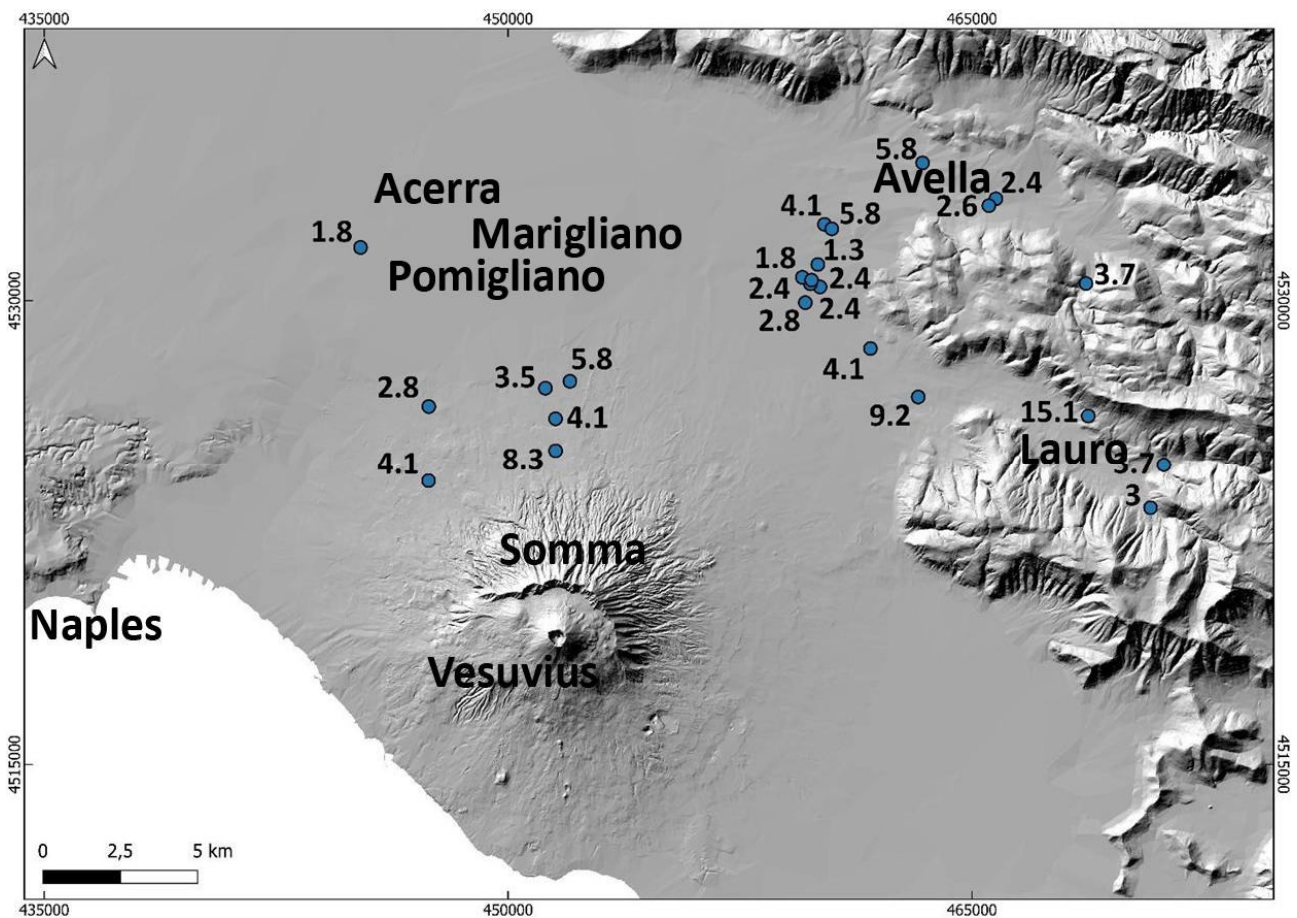
711

712 Fig. 165. a) Sites with evident erosion traces at the base of the lahar units; b) Sites in which multiple depositional flow  
 713 units are vertically identified. Both evidences corroborate the interpretation of the depositional mechanisms, as well as  
 714 constrain the choice of the shallow layer approach for the lahar models and simulations (de'Michieli Vitturi et al., this  
 715 issue; Sandri et al., this issue).

716

717 Evidence Occurrences of oversize-large clasts and boulders -are observed-reported in all the studied  
 718 areas invaded by the lahars, with a distribution that is similar to follows the one of the lahar deposits  
 719 themselves (but with less proportions), and in particularly both are found at the mouth of the valleys,  
 720 and in the alluvial plain (Fig. 15a). The presence of the erosional features (Fig. 16a), and the fact that  
 721 the deposits are ubiquitously mostly composed of massive and relatively thick units (Fig. 16b),  
 722 suggest that high sediment transport and deposition were not exclusive processes both occurred, i.e.  
 723 they both occurred even at local scale in the same area (Doronzo and Dellino, 2013; Roche, 2015).  
 724 Such occurrences of erosion and accumulation of multiple units were useful to inform the lahar  
 725 modelling of de'Michieli Vitturi et al. (this issue).

726 We calculated local velocities of the syn- and post-eruptive lahars based on the biggest clasts that are  
 727 found in the deposits at various stratigraphic heights, with boulder dimensions from several  
 728 centimeters to a meter, and for flow density  $\geq$  water density (Appendix 4A). The faster the lahar the  
 729 higher the capability of its flow to entrain bigger external clasts. This occurred at locations where  
 730 such clasts were freely available on the substrate, or where the lahars impacted and damaged  
 731 anthropogenic structures.  
 732



733 Fig. 176. Average lahar velocities (in m/s) estimated with a point-by-point reverse engineering approach.  
 734

735  
 736 Then, we used the flow velocities (Fig. 176) to calculate local dynamic pressures of the lahars (Fig.  
 737 187) as a function of the clast properties (size, density and shape). The obtained estimations are used  
 738 by Sandri et al. (submitted this issue) to validate the pProbabilistic hHazard aAssessment of lahars  
 739 from Vesuvius eruptions.  
 740

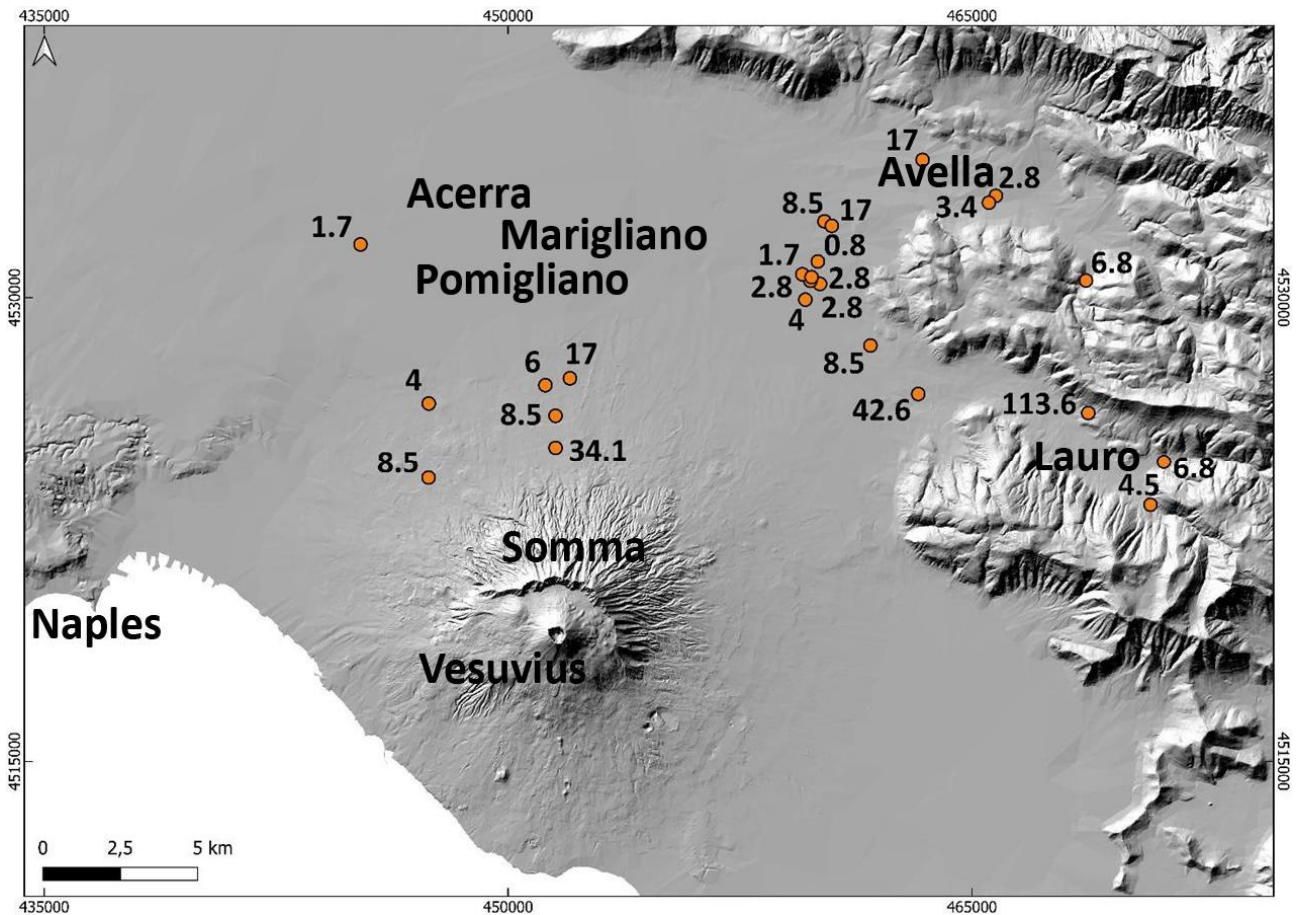


Fig. 187. Average lahar dynamic pressures (in kPa) estimated with a point-by-point reverse engineering approach.

741  
742  
743

744 The data presented in Figs. 176 and 187 represent respectively minimum local values of the flow  
 745 velocity and dynamic pressure, respectively, useful to assess some minimum impact of the lahars in  
 746 the alluvial plain. An approximation of this point-by-point approach is that the values were calculated  
 747 for the finding locations of the clasts in the deposits, meaning that the values are overestimated for  
 748 those exact locations, while they should more properly be referred to the immediate surroundings  
 749 upstream. ~~In particular, w~~We did a parametric test to quantify the sensitivity for different physical  
 750 states of the multiphase flow; depending on initial fluidization and flow density, and considering two  
 751 end members, from a non-fluidized case to an initially fluidized and non-expanded case (see  
 752 Appendix 4A; Roche et al., 2013). From the performed analysis ~~(see Appendix 4)~~, we found that the  
 753 most typical values are referred to the initially fluidized and slightly expanded case (that is a few %  
 754 more expanded than the non-expanded case), with most of the points falling in the range of velocity

755 of 2-4 m/s, and dynamic pressure of 4-8 kPa.

756 Lastly, in eight ~~points-locations~~ we found the lahar deposits ~~emplaced~~ against meter-sized obstacles,  
757 from which we estimated, by comparison, local flow heights of the order of 1-1.5 m, and particle  
758 volumetric concentrations of ~30% or more, i.e. the deposit thickness is ~1/3 of the lahar thickness  
759 ~~(cf. Capra et al., 2018). On the other hand, it is reasonable to argue that these are local values, and~~  
760 ~~that flow height, particle concentration, and deposit thickness significantly varied over space due to~~  
761 ~~the multiphase nature of the lahars (see de' Michieli Vitturi et al., submitted; Sandri et al., submitted).~~

762

## 763 5. Discussion

764 The historical sources used as benchmark for ~~the problem of the~~ lahars around Somma-Vesuvius and  
765 in the Apennine valleys remark the frequent and broad impact that explosive eruptions of Vesuvius  
766 had in historical times. Some of the eruptions ~~occurred~~ in the last four centuries (e.g., 1631, 1822,  
767 1906 and 1944) ~~reached contemporaneously and repeatedly over time~~ impacted on a number of  
768 municipalities ~~due to the explosive character of the events~~, particularly ~~in~~ during the sub-Plinian  
769 eruption of 1631. Heavy rain events caused remobilization of the primary pyroclastic deposits,  
770 triggering multiple lahars during or immediately after the eruption up to a few years (syn-eruptive  
771 lahars; Sulpizio et al., 2006); post-eruptive lahars were triggered on the longer term.

772 On the other hand, the ~~472~~ Pollena eruption had an even wider impact, both in terms of primary  
773 pyroclastic deposition and secondary (lahar) impact. For this event, the historical sources are scarce  
774 ~~or to~~ absent.

775 The analysis of – and realization of a database with – more than 500 stratigraphic sections were done,  
776 which also includes the sedimentological features ~~both~~ of primary (fall, flows) and secondary (the  
777 lahars, alluvial events) deposits relative to the two sub-Plinian Vesuvius eruption case–studies ~~from~~  
778 Vesuvius, Pollena and 1631. The detailed reconstruction and mapping of ~~these the primary~~ deposits  
779 allow an updating of the pyroclasts distribution on the territory allowed to update the area affected by

780 ~~pyroclastic deposits dispersal~~, ~~as and it was found that~~ both ~~the~~ eruptions had an impact larger than  
781 previously known. In particular, the stratigraphic and sedimentological reconstruction of the deposits  
782 was done not only in ~~open spaces~~ the countryside but also close to urban areas, and this is important  
783 in terms of local impact of the lahars ~~vs. broad impact~~ in the environment. Specifically, such impact  
784 investigation was done in urban areas including archaeological findings (e.g., ~~villages, urban~~  
785 structures, walls, etc...).  
786 These findings include not only new data from the Somma-Vesuvius plain, but also more distal  
787 ~~deposits data~~ from Lauro Valley and Avella-Baiano Valley (Apennines), which were subjected to  
788 heavy remobilization ~~also~~ of the ~~finer~~ primary deposits ~~as for the presence of~~ including the widely-  
789 dispersed fine ash deposits ~~present in both proximal and distal areas~~ formed in the late stage of the  
790 eruptions. Indeed, the accumulation areas that were reconstructed reveal an enlargement and extra  
791 2047% (Pollena eruption) and 230% (1631 eruption) coverage that was not previously known ~~and~~,  
792 ~~considering the physical characteristics of the ash, it and this~~ should be considered in ~~any the~~ hazard  
793 and impact evaluation in the Campanian plain and on the nearby Apennine reliefs. The full database  
794 ~~thus~~ allows a more precise reconstruction of the new isopachs, both for the Pollena and 1631  
795 eruptions, which is possible given the high number of data points in the study area.  
796 With particular reference to the lahar deposits, the syn-eruptive ones ~~that were emplaced~~ occurred by  
797 relatively short-term (during or immediately after the eruption) events, ~~stand and were~~ directly  
798 emplaced on the primary pyroclastic deposits, both for the Pollena and 1631 eruptions ~~case studies~~.  
799 Also, there are not any significant erosion surfaces nor humification traces in the sequences due to  
800 prolonged exposure of the primary deposits, testifying that the secondary emplacement was quite  
801 immediate (max a few years; Sulpizio et al., 2006) after or even during the eruption. The syn-eruptive  
802 features ~~of these deposits~~ are also testified by the absence of ~~anthropic~~ anthropogenic traces or  
803 humified surfaces at the base of or within ~~interbedded in~~ the ~~deposits~~ lahar deposits, as further  
804 evidence of a very short-term time span between the eruptions and the lahar events. ~~Another~~  
805 interesting features ~~are is~~ the presence of multiple depositional flow units in the lahar deposits, as

806 evidenced by granulometric grain-size changes, some clast alignments and concave erosion surfaces  
807 inside within the ~~lahar deposits~~ lahar deposits. Such flow-depositional units were ~~emplaced~~ formed by  
808 en-masse deposition-emplacement (with reference to ~~each-single~~ flow pulse), while the whole lahar  
809 deposits were formed by rapid progressive aggradation of the various flow units (Vallance and Scott,  
810 1997; Doronzo, 2012; Roche, 2012; Smith et al., 2018; Martí et al., 2019; Guzman et al., 2020; see  
811 also Sulpizio et al., 2014, p. 56), which does not contradict the principle of superposition. and this This  
812 can be argued by the generally massive facies of each flow unit in the deposits, and by the presence  
813 of water escape structures that cross vertically the entire ~~lahar-deposits~~ sequences. ~~Theis~~ latter  
814 evidence testifies a rapid ~~and-contemporaneous~~ water loss through vertical escaping “pipes” during  
815 or soon after the emplacement-aggradation of the sequences. In other words, the various flow units  
816 (layers) must decouple from the transport system, and such decoupling occurs unit-by-unit and not  
817 particle-by-particle (Sulpizio et al., 2006, 2014; Roche, 2012; Doronzo and Dellino, 2013; Breard  
818 and Lube, 2017; Smith et al., 2018), through a massive accumulation rate (Duller et al., 2008;  
819 Doronzo et al., 2012; Martí et al., 2019).

820 The analysis of the Pollena lahar lithofacies allowed the identification of ~~mainly~~ two main deposit  
821 categories. The first one occurs ~~over-on~~ an area that extends for more than 10 km north of Mount  
822 Somma, and the second one occurs on an area ~~which-that~~ extends west of the Apennines. For the  
823 latter, we can recognize two significant sub-categories of deposits, corresponding to the main valleys  
824 in northwest-southeast direction, Avella-Baiano Valley and Lauro Valley. ~~Theis~~ difference between  
825 the first and the second deposit categories seems to reflect the type of primary deposits that ~~was-were~~  
826 remobilized ~~and~~ (~~just~~ fine ash vs. ash and lapilli). ~~In the first area Avella-Baiano Valley~~ the area north  
827 of Mount Somma, which also comprises the municipalities of Acerra and Afragola, the primary lapilli  
828 fallout deposits ~~is in fact not deposited~~ are absent, ~~while On the other hand~~ In this part of the plain,  
829 there is almost always a very thin level-layer of phreatomagmatic ash is widely present in the  
830 Plain, while and thick, fine-grained pyroclastic current deposits are present in the ~~Mt.~~ Mount Somma

831 valleys ~~feeding the lahars~~ that fed some of the lahars. ~~The other basin comprises many~~In Avella-  
832 ~~Baiano Valley and Lauro Valley, which also comprises the~~ municipalities ~~in the area~~ around Nola  
833 (Fig. 1 and Appendix 3C), ~~where~~ the lahar deposits are generally coarser, and consist of multiple  
834 depositional units with different lithofacies (Tab. 3). In this case, both ~~granulometry grain-size~~ and  
835 componentry indicate ~~the that lahar~~ deposits resulted from the remobilization of the fallout deposits.  
836 ~~Such considerations also derive from the full compilation of the geospatial database.~~ A volume  
837 estimation of the remobilized syn-eruptive deposits, based on a QGIS calculation, is of  $73 \times 10^6 \text{ m}^3$   
838 for the northern Vesuvius area, and  $42 \times 10^6 \text{ m}^3$  for the Lauro Valley.

839 Referring to the 1631 eruption, previous maps have shown the distribution of the 1631 lahar deposits  
840 toward east, basically following the distribution of the primary pyroclastic fall deposits (Sulpizio et  
841 al., 2006), while in Figs. 109 and 110 we show a significantly larger distribution area particularly  
842 toward ~~the~~ north (Somma-Vesuvius ramps and ~~p~~Plain) and east (~~mountain~~ Apennines valleys), and  
843 less toward the ~~SE~~southeast. In particular, this distribution is well explained by the wide distribution  
844 of the ash fallout deposit toward both north and northeast (Fig. 6), remobilized during the lahar  
845 generation ~~along~~ both ~~from the Mount~~ Somma and Apennine slopes. On the other hand, looking at  
846 the ~~average~~ deposit thicknesses, they reach ~~on average~~ half a meter ~~to in~~ the ~~N~~north and ~~NE~~northeast,  
847 while reaching a couple of meters in some ~~points locations~~ ~~to in~~ the ~~NE~~northeast (aligned with the  
848 dispersion axis of the primary fallout deposits and out of the Apennine valleys).

849 The sedimentological analyses carried out on a number of samples from the different studied sectors  
850 (Somma-Vesuvius, Lauro Valley, Avella-Baiano Valley) are useful for discriminating the various  
851 factors that contributed to ~~the initiation of the lahars and~~ emplacement of their ~~lahar~~ deposits. The  
852 samples ~~for from~~ Lauro Valley and Avella-Baiano Valley are coarser (but have a significant finer  
853 tail) than the ones for Somma-Vesuvius, and this can depend on three factors: i) ~~depositional~~  
854 ~~mechanisms~~ genetic types of the primary pyroclastic deposits (fall vs. flow); ii) interaction between  
855 lahars and morphology (valley vs. plain); iii) major ~~involvement~~ remobilization ~~for in~~ Lauro Valley

856 and Avella-Baiano Valley of the distal ~~fine~~-phreatomagmatic fine ash deposits formed in the ~~final-late~~  
857 eruptions stages. In other words, the primary grain sizes involved in the remobilization (finer and  
858 higher-water retention for Somma-Vesuvius), as well as the general topography (gentler but longer  
859 ramp for Somma-Vesuvius) likely acted as the main factors directly impacting the distribution of the  
860 lahar deposits, and the decay of the flow velocities and dynamic pressures in the area. Interestingly,  
861 an emplacement temperature (~120 °C) of the lahar deposits was calculated for those generated along  
862 the Somma-Vesuvius slopes, indicating a relatively hot provenance after remobilization of the  
863 pyroclastic current deposits. Instead, the remobilization from the Apennines sectors involved only  
864 cold fallout deposits. The sampled clasts might have been incorporated multiple times by the flows,  
865 and the heating/cooling processes that we interpret as indicating  $T_{dep}$  in the diagrams are the last to  
866 have occurred and affected the samples. Besides, a third heating component is clearly observed for  
867 some of them. The paleomagnetic ~~data-directions of flow direction~~ are statistically distinguishable also  
868 indicate, supporting that the lahar emplacement at Nola and Acerra was not synchronous, as ~~a~~ further  
869 evidence of the different timing ~~and hence likely different~~ detachment areas involved during the  
870 pyroclasts remobilization. However, the comparison with the paleosecular variation curves of the  
871 Earth's magnetic field does not allow to better constrain the entity of the time span between the two  
872 lahar events. The parental lahars acted as mass flows capable of entraining outsized clasts (where  
873 available) from substrate under the action of shallow-layer flow velocity and dynamic pressure  
874 (de' Michieli Vitturi et al., this issue), then emplaced massive flow units with uplifted external clasts  
875 set into the much finer matrix (see Roche, 2015). In ~~various-some~~ lahar units, multiple-various clasts  
876 have been found, showing some alignment that depends on the mechanisms of entrainment and uplift  
877 (with respect to substrate) within the flow.

878 In terms of local impact in the Pollena case study (the largest one), while most of the calculated points  
879 (44) fall in the range of lahar velocity of 2-4 m/s and dynamic pressure of 4-8 kPa, a few peak values  
880 of velocity of 13-15 m/s and dynamic pressure of 90-115 kPa are also calculated, which are directly  
881 related to meter-sized clasts entrained into the lahars on the steep slopes, then deposited downstream



882 of alluvial fans. Such values of the velocity and dynamic pressure are well comparable with those  
883 calculated for lahars that occurred recently at Ruapehu in 2007 (Lube et al., 2012) and Merapi in 2011  
884 (Jenkins et al., 2015), and in historical times at El Misti (Thouret et al., 2022). In particular, the  
885 estimated velocities and pressure agree with those of Lube et al. (2012) and Jenkins et al. (2015).  
886 Moreover, multiplying velocity and density gives a power per unit surface, so those most  
887 representative values correspond to a flow power per unit surface of  $8 \cdot 10^3 - 3.2 \cdot 10^4 \text{ W/m}^2$ , with peak  
888 values of  $1.17 \cdot 10^6 - 1.72 \cdot 10^6 \text{ W/m}^2$ , in agreement with typical values reported for floods and  
889 megafloods (Russell and Knudsen, 1999; Whipple et al., 2000; Carling, 2013).

890

## 891 6. Conclusions

892 ~~A number of points can be highlighted after the~~The integration of the historical, stratigraphic,  
893 sedimentological, laboratory, and impact parameter analyses carried out in the Vesuvius area allow  
894 us updating on the lahar invasion related to ~~for~~ the Pollena and 1631 eruptions. In general, the physical  
895 characteristics of the analyzed deposits indicate that syn-eruptive lahars are related to the rapid  
896 remobilization of large volumes of pyroclastic material, which is mainly fine-grained and almost  
897 exclusively derived from the accumulation of products related to a single eruption. The analysis also  
898 shows that tardive (post-eruptive) mass flows are common, and involve multiple and variably altered  
899 deposits, and that their energy and frequency are progressively lower over time, after the last eruption  
900 has occurred. In particular, a higher impact both from primary and secondary phenomena is  
901 something that should be accounted in the Vesuvius area and that;

- 902 i) The new isopach maps of the Pollena and 1631 eruptions allow us to infer a larger impact  
903 than previously known for these two sub-Plinian events of the Vesuvius. Thus, it is worth  
904 reconsidering the territorial impact that sub-Plinian eruptions can have in the Vesuvius  
905 (but not only) area. In particular, the ash deposits can have a high impact in relation to  
906 their high density and low permeability.

- 907 ii) The primary impact from fallout and pyroclastic current processes in the Vesuvius area  
908 was - and may be in the future – followed by the secondary impact from lahars generated  
909 during or immediately after the eruption events. Both impacts can have a wide distribution,  
910 because they are directly controlled by the primary deposits distributions, both around  
911 Somma-Vesuvius and in the Apennines valleys.
- 912 iii) The runouts of such lahars were significant both for the Pollena and 1631 eruptions, by  
913 reaching distances of 10 to 15 km from the sources, and their deposits geometry is tabular-  
914 like with average thicknesses of 0.5 to 1 m.
- 915 iv) The paleotemperature data highlight a relatively hot dynamics (~120 °C) for those lahar  
916 flow pulses that traveled [along-down](#) the Somma-Vesuvius slopes because of pyroclastic  
917 current deposit remobilization. This did not occur from the Apennines sectors, where  
918 [pyroclastic currents did not get to, and](#) only cold fallout deposits were remobilized.
- 919 v) A reverse engineering approach allowed to calculate the local lahar velocities (2-4 m/s,  
920 with peaks of 13-15 m/s), dynamic pressures (4-8 kPa, with peaks of 90-115 kPa), and  
921 solid volumetric concentration (~30%, implying a 1:3 ratio between deposit and flow  
922 thickness), on the basis of the external clast properties entrained into the flows then  
923 emplaced into the ash matrix, and on the presence of the lahar deposits in proximity of  
924 obstacles and archaeological findings.

925 As a general conclusion, we have demonstrated that the areal impact of both primary deposits and  
926 lahars, in case of sub-Plinian events at Somma-Vesuvius, involves a territory wider than  
927 previously known and for several years, with possible decreasing damages over time.

## 928

### 929 **Appendix A. Calculation of lahar velocities and dynamic pressures**

930 A theoretical scheme is presented to quantify local [velocities and](#) dynamic pressures of the lahars, by  
931 inverting the field features at selected locations. The final goal is to map the values of [velocity and](#)

932 dynamic pressure to assessing the hazard from lahars in the study area. Flow dynamic pressure,  $P_{dyn}$ ,  
933 results from a combination of flow density,  $\rho_f$ , and flow velocity,  $v$ , and is defined as follows

$$934 \quad P_{dyn} = 0.5 \rho_f v^2 \quad (A1)$$

935 In the study area, the original flow was a multiphase flow of water + pyroclastic sediment, which  
936 during remobilization evolved into a flow of water + pyroclastic sediment + external clasts.  
937 Generically, flow density results from a combination of particle density,  $\rho_p$ , and water density,  $\rho_w$ ,  
938 through particle volume concentration,  $C$ , and is defined as follows

$$939 \quad \rho_f = \rho_p C + \rho_w (1 - C) \quad (A2)$$

940 In order to define flow velocity, we take into account stratigraphic and sedimentological  
941 characteristics of the lahar [depositsflow units](#): i) they are ubiquitously massive, and result from  
942 remobilization of the primary pyroclastic deposits then emplacement from mass flows; ii) they  
943 contain big external clasts entrained [\(by dynamic pressure\)](#) and uplifted [\(also by pore pressure\)](#) from  
944 substrate into the flows. With these field characteristics, flow velocity can be expressed as a  
945 combination of entrained clast properties and flow density, and is defined as follows (modified after  
946 Roche, 2015)

$$947 \quad v = \sqrt{\frac{X\psi(\rho_c - \rho_w)g}{\gamma\rho_f}} \quad (A3)$$

948 where  $X$  is clast small axis,  $\psi$  is clast shape factor,  $\rho_c$  is clast density,  $g$  is gravity acceleration and  $\gamma$   
949 is an empirical constant. Eq. 3 allows quantifying the incipient motion of the big clasts, and gives  
950 minimum values of flow velocity required to entrain and uplift the clasts from substrate, [possibly](#)  
951 [probably](#) more than once, before being emplaced into the lahar deposits [by flow velocity drop](#). Such  
952 equation has been originally derived in laboratory experiments for a multiphase flow of air +  
953 sediment, and is highly performing at  $\rho_f \sim 1000 \text{ kg/m}^3$  (hindered settling) for dense pyroclastic  
954 currents controlled by topography then opened to alluvial plain (Martí et al., 2019), which is a case  
955 similar to the lahars in the study area. Substituting Eq. 3 into Eq. 1 and simplifying gives

$$P_{dyn} = 0.5 \frac{X\psi(\rho_c - \rho_w)g}{\gamma} \quad (A4)$$

957 For given clast properties, flow dynamic pressure has a unique value, while flow velocity is a function  
 958 of flow density. Indeed, the present scheme is a spot model that basically depends on, and is limited  
 959 to, the finding of big clasts and boulders within the lahar deposits. An approximation is that velocity  
 960 and dynamic pressure are calculated for the locations where the clasts are found in the deposits,  
 961 meaning that the calculated values are overestimated for those exact locations, while they are more  
 962 properly referred to the immediate surroundings upstream.

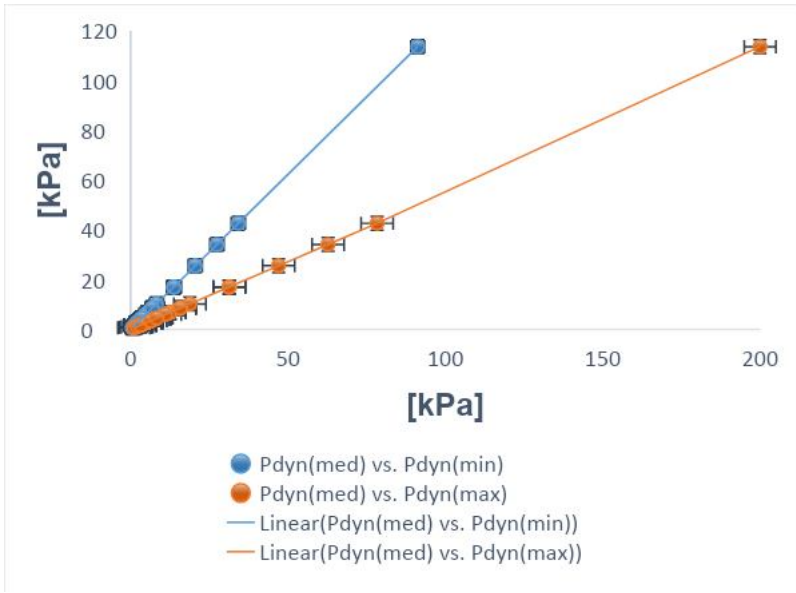
963 At the selected locations in the study area, we collected the dimensions of the biggest clasts found in  
 964 the lahar deposits, and we characterized ~~petrographically~~ lithologically the clasts in the field, to  
 965 calculate flow dynamic pressures using Eq. 4. We used the following values for the various  
 966 parameters in the calculations:  $\Psi$  (ellipsoid) = 0.66;  $\rho_c$  (limestone) = 2500 kg/m<sup>3</sup>;  $\rho_c$  (ceramic) = 2000  
 967 kg/m<sup>3</sup>;  $\rho_c$  (brick) = 2000 kg/m<sup>3</sup>;  $\rho_c$  (tephra) = 1500 kg/m<sup>3</sup>;  $\rho_c$  (lava) = 2500 kg/m<sup>3</sup>;  $\rho_c$  (iron) = 8000  
 968 kg/m<sup>3</sup>;  $\rho_w$  = 1000 kg/m<sup>3</sup>;  $g$  = 9.81 m/s<sup>2</sup>;  $\gamma$  = 0.031 – 0.071. Also, we calculated flow velocities using  
 969 Eq. 3, in the following range of flow density:  $\rho_w \leq \rho_f \leq \rho_p$ , where  $\rho_w$  = 1000 kg/m<sup>3</sup> and  $\rho_p$  = 2000  
 970 kg/m<sup>3</sup>. In this way, flow density spans from two extreme cases: i)  $\rho_f = \rho_w$ , negligible pyroclastic  
 971 sediment and external clasts, so water flow only; ii)  $\rho_f = \rho_p$ , negligible water and dominant pyroclastic  
 972 sediment, so ash flow only. For the empirical constant in Eq. 3, we used three different values to test  
 973 the sensitivity with respect to different physical states of the multiphase flow:  $\gamma$  (non-fluidized) =  
 974 0.031;  $\gamma$  (initially fluidized and slightly expanded) = 0.057;  $\gamma$  (initially fluidized and non-expanded)  
 975 = 0.071 (see Roche et al., 2013; Fig. A1).

976 Regarding flow velocity, after calculation we can rewrite Eq. 3 in a simpler form (to more directly  
 977 relate velocity to density) as follows

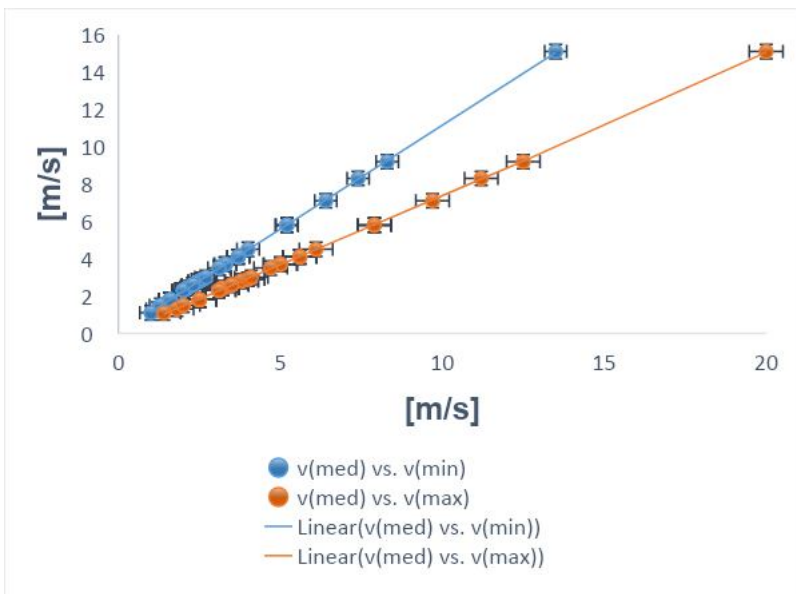
$$v = \frac{a}{\sqrt{\rho_f}} \quad (A5)$$

979 where  $a > 0$  depends on clast properties, and its square has dimension of pressure. On the other hand,

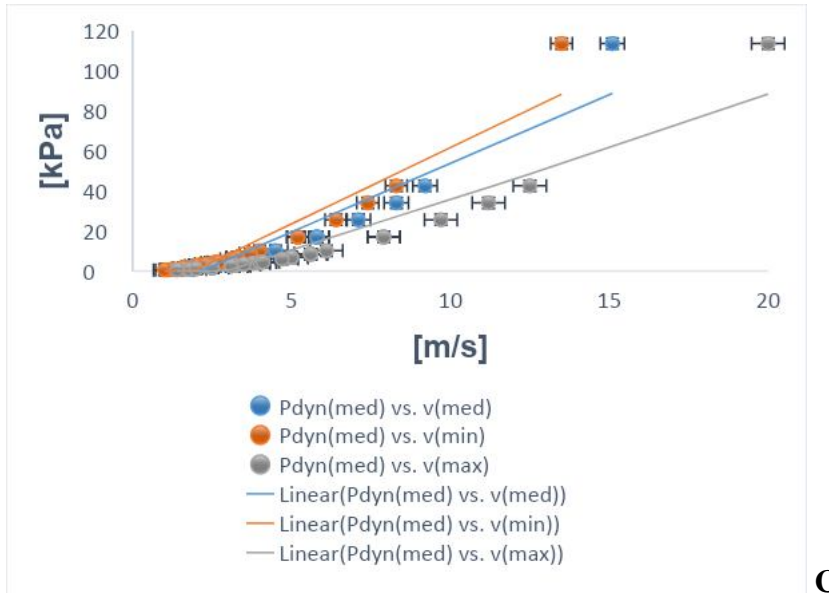
980 it is not straightforward to constrain local flow velocities with unique values of flow densities, mostly  
981 because small variations of velocity correspond to large variations of density, and this is particularly  
982 valid for volcanoclastic mass flows (Carling, 2013; Jenkins et al., 2015; Roche, 2015; Martí et al.,  
983 2019; Guzman et al., 2020; Thouret et al., 2022).



984 **A**



985 **B**



986

987 Fig. A1. **A**, dynamic pressure for the initially-fluidized and slightly expanded case vs. dynamic pressure for the initially-  
 988 fluidized and non-expanded (blue) and non-fluidized (orange) cases; **B**, velocity for the initially-fluidized and slightly  
 989 expanded case vs. velocity for the initially-fluidized and non-expanded (blue) and non-fluidized (orange) cases; **C**,  
 990 dynamic pressure for the initially-fluidized and slightly expanded case vs. velocity for the initially-fluidized and slightly  
 991 expanded (blue), vs. velocity for the initially-fluidized and non-expanded (orange), vs. velocity for the non-fluidized  
 992 (grey) cases.

993

994 At some locations in the study area, we found lahar deposits against meter-scale manufacturing  
 995 obstacles (Di Vito et al., 2009). The peculiarity is that the deposits in proximity of the obstacles are  
 996 thicker than the correlated ones in the free field, but never reach the top of the obstacles themselves.  
 997 This means that the lahars were not much expanded, so unable to overcome the obstacles as stratified  
 998 flows would have done (cf. Spence et al., 2004; Gurioli et al., 2005; Doronzo, 2013; Breard et al.,  
 999 2015). With this field evidence, we can assume that local flow height,  $H$ , was similar to deposit  
 1000 thickness against the obstacle,  $h_o$ , as follows

$$1001 \quad H \approx h_o \quad (A6)$$

1002 In order to estimate flow density using Eq. 2, we focus on particle volumetric concentration. For well-  
 1003 sorted deposits, such concentration can be defined with an average value over flow height as follows

1004 (modified after Doronzo and Dellino, 2013; see also Eq. 30 in de' Michieli Vitturi et al., [submitted this](#)  
1005 [issue](#))

$$1006 \quad C = \frac{h_f}{H} \quad (A7)$$

1007 where  $h_f$  is deposit thickness in the free field. Substituting Eq. 6 into Eq. 7 gives

$$1008 \quad C \approx \frac{h_f}{h_o} \quad (A8)$$

1009 In particular,  $h_f$  refers to those lahar deposits relatively close to the obstacles, but which were not  
1010 affected by them during emplacement, i.e. close but not so much. We assessed that correlation taking  
1011 into account the stratigraphic and sedimentological characteristics of the lahar deposits, and the fact  
1012 that Eq. 7 performs better with layers emplaced after remobilization of primary pyroclastic fallout or  
1013 dominantly ash flow deposits.

1014 Lastly, we macroscopically assessed erosion in the field, by characterizing the unconformities present  
1015 both on the primary pyroclastic and lahar deposits. In particular, the syn-eruptive lahar deposits  
1016 consist of more than one flow unit, so it is important to understand how the different flow pulses  
1017 interacted with each other during emplacement. The main unconformities that are found in the field  
1018 are referred to the partial absence of a flow unit, and the loss of lateral continuity despite some flat  
1019 geometry of the deposits. On the other hand, at some locations we were not able to assess if erosion  
1020 occurred or not due to multiple open issues: i) ~~eventual-possible~~ absence of the primary pyroclastic  
1021 deposits; ii) ~~eventual-possible~~ exclusive presence of the post-eruptive lahar deposits; iii) impossibility  
1022 to get to some outcropping deposit base and ~~eventual-possible~~ unconformities.

## 1023

## 1024 **Appendix B. Paleo-temperature and paleo-direction determinations**

1025 The magnetic fabric of a deposit was investigated by measurements of the magnetic susceptibility  
1026 and its anisotropy (AMS). AMS was measured with a Kappabridge KLY-3 (AGICO), and data were

1027 elaborated by the software Anisoft5 (AGICO). AMS depends on the type, concentration, and  
1028 distribution of all the minerals within the specimen. It is geometrically described by a triaxial  
1029 ellipsoid, whose axes coincide with the maximum ( $k_1$ ), intermediate ( $k_2$ ) and minimum ( $k_3$ )  
1030 susceptibility directions. The magnetic fabric of a specimen is then described by the direction of the  
1031  $k_1$  axis, the magnetic lineation (L) and that of the  $k_3$  axis, which is parallel to the pole of the magnetic  
1032 foliation plane (F). Besides, the modulus of the susceptibility axes provides some magnetic  
1033 parameters useful to express the intensity of the anisotropy ( $P_j$ ) and the oblate/prolate fabric  
1034 occurrence (T) (Jelinek, 1981). Generally, sedimentary vs. pyroclastic deposits fabric, here  
1035 considered as the proxy of the lahar fabric, is oblate with a horizontal to gently imbricated (less than  
1036  $20^\circ$ ) magnetic foliation. The magnetic lineation is normally clustered along the foliation plunge. In  
1037 this case, both the F imbrication and the L direction can provide the local flow direction. Other times,  
1038 L is orthogonal to the F plunge or F is statistically horizontal, and it is not possible to infer the flow  
1039 direction.

1040 For  $T_{dep}$  estimation, pottery sherds were subjected to progressive thermal demagnetization (PTD),  
1041 with heating steps of  $40^\circ\text{C}$ , up to the Curie Temperature ( $T_C$ ), using the Schonstedt furnace and the  
1042 spinner magnetometer JR6 (AGICO). The rationale of the method has been described in detail in  
1043 several papers (McClelland and Druitt, 1989; Bardot, 2000, Porreca, 2007; Paterson et al., 2010; Lesti  
1044 et al., 2011), many of them dedicated to PDCs of the [Vesuvian-Vesuvius](#) area (Cioni et al., 2004; Di  
1045 Vito et al., 2009; Giordano et al., 2018; Zanella et al., 2007; 2018; 2015). Typically, measurements  
1046 are made on accidental lava lithics that were entrained during pyroclastic or lahar flows. In this case,  
1047 we had the opportunity to estimate the  $T_{dep}$  by measuring ancient pottery artifacts. Briefly, pottery is  
1048 characterized by a thermal remanent magnetization (TRM) acquired during its manufacture and its  
1049 subsequent history of daily use. Whenever it is heated, part of its TRM, the one associated with  
1050 blocking temperatures ( $T_b$ ) below the heating one ( $T_h$ ), is overwritten. Without alteration phenomena,  
1051 the heating/cooling is a reversible process, except for the magnetic directions. The original TRM  
1052 shows a random paleomagnetic direction, due to the transport during emplacement. Subsequent



1053 TRMs show directions parallel to the Earth's magnetic field during their cooling. This is clearly  
1054 illustrated in the Zijdeveld diagrams. The composition of the different magnetization components  
1055 reveals thermal intervals characteristic of the heating history of the potsherd. Of course, this  
1056 explanation is simplified, but the method is well-established and has been shown to work well with  
1057 heated artifacts, such in the case of tiles and pottery embedded in the PDC deposits at Pompeii  
1058 (Gurioli et al., 2005; Zanella et al., 2007), Afragola (Di Vito et al., 2009) and Santorini (Tema et al.,  
1059 2015). In case of lahar, we expect low  $T_{\text{dep}}$  or cold deposits. This can be a major concern because of  
1060 the difficulties to distinguish between the TRM secondary components, and the chemical (CRM) and  
1061 viscous (VRM) remanent magnetization. The CRM may develop due to mineralogical changes during  
1062 reheating (McClelland, 1996). Instead, VRM is typical of ferromagnetic grains with low  $T_b$  and often  
1063 occurs in most rocks. Following Bardot and McClelland (2000) relationship for time intervals in the  
1064  $10^2$ – $10^6$  year range,  $T_b = 75 + 15 \log$  (acquisition time in years), and using the Pollena eruption date  
1065 (472 [ADCE](#)), we obtain a lower limit of the  $T_b$  around 123 °C. This means that this temperature helps  
1066 us in discriminating between “hot” ( $T_b > 120$  °C) or “cold” lahar ( $T_b < 120$  °C).

1067 Finally, routine magnetic measurements on the lahar matrix were done on the lahar matrix to  
1068 determine the Characteristic Remanent Magnetization (ChRM) by Thermal and Alternating Field  
1069 demagnetizations. The direction of the Earth's Magnetic Field during the Pollena eruption is well-  
1070 known (Zanella et al., 2008). If the sampled lahars were emplaced shortly after the eruption, both the  
1071 secondary TRMs and the matrix of the lahars should show a remanent magnetization direction similar  
1072 to the Pollena ones. ChRMs can also test if the two lahars (Acerra and Nola) are coeval.

1073

## 1074 **Appendix C. Description of the studied areas**

### 1075 *Area 1 – Nola*

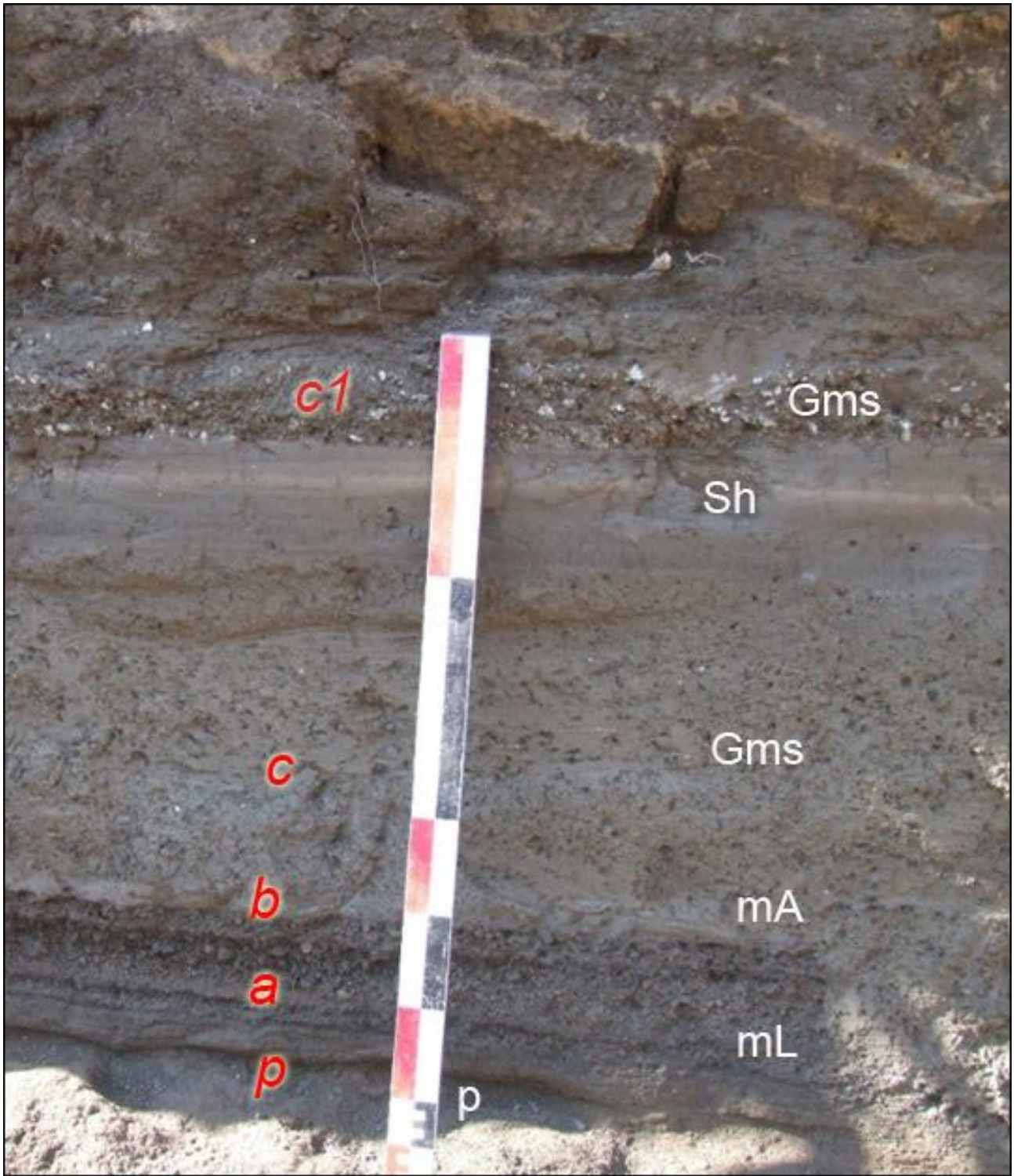
1076 In the area surrounding Nola, it is possible to recognize the complete fallout sequence of the Pollena  
1077 eruption (a in [Ffig. C1](#) and [C2](#)), which usually covers ploughed soils (p in [Ffig C1](#)) and late Roman

1078 archaeological remains. The sequence is composed ~~by of~~ an alternation of coarse pumice and thin ash  
1079 fallout layers. Its top is always made of a ~~cohesive fine~~ ash bed related to the phreatomagmatic phase  
1080 of the eruption (b in ~~F~~fig. C1 and C2), with a thickness ranging from 1 to 14 cm due to erosion. They  
1081 are almost always overlain by lahar deposits composed of several flow units (c in ~~F~~fig. C1 and C2)  
1082 with a large thickness variability due to channeling and presence of barriers and ~~edifices~~buildings.  
1083 They sometimes include blocks, tiles, and other archaeological remains.

1084 In Fig. C1, above the primary deposit, there is an example of a well-exposed sequence composed ~~by~~  
1085 ~~of~~ at least five units (c in ~~F~~fig. C1). The first one is a massive and matrix-supported deposit composed  
1086 ~~by of~~ fine and not vesiculated ash (lithofacies Gms), with fragments of greenish to blackish scoriae  
1087 and minor fragments of pumices, lavas and limestones. The fragments are cm-sized and are both  
1088 angular and rounded. The second flow unit is similar to the one below, but is darker and contains less  
1089 coarse fragments. Its matrix is composed ~~by of~~ an alternation of fine to medium ash layers. It follows  
1090 a plane-parallel sequence of well-sorted fine sand and silt layers characterized by the lithofacies fM.  
1091 A massive deposit follows upward, it is progressively humified and contains abundant reworked and  
1092 rounded pumice clasts from the Avellino eruption. The top humified surface is almost always eroded  
1093 by anthropogenic activity and is generally ploughed (p1 in Fig. ~~C24~~), ~~whose surface~~. ~~It~~ is overlain by  
1094 the primary deposits of the 1631 eruption ~~of 1631~~ (d in Fig. C2). It is few cm thick and is composed  
1095 ~~by of~~ a basal layer of dark coarse ash (small pumice fragments), overlain by a ~~very cohesive and~~  
1096 massive ash bed, containing abundant accretionary lapilli. The following deposit thickens in the  
1097 ~~plowing ploughing~~ furrows and depressions, and is composed ~~by of~~ massive fine-ash beds,  
1098 vesiculated and cohesive, and is interpreted as a lahar deposit (lithofacies mM) (e in Fig. C2). This  
1099 deposit (e in Fig. C3) overlies the foundations of Palazzo Orsini (blocks in Fig. C3), now seat of the  
1100 Court of Nola and built in the second half of the XV century (Fig. C3). The top is always eroded by  
1101 the modern anthropogenic activity, and locally by deposits of recent eruptions of Vesuvius (e.g., 1822,  
1102 1906).



1103



1104

1105

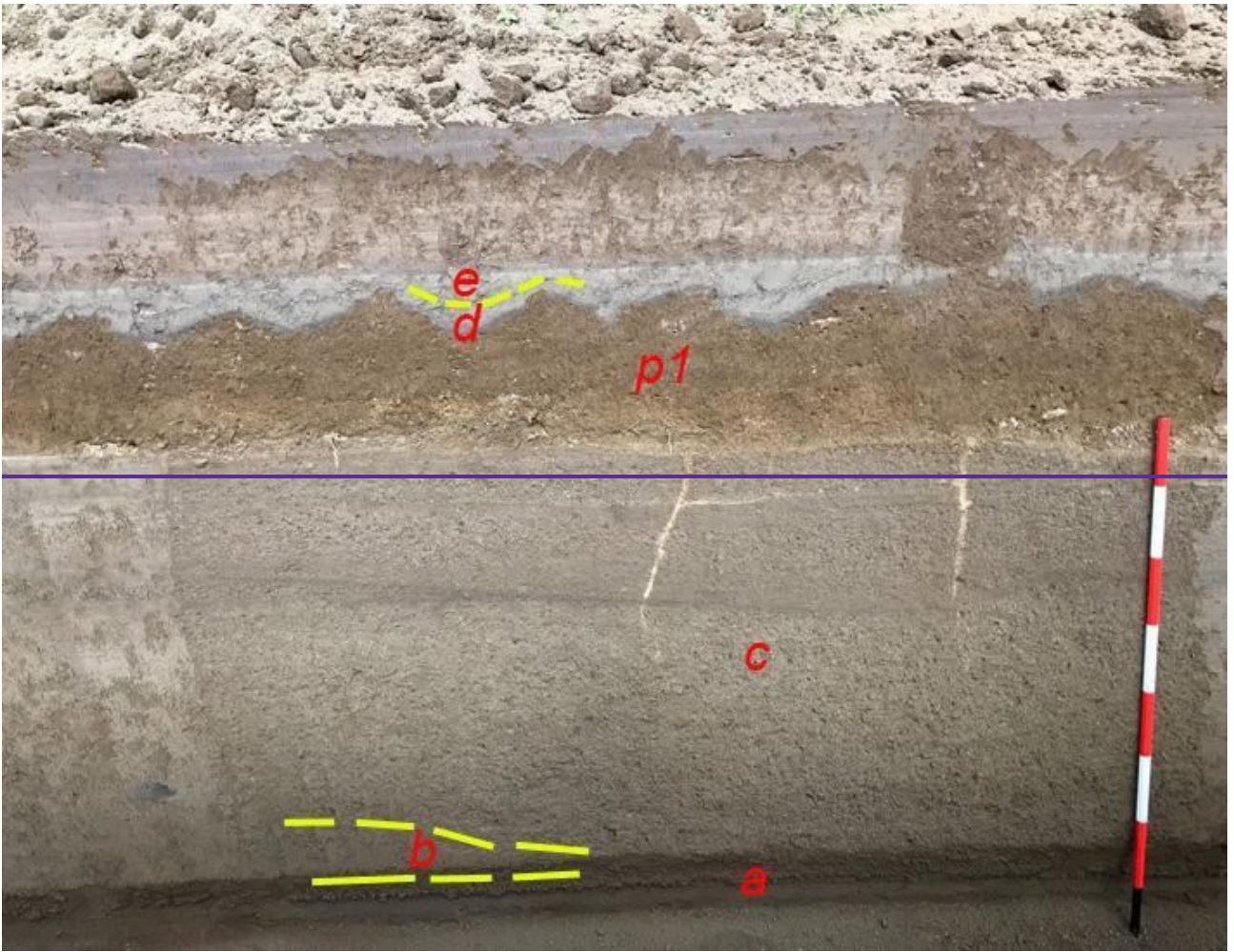
1106

1107

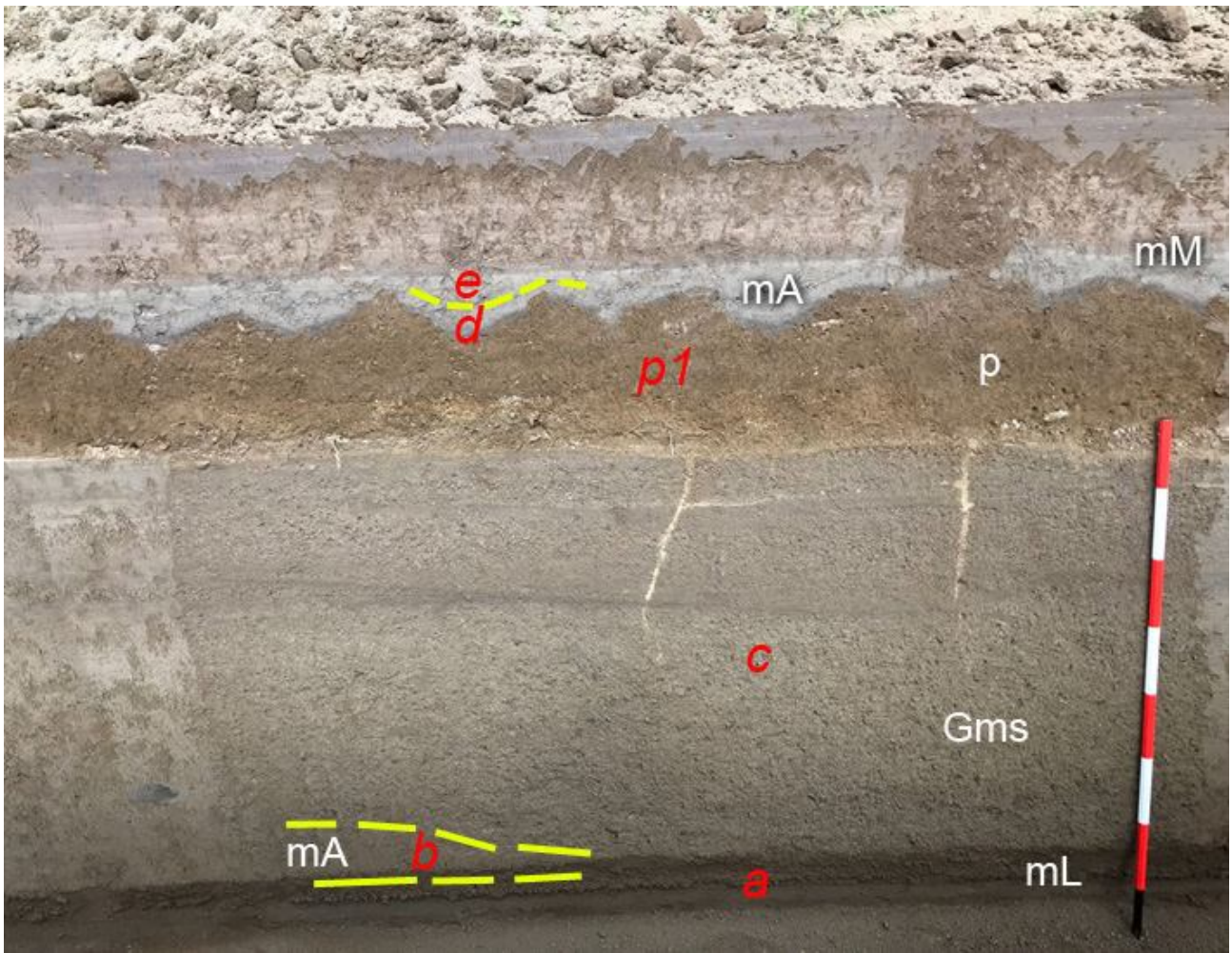
1108

1109

Fig. C1. Nola, Pollena fallout deposits overlain by at least five lahar units. In particular: p = paleosol; a = alternation of coarse and fine fallout sequence of the Pollena eruption; b = final ash fallout of the eruption; c = sequence of syn-eruptive lahars; c1 = post-eruptive lahar containing white pumice fragments of the Pomici di Avellino eruption. For the description of lithofacies see Tab. 2.



1110



1111

1112 Fig. C2. Pollena lahar deposits overlain by a cultivated paleosol, and by the 1631 ash fallout and lahars. In particular: a  
 1113 = alternation of coarse and fine fallout sequence of the Pollena eruption; b = final ash fallout of the eruption, partially  
 1114 eroded; c = sequence of three lahar units; p1 = ploughed paleosol; d = 1631 ash fallout deposit mantling the undulated  
 1115 paleosol; e = lahar deposit composed of a massive ash layer. For the description of lithofacies see Tab. 2.

1116





1118

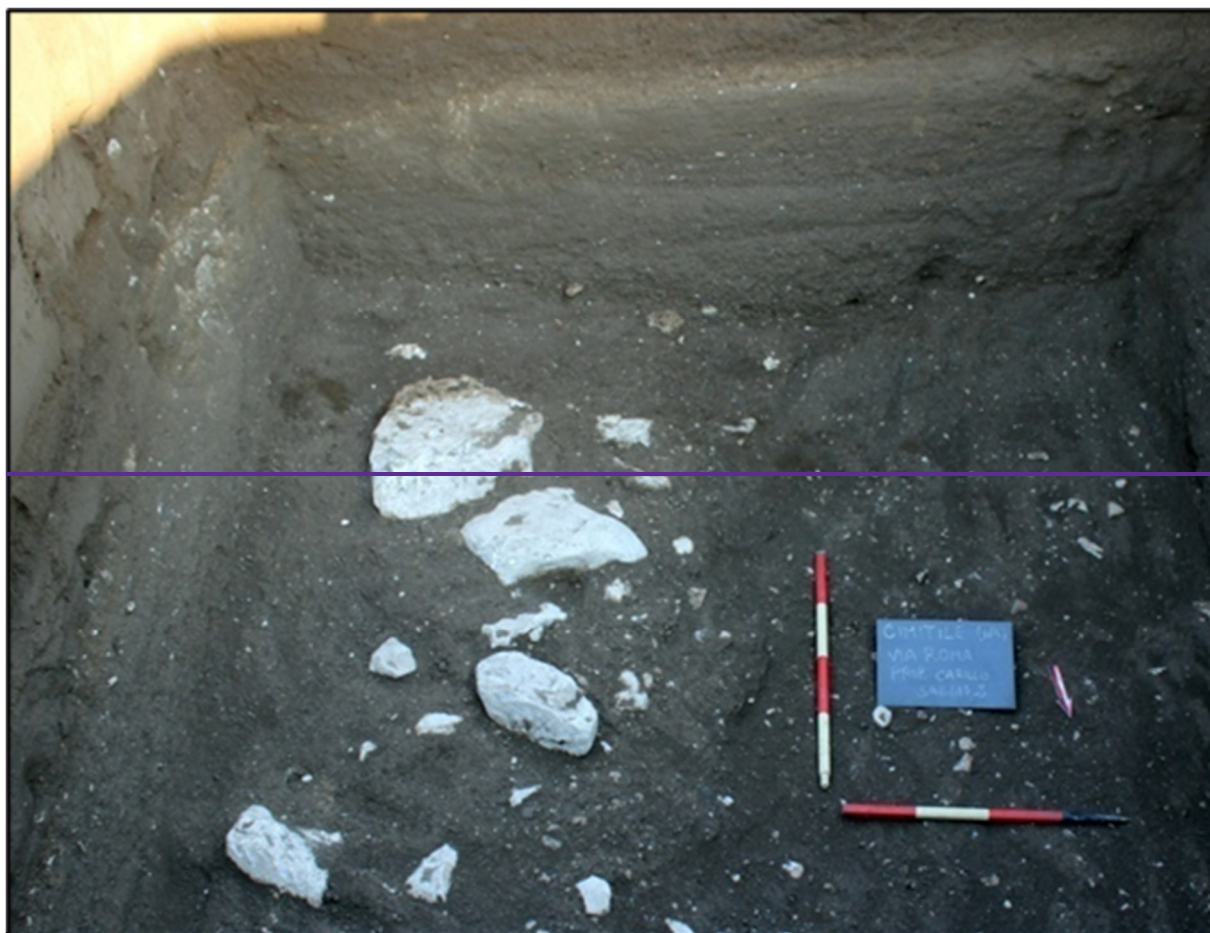
1119 Fig. C3. Palazzo Orsini, Nola (1631 fallout and lahars). In particular: d = 1631 ash fallout deposit overlying the  
 1120 foundations of the building (in the inset); e = syn-eruptive lahar deposit. For the description of lithofacies see Tab. 2.

1121

1122 In Nola and in the nearby Cimitile, the effects on the territory of the lahar emplacement related to the  
 1123 Pollena eruption are testified by numerous archaeological remains. The Nola and Cimitile areas are  
 1124 covered by thick sequences of fallout and lahar deposits. In fact, the previous ground level was at  
 1125 least 2-3 m below the present one. This effect is well visible in the Amphitheater Laterizio, which



1126 was completely filled by the primary and secondary deposits, and the same in Cimitile, where in the  
1127 archaeological site of the Early Christian basilicas the present ground level is about two meters higher  
1128 than the one before the eruption. It is worth noting that in Cimitile the flows were able to carry  
1129 limestone blocks of 50 cm in diameter, likely along the main flow direction of the lahars (Fig. C4).



1130



1131

1132 Fig. C4. Cimitile. Sequence of three m-thick syn-eruptive lahar units with the evidences of transport of calcareous block  
 1133 (up to 50 cm). The largest are in the lower unit. The base of the lahar sequence and the underlying fallout deposit of the  
 1134 Pollena eruption are not visible in the photo. For the description of lithofacies see Tab. 2.

1135

1136 *Area 2 – Acerra-Afragola*

1137 The Acerra and Afragola territories are located north and north-west of Vesuvius, and are almost flat  
 1138 areas crossed by the Clanis river. Both the coarse fallout deposits of the Pollena and 1631 eruptions  
 1139 are absent in this area. Here, only a thin, centimetric ash bed overlies the Late Roman paleosoil. This  
 1140 fine ash bed, which we correlate with the final phreatomagmatic phases of the Pollena eruption, is  
 1141 homogeneous, cohesive and mantles the ground without any significant lateral variation. The  
 1142 overlying deposit is characterized by high thickness variations, it is generally massive and contains  
 1143 vesicles from circular to flattened and coated by fine ash. It has a matrix-supported texture and is  
 1144 composed of fine to very fine, very cohesive ash, and contains scattered and more or less abundant  
 1145 pumice and lithic fragments (lithofacies mM) and remains of vegetation (Barone et al., 2023). From

1146 one to three depositional units have been recognized, marked by unconformities, and differences in  
1147 grain-size or color. The uppermost unit always contains white pumice fragments of the Avellino  
1148 eruption. Very common are drying out structures and water escape structures, which are vertical  
1149 structures (Fig. C5); looking like fractures a few cm large, filled by finer material transported by the  
1150 escaping water, formed soon after the emplacement of the sequence of the syn-eruptive lahars (Fig.  
1151 C5). The maximum thickness recorded in this area is about 90 cm.



1152  
1153 Fig. C5. Lahar deposit (unit 2) in Acerra overlaying a cultivated paleosol (unit 3). The index finger indicates a water  
1154 escape structure crossing the sequence of lahars. For the description of lithofacies see Tab. 2.

1155  
1156 The top is almost always horizontal due to the erosion related to the modern anthropogenic activity,  
1157 and only in a few exposures it is capped by a paleosol, with traces of human presence of the Medieval  
1158 times and of the deposits of the 1631 eruption as well. The base of this latter deposit is a cm-thick

1159 fine-ash bed with an internal plane-parallel layering emplaced by fallout. It underlies a massive  
1160 deposit with high thickness variations (max 20 cm) at the outcrop scale. It is composed by of fine  
1161 ash, cohesive and vesiculated and contains scattered small pumice fragments (lithofacies mM). The  
1162 pumice fragments are vesicular, dark gray to blackish, highly porphyritic with leucite, pyroxene and  
1163 feldspar crystals. The stratigraphic position and lithology confirm their attribution to the 1631 primary  
1164 and secondary (lahars) deposits.

1165

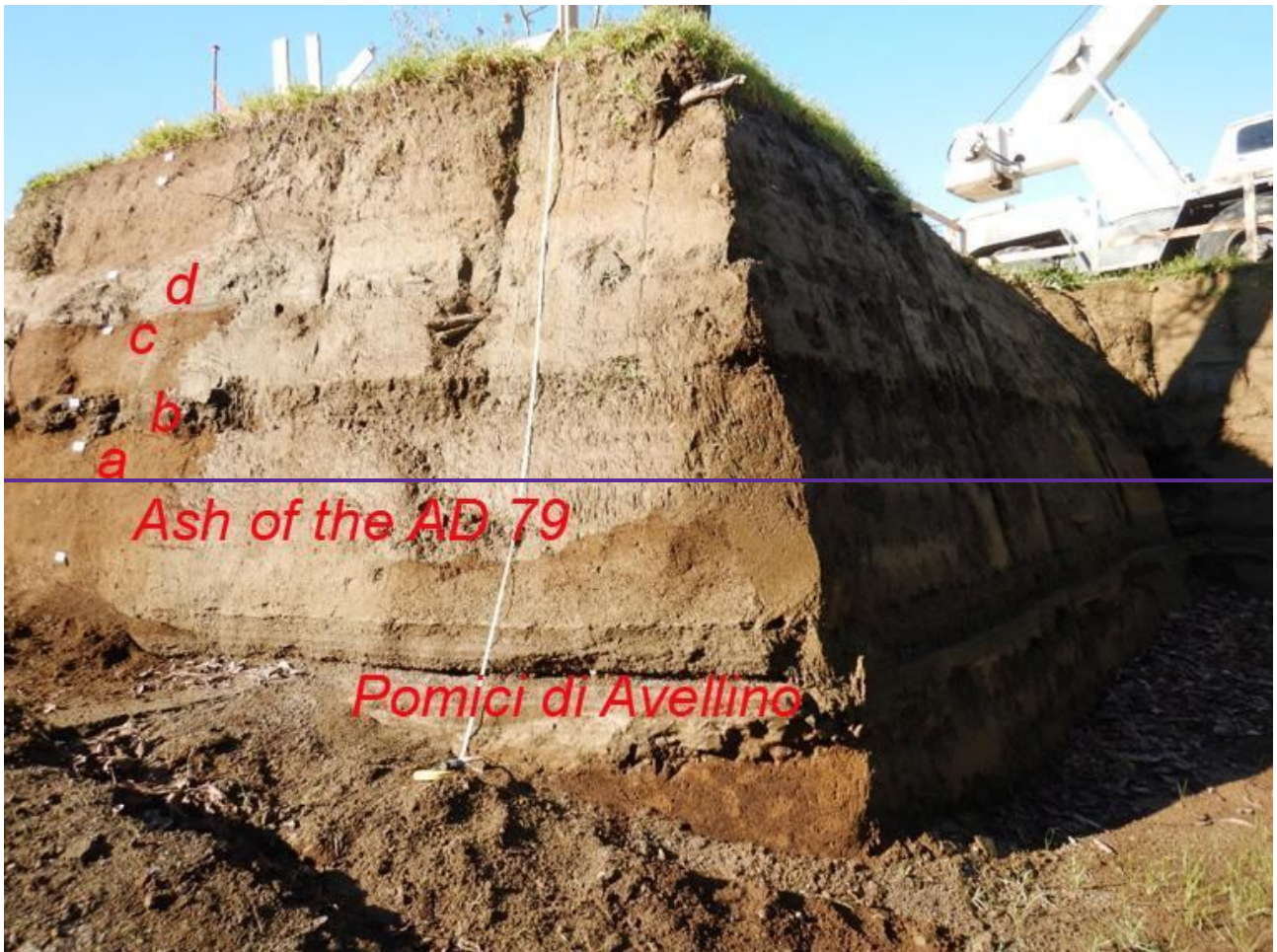
### 1166 *Area 3 – Pomigliano-Marigliano*

1167 This area is located along the northern outer part of the Vesuvius apron (Santacroce et al., 2003). The  
1168 studied sequences start from the paleosoil developed on top of the ash deposits of the AD 79  
1169 eruption. The paleosoil is mature and contains pottery fragments till the II century AD. Its top is  
1170 undulated with traces of ploughing spaced about 50 cm (a in Fig. C6). Representative sequences of  
1171 the area include a basal ash layer with a thickness ranging from 1 to 4 cm (b in Fig. C7), thickening  
1172 in the depressions, cohesive and locally vesiculated. It is here interpreted as co-ignimbritic ash  
1173 emplaced by fallout during the phreatomagmatic final phases of the Pollena eruption. Upwardly, the  
1174 sequence includes several lahar units from massive to slightly stratified, composed by of fine and  
1175 very cohesive ash, and containing scattered greenish pumice fragments (lithofacies mM) (b1 in Fig.  
1176 C7). Locally this deposit, also in the case of multiple units, is cut by vertical drying cracks. The  
1177 sequence is overlain by a 25-30 cm thick mature paleosoil, containing cultivation traces and majolica  
1178 fragments (c in Figs. C6 and C7).

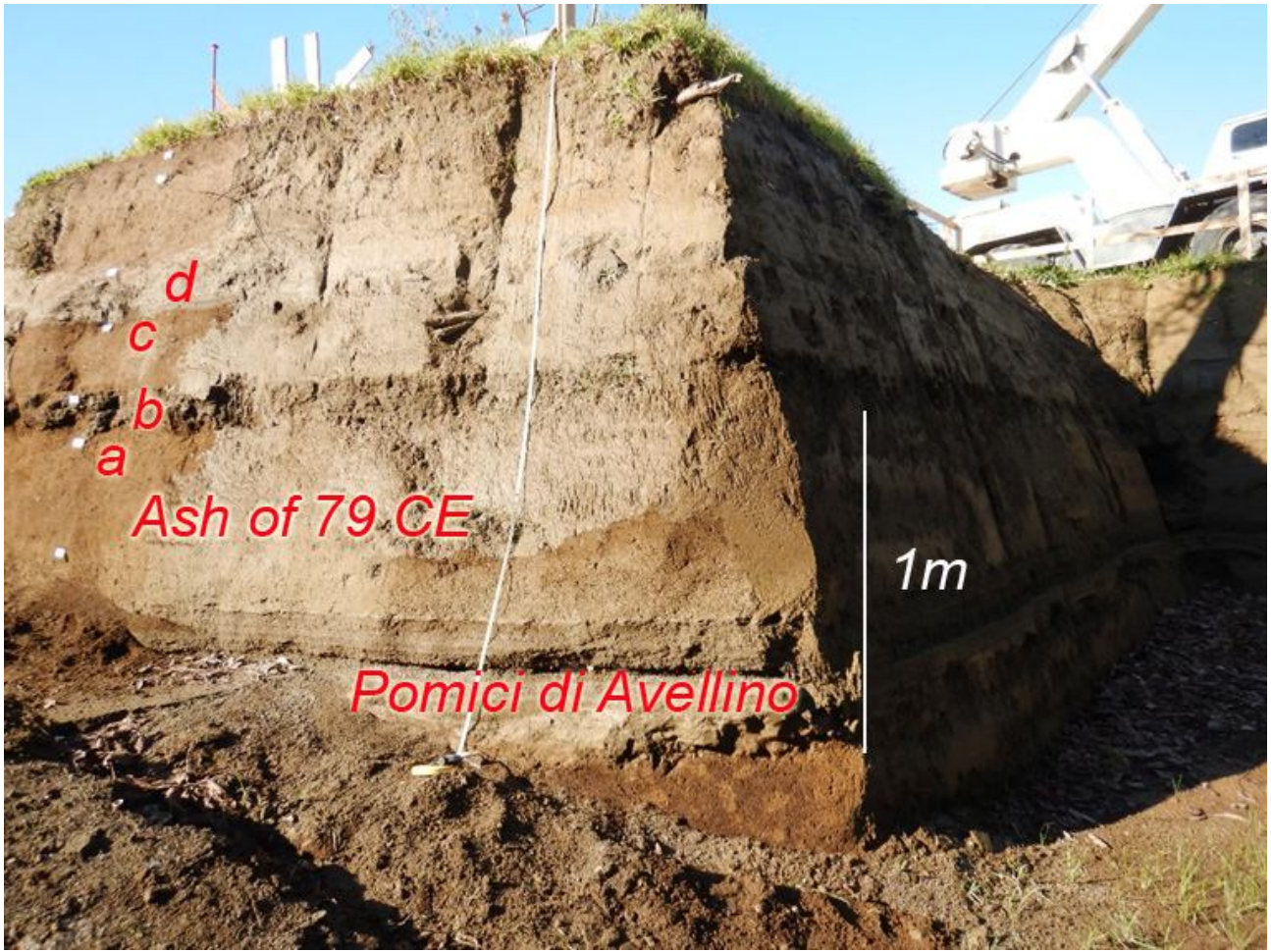
1179 The top of this paleosoil is undulated and covered by the primary deposit of the 1631 eruption (d in  
1180 Fig. C7). This latter is represented by a discontinuous medium-to-fine ash layer, slightly laminated  
1181 for contrasting grain-size, up to 5 cm thick, with a gray to violet color, and containing dark pumice  
1182 fragments and loose crystals of leucite, pyroxene and biotite (Fig. C7). Its thickness variation is due  
1183 both to slight internal variations (thickening in correspondence of depressions) and erosion by the  
1184 following lahars. These latter are composed of one to three flow units (d1 in Fig. C7), with a

1185 cumulative total thickness varying from 10 to 45 cm. They are composed of massive fine and very  
1186 cohesive ash, and contain rare scattered dark pumice fragments similar to those of the 1631 eruption  
1187 (lithofacies mM). These sequences are overlain by recent, cultivated soil. Locally, thin ash beds of  
1188 the recent Vesuvius activity (like 1822, 1906) overlie the 1631 deposits.

1189



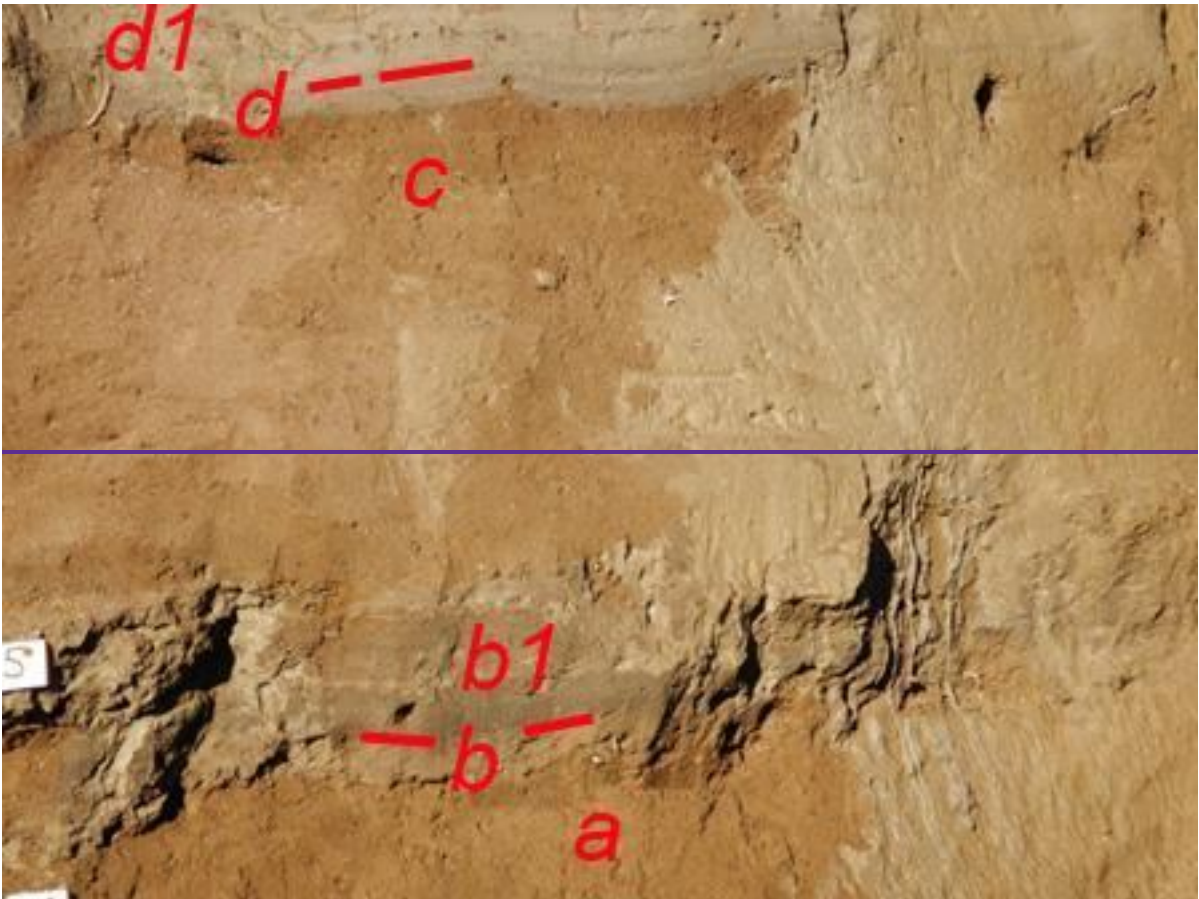
1190



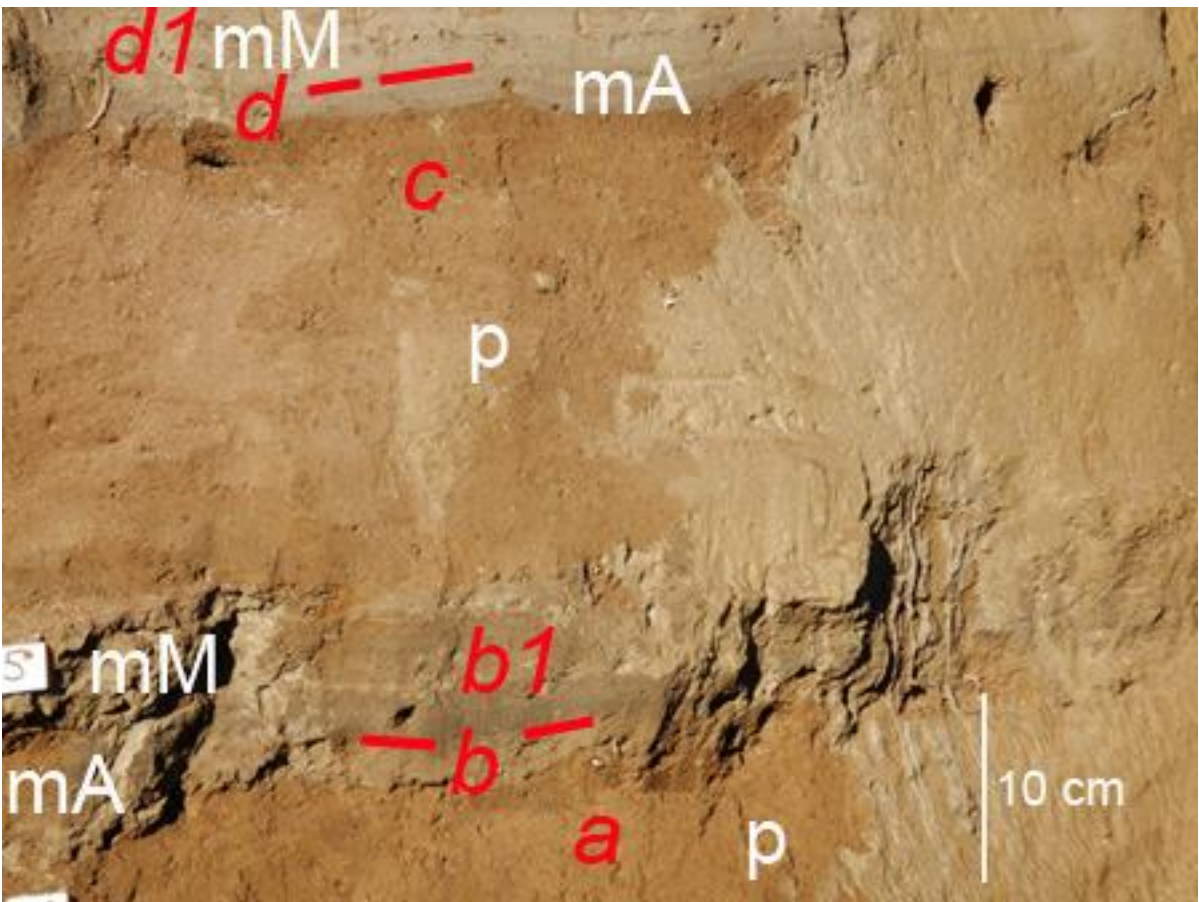
1191

1192 Fig. C6. Pomigliano locality. Sequence of deposits including bottom to top: Bronze Age paleosol, Pomici di Avellino  
 1193 (unit EU 5 of Di Vito et al., 2009), paleosol developed on top of Pomici di Avellino and buried by the Pollena eruption  
 1194 deposits. In the central part, fine ash deposits of the 79 CE eruption are visible. The top of the paleosol is undulated and  
 1195 ploughed. In particular: a = paleosol of Roman Age; a,b) = primary and secondary deposits of the Pollena eruption; c) =  
 1196 paleosol between Pollena and 1631 deposits; d) = 1631 primary and secondary deposits. Further details in Fig. C7.

1197



1198



1199

1200 Fig. C7. Particular of the Fig. C6: a) paleosoil containing potteries of the II Cent. AD; b) ash deposit of the Pollena  
1201 eruption; b1) syn-eruptive lahars of the Pollena eruption; c) paleosoil between Pollena and 1631; d) primary deposits  
1202 of the 1631 eruption, overlain by syn-eruptive lahars (d1). [For the description of lithofacies see Tab. 2.](#)

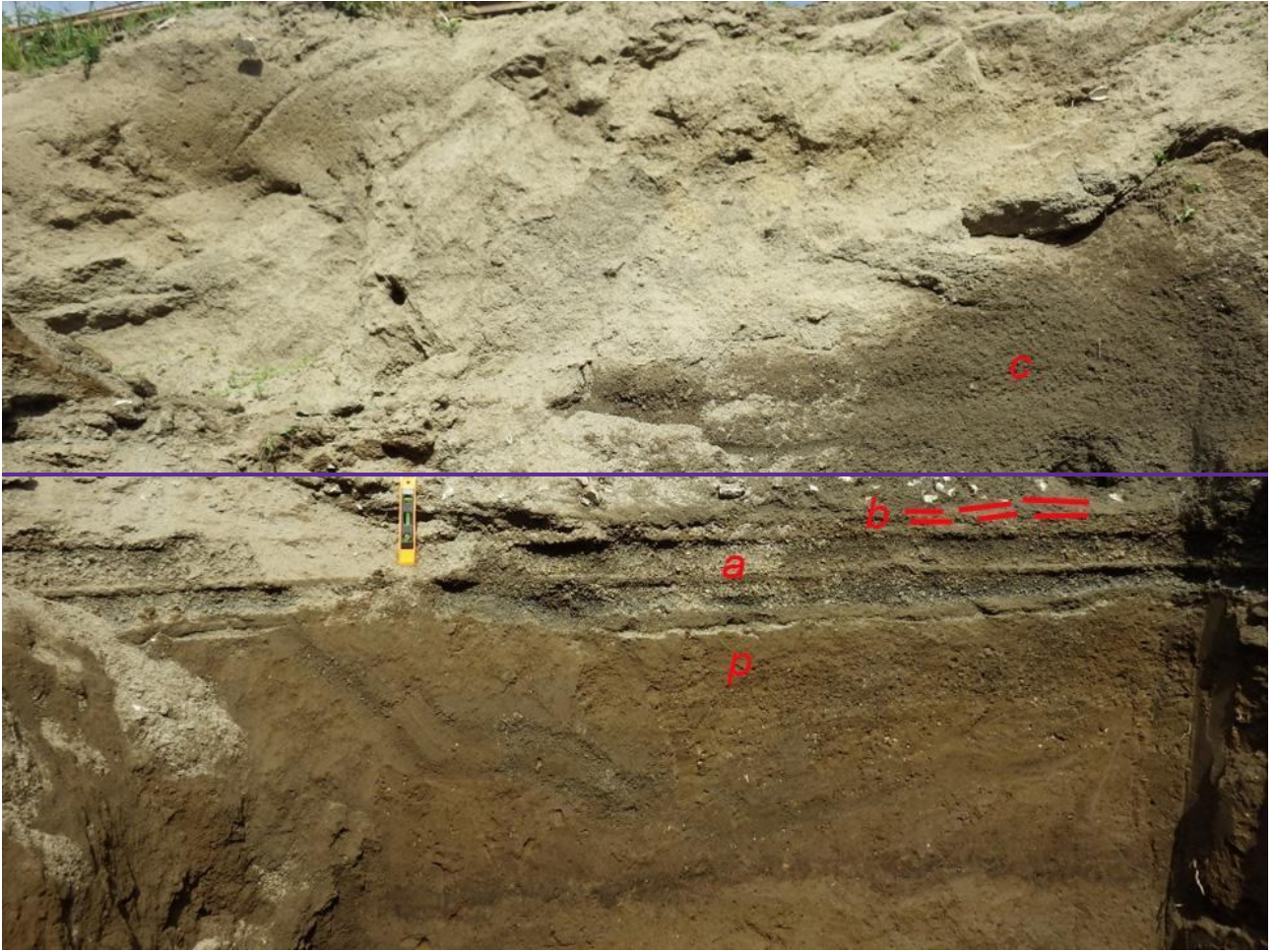
1203

#### 1204 *Area 4 – Avella-Baiano Valley*

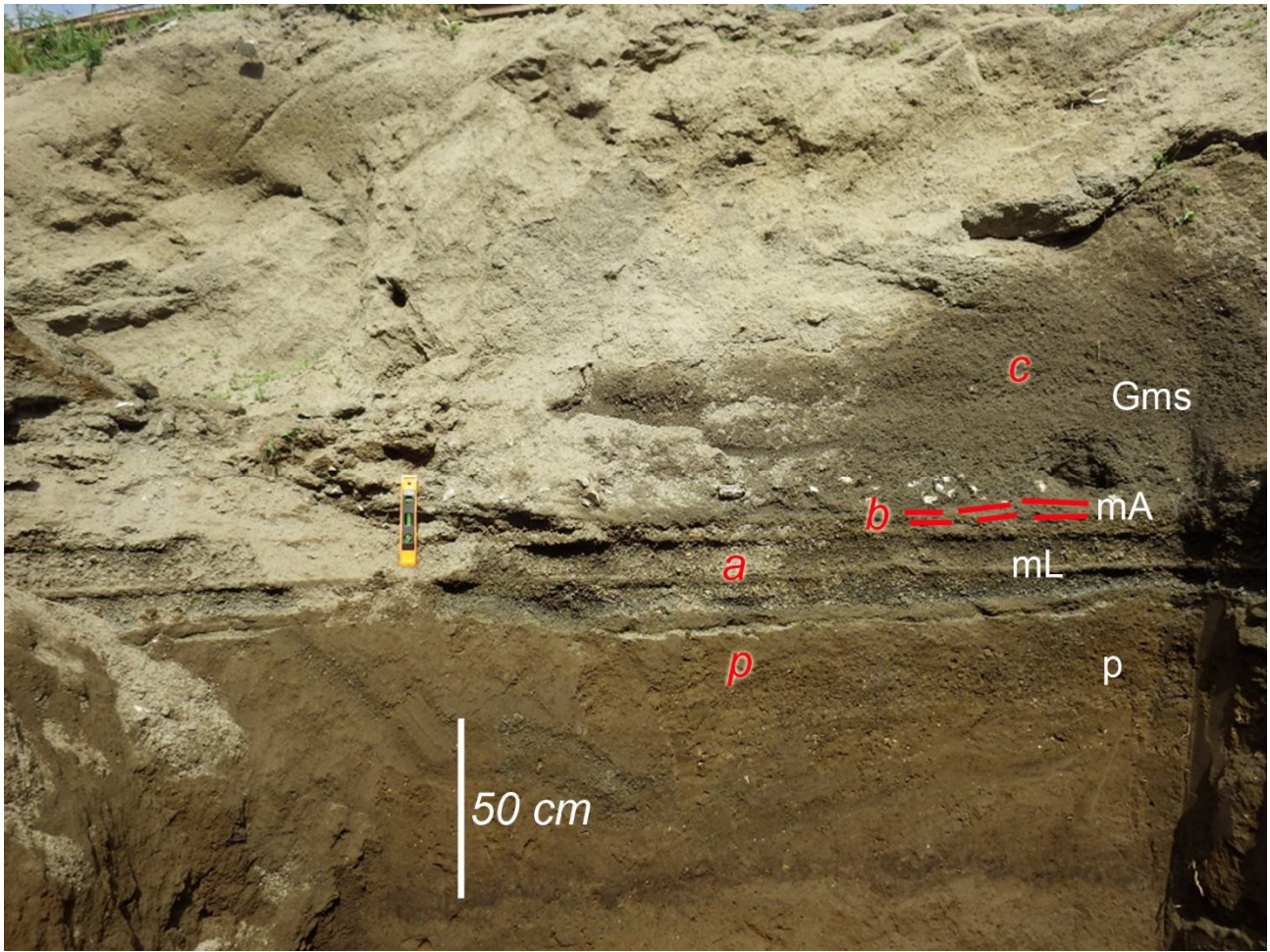
1205 We have analyzed several sequences along the *Avella-Baiano Valley*, both exposed and excavated  
1206 for the present work. Here the sequences of primary deposits are often affected by deep erosion, in  
1207 fact, in some places the Pollena primary deposits are completely lacking and only the syn-eruptive  
1208 lahar deposits are present on top of the late Roman paleosoil. Where preserved, the paleosoil has often  
1209 an undulated surface due to cultivation (ploughing and hoeing). The Pollena eruption sequence  
1210 consists of an alternation of coarse pumice and fine ash layers emplaced by fallout (a in Fig. C8). It  
1211 is up to 50 cm thick and ends with a cohesive yellowish ash layer (b in Fig. C8), overlain by the lahar  
1212 deposits, generally composed [by of](#) 2-3 flow units (c in Fig. C8). The total thickness of the lahars is  
1213 largely variable with maxima at the base of the slopes where it can reach 2-3 m. In some excavations  
1214 we did not reach the base of the deposit, deeper than 3.5 m. In Fig. C8, it is possible to observe a  
1215 complete sequence of [the Pollena](#) deposits ~~of Pollena~~ overlying a late Roman paleosoil. The sequence  
1216 includes the fallout layers and thick lahar deposits. These latter are always massive, matrix-supported,  
1217 and contain abundant scattered pumice and lithic fragments (lithofacies Gms). In some cases, the  
1218 lower part contains several limestone fragments up to 10 cm in diameter. The described deposit has  
1219 been also found in the Roman Amphitheatre of Avella, where it has a variable thickness (order of  
1220 decimetric). Here, it has been almost all excavated and only remnants are presently exposed.

1221 Generally, the upper part of the sequences is composed [by of](#) an alternation of plane-parallel to cross-  
1222 layered sands and gravels, with abundant rounded limestone fragments, emplaced by several alluvial  
1223 episodes (post-eruptive) (lithofacies Sh-Ss). In these post-eruptive deposits, it is not uncommon to  
1224 find terracotta fragments from the Imperial Roman age.





1225



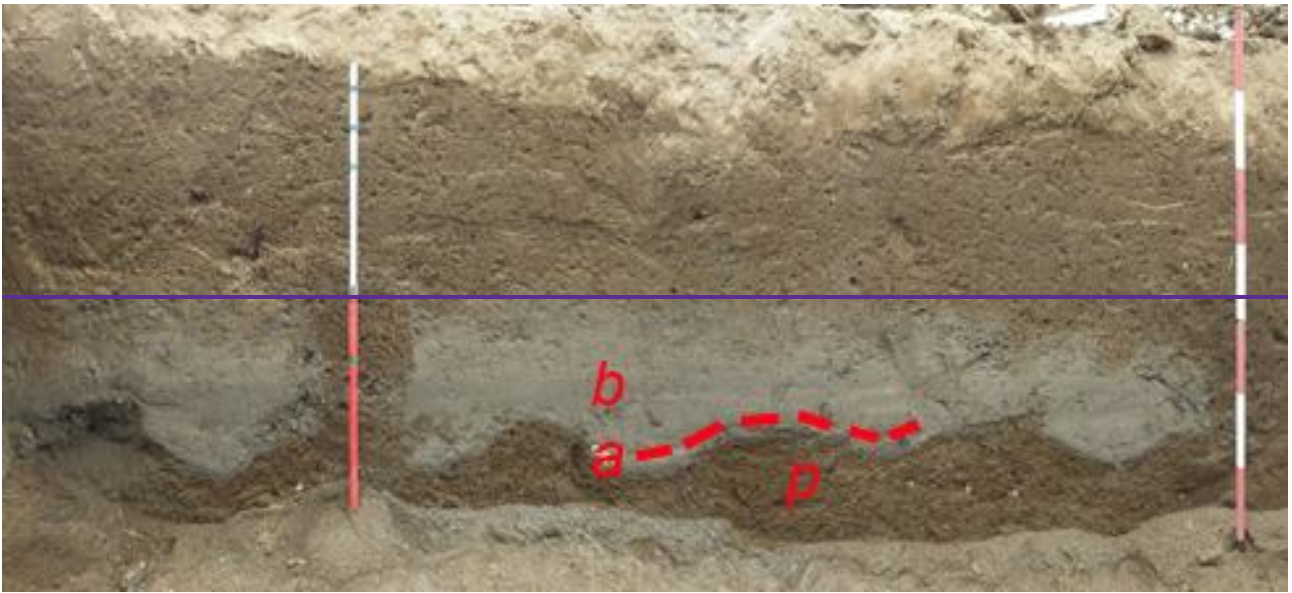
1226

1227 Fig. C8. Avella-Baiano Valley [Avella valley](#). The Pollena primary deposit (a,b) lies on a ploughed soil (p), and is covered  
 1228 by at least three flow units of lahars (c). [For the description of lithofacies see Tab. 2.](#)

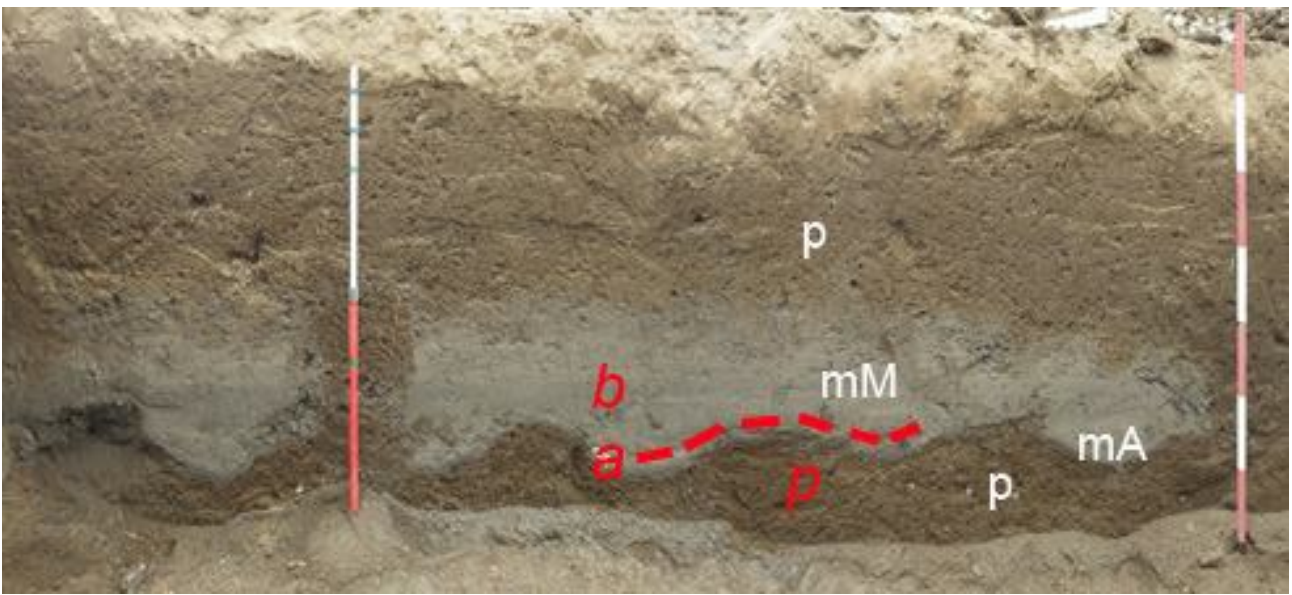
1229

1230 The Pollena primary and secondary sequences are overlain by a mature paleosol with frequent  
 1231 evidence of cultivation (ploughing, p in Fig. C9) and locally by the 1631 eruption deposits. The  
 1232 primary deposit related to the 1631 eruption is not always present. It is up to 2 cm (a in Fig. C9) thick  
 1233 ash layer, gray-violet in color deposited by fallout deposit and overlaying a ploughed paleosol (p in  
 1234 Fig. C9). It is overlain by lahar deposits (b in Fig. C9) composed [by of](#) several units and characterized  
 1235 by contrasting grain-sizes. The deposits are composed of medium ash, are massive and matrix-  
 1236 supported, and contain abundant scattered mm- to cm-sized pumice fragments (all with the same  
 1237 lithology of the primary deposits) and sometimes vegetal remain traces (lithofacies Gms).

1238



1239



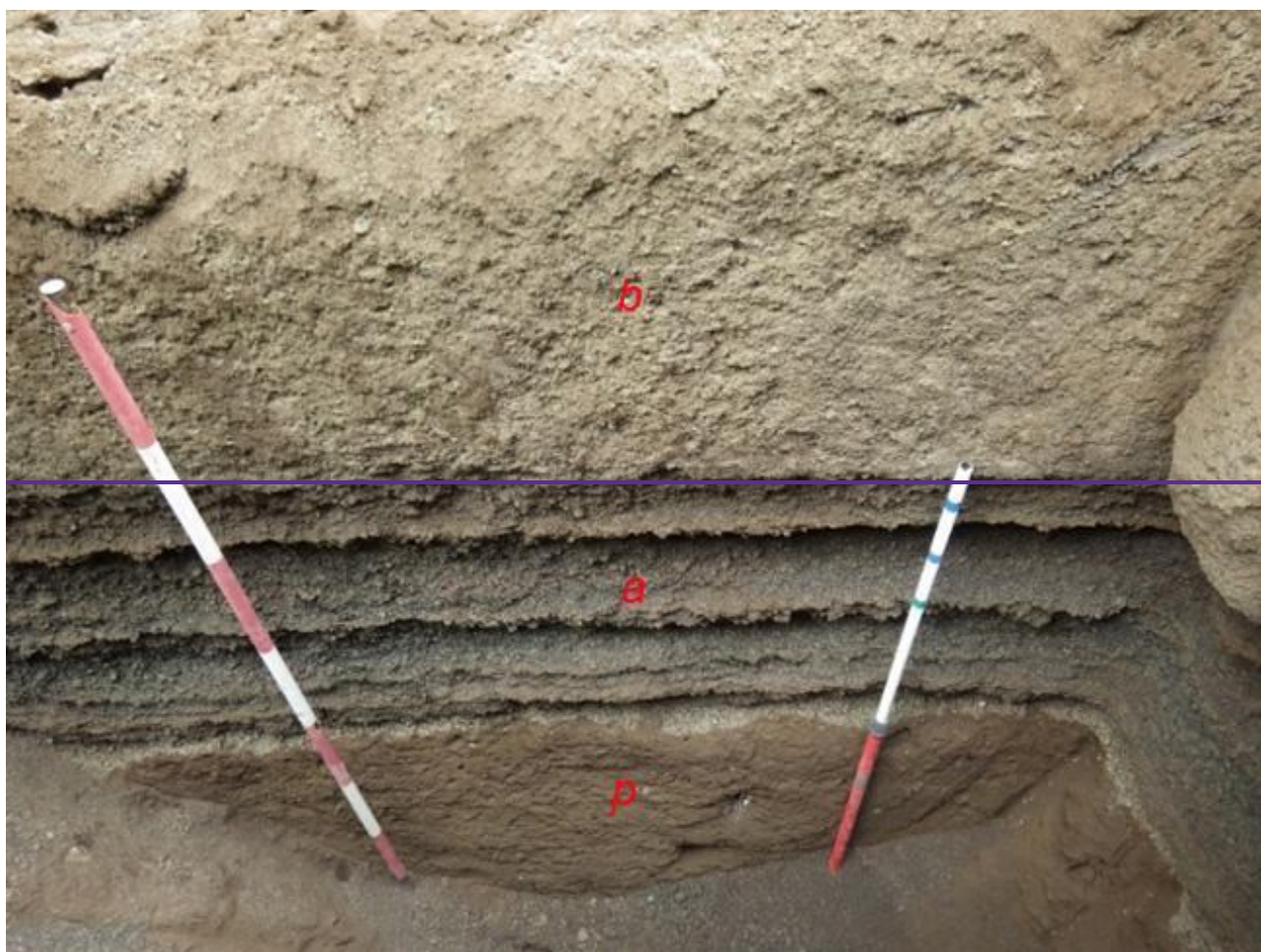
1240 Fig. C9. Avella-Baiano Valley *Avella valley*: particular of the 1631 primary (a) and secondary deposits (b, syn-eruptive  
 1241 lahars) in a trench at Cicciano locality. [For the description of lithofacies see Tab. 2.](#)

1242

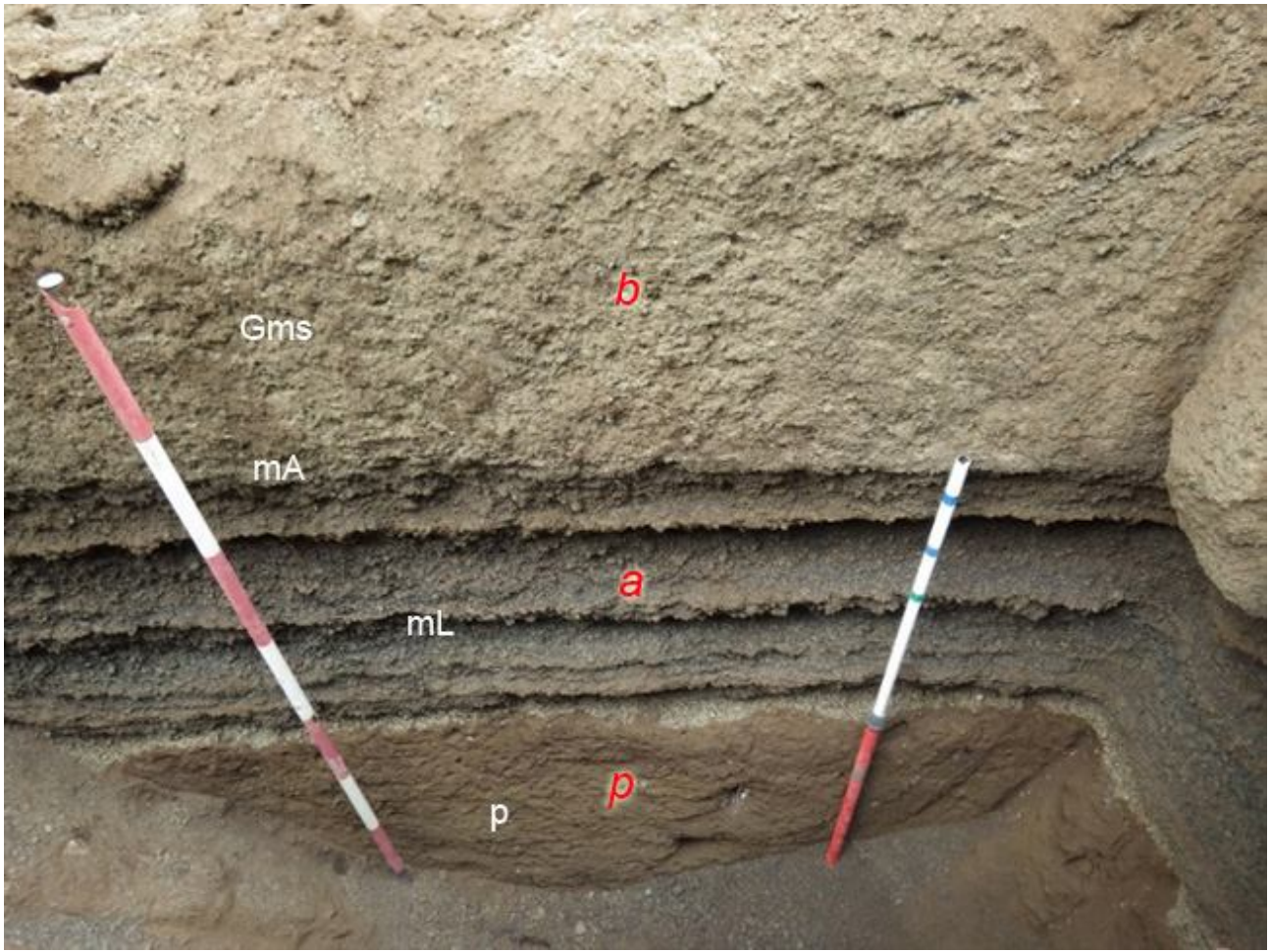
1243 *Area 5 – Lauro Valley* *Vallo di Lauro*

1244 Lauro Valley *Vallo di Lauro* has characteristics similar to the Avella-Baiano Valley *Avella valley*, but  
 1245 the primary deposits of Pollena and 1631 eruptions are thicker (Figs. 5 and 6) and coarser. In this  
 1246 valley, also the sequences are locally deeply eroded. In fact, the deposits of the Pollena eruption  
 1247 (normally 50-70 cm thick) (Fig. C10) are sometimes missing. They overlie a mature paleosol with  
 1248 abundant traces of cultivation. Overall, the characteristics of the deposits are very similar to the ones

1249 of the Nola area. The overlying lahar deposits are always massive, matrix-supported, and composed  
1250 of fine and very cohesive ash with abundant scattered pumices and lithic fragments (similar in  
1251 lithology to those of the primary deposits) (lithofacies Gms). These deposits have a high variable  
1252 thickness, with a measured maximum ~~up to~~ of 2 m, but sometimes reduced by erosion. In some  
1253 trenches the base of the sequences was deeper than the investigated depth (>3.5 m).  
1254



1255



1256

1257 Fig. C10. Lauro Valley, Pago del ~~Lauro Valley~~ ~~Vallo~~ ~~Vallo di Lauro~~. In particular: a = Sequence of the Pollena fallout  
 1258 deposits (a) overlain by syn-eruptive lahars (b); p = At the base the late Roman paleosol at the base (p). For the  
 1259 description of lithofacies see Tab. 2.

1260

1261 It is possible to evaluate the effects of the lahars on building in the Roman Villa di Lauro, at Taurano,  
 1262 where a 70 cm thick fallout is overlain, without paleosol, by syn-eruptive lahars which engulfed and  
 1263 transported pieces of walls, bricks and potteries. The lahar deposits are matrix supported and  
 1264 composed by of fine to coarse ash and contain abundant pumice lapilli (all similar to the Pollena  
 1265 fallout deposits). They are massive, cohesive and have a thickness up to about 1 m, thickening in  
 1266 depressions and near barriers (Fig. C11).

1267 The sequence related to the eruption of 1631 is not always present, but it is possible to find its primary  
 1268 deposit, composed by of a basal layer of stratified fine and medium thin ash beds, and minor dark

1269 pumice and lithic fragments overlain by a thin, very fine and cohesive accretionary lapilli-rich ash  
1270 bed. The maximum measured thickness is 30 cm. The overlying lahar deposits are massive and  
1271 matrix-supported, composed of fine to coarse ash and contain abundant pumice fragments of the  
1272 primary deposit.



1273

1274 Fig. C11. Taurano (Villa Lauro), baulk showing a thick sequence of [the Pollena syn-eruptive](#) lahar units filling the Roman  
1275 Villa. Some units engulf and transport pieces of walls and large blocks. [The fallout sequence is not exposed in the Villa,](#)  
1276 [likely due to the presence of a roof. The deposit below the damaged walls is composed of multiple lahar units represented](#)  
1277 [by the Gms lithofacies \(see Tab. 2\).](#)

1278

### 1279 **Author contribution**

1280 MDV: conceptualization, investigation, methodology, writing - original draft preparation, writing -  
1281 review & editing, funding acquisition; IR: data curation, investigation, writing - original draft  
1282 preparation; SdV: investigation, writing - original draft preparation, writing - review & editing; DMD:

1283 investigation, methodology, data curation, writing - original draft preparation, writing - review &  
1284 editing; MB: data curation, methodology, writing - original draft preparation; MdMV: writing -  
1285 review & editing; MR: conceptualization, writing - review & editing; LS: writing - review & editing;  
1286 GZ: investigation, writing - review & editing; EZ: investigation, methodology, writing - original draft  
1287 preparation; AC: conceptualization, writing - review & editing, funding acquisition.

1288

## 1289 **Acknowledgements**

1290 This work benefited of the agreement between Istituto Nazionale di Geofisica e Vulcanologia and  
1291 the Italian Presidenza del Consiglio dei Ministri, Dipartimento della Protezione Civile (DPC),  
1292 Convenzione [INGV-DPC All. B2](#). [The work was also supported by the INGV project Pianeta](#)  
1293 [Dinamico—Working Earth \(CUP 1466 D53J19000170001—“Fondo finalizzato al rilancio degli](#)  
1294 [investimenti delle 1467 amministrazioni centrali dello Stato e allo sviluppo del Paese”, legge](#)  
1295 [145/2018\)—Task V3 \(MDV\)](#). The paper does not necessarily represent DPC official opinion and  
1296 policies. [We thank very much Ulrich Kueppers, Lucia Capra and an anonymous reviewer for their](#)  
1297 [help in improving this manuscript in the revision process.](#)

1298

## 1299 **References**

- 1300 Acocella V and Funiciello R (2006) Transverse systems along the extensional Tyrrhenian margin of  
1301 Central Italy and their influence on volcanism. *Tectonics* 25,1-24.
- 1302 Arguden AT and Rodolfo KS (1990) Sedimentologic and dynamic differences between hot and cold  
1303 laharic debris flows of Mayon Volcano, Philippines. *Geological Society of America Bulletin* 102,  
1304 865-876.
- 1305 Bardot L (2000) Emplacement temperature determinations of proximal pyroclastic deposits on  
1306 Santorini, Greece, and their implications. *Bulletin of Volcanology* 61, 450-467.
- 1307 Bardot L, McClelland E (2000) The reliability of emplacement temperature estimates using  
1308 paleomagnetic methods: a case study from Santorini, Greece. *Geophysical Journal International* 143,  
1309 39-51.

- 1310 Bartole R (1984) Tectonic Structure of the Latian-Campanian Shelf (Tyrrhenian Sea). *Bollettino di*  
1311 *Oceanologia Teorica Applicata* 2, 197-230.
- 1312 [Baumann V, Bonadonna C, Cuomo S, Moscariello M \(2020\) Modelling of erosion processes](#)  
1313 [associated with rainfall-triggered lahars following the 2011 Cordon Caulle eruption \(Chile\). \*Journal\*](#)  
1314 [of \*Volcanology and Geothermal Research\* 390, 106727.](#)
- 1315 Bisson M, Pareschi MT, Zanchetta G, Sulpizio R, Santacroce R (2007) Volcaniclastic debris-flow  
1316 occurrences in the Campania region (Southern Italy) and their relation to Holocene–Late Pleistocene  
1317 pyroclastic fall deposits: implications for large-scale hazard mapping. *Bulletin of Volcanology* 70,  
1318 157-167.
- 1319 Bisson M, Spinetti C, Sulpizio R (2014) Volcaniclastic flow hazard zonation in the Sub-Apennine  
1320 Vesuvian area using GIS and remote sensing. *Geosphere* 10, 1419-1431.
- 1321 Bisson M, Zanchetta G, Sulpizio R, Demi F (2013) A map for volcaniclastic debris flow hazards in  
1322 Apennine areas surrounding the Vesuvius volcano (Italy). *Journal of Maps* 9, 230-238.
- 1323 Blott SJ and Pye K (2001) Gradistat: A Grain Size Distribution and Statistics Package for the Analysis  
1324 of Unconsolidated Sediments. *Earth Surface Processes and Landforms* 26, 1237-1248.
- 1325 Braccini GC (1632) Dell'Incendio Fattosi nel Vesuvio a XVI di Dicembre MDCXXXI. Secondino  
1326 Roncagliolo, 104 pp.
- 1327 Brancaccio L, Cinque A, Romano P, Roszkopf C, Russo F, Santangelo N, Santo A (1991)  
1328 Geomorphology and neotectonic evolution of a sector of the Tyrrhenian flank of the Southern  
1329 Apennines (Region of Naples, Italy). *Zeitschrift für Geomorphologie Supplement Bd.* 82, 47-58.
- 1330 Breard ECP, Lube G, Cronin SJ, Valentine GA (2015) Transport and deposition processes of the  
1331 hydrothermal blast of the 6 August 2012 Te Maari eruption, Mt. Tongariro. *Bulletin of Volcanology*  
1332 77, 100.



- 1333 [Breard ECP, Lube G \(2017\) Inside pyroclastic density currents – uncovering the enigmatic flow](#)  
1334 [structure and transport behaviour in large-scale experiments. Earth and Planetary Science Letters 458,](#)  
1335 [22-36.](#)
- 1336 Brocchini D, Principe C, Castradori D, Laurenzi MA, Gorla L (2001) Quaternary evolution of the  
1337 southern sector of the Campanian Plain and early Somma-Vesuvius activity: insights from the Trecase  
1338 1 well. *Mineralogy and Petrology* 73, 67-91.
- 1339 [Capra L, Sulpizio R, Marquez-Ramirez VH, Coviello V, Doronzo DM, Arambula-Mendoza R, Cruz](#)  
1340 [S \(2018\) The anatomy of a pyroclastic density current: the 10 July 2015 event at Volcan de Colima](#)  
1341 [\(Mexico\). Bulletin of Volcanology 80, 34.](#)
- 1342 Carling PA (2013) Freshwater megaflood sedimentation: What can we learn about generic processes?  
1343 *Earth-Science Reviews* 125, 87-113.
- 1344 Carrara E, Iacobucci F, Pinna E, Rapolla A (1973) Gravity and magnetic survey of the Campanian  
1345 volcanic area, S. Italy. *Bollettino di Geofisica Teorica e Applicata* 15, 39-51.
- 1346 Cas RAF, Wright HMN, Folkes CB, Lesti C, Porreca M, Giordano G, Viramonte JG (2011) The flow  
1347 dynamics of an extremely large volume pyroclastic flow, the 2.08-Ma Cerro Galán Ignimbrite, NW  
1348 Argentina, and comparison with other flow types. *Bulletin of Volcanology* 73, 1583-1609.
- 1349 Cinque A and Robustelli G (2009) Alluvial and coastal hazards caused by long-range effects of  
1350 Plinian eruptions: The case of the Lattari Mts. After the AD 79 eruption of Vesuvius. *Geological*  
1351 *Society London Special Publications* 322, 155-171.
- 1352 [Cioni R, Santacroce R, Sbrana A \(1999\) Pyroclastic deposits as a guide for reconstructing the multi-](#)  
1353 [stage evolution of the Somma-Vesuvius Caldera. Bulletin of Volcanology 60, 207-222.](#)
- 1354 Cioni R, Gurioli L, Lanza R, Zanella, E (2004) Temperatures of A.D. 79 pyroclastic density current  
1355 deposits (Vesuvius, Italy). *Journal of Geophysical Research* 109, B02207.

- 1356 Costa JE (1997) Hydraulic modeling for lahar hazards at Cascades volcanoes. Environmental  
1357 Engineering Geoscience 3, 21-30.
- 1358 D'Argenio B, Pescatore TS, Scandone P (1973) Schema geologico dell'Appennino meridionale  
1359 (Campania e Lucania). In: Moderne vedute sulla geologia dell'Appennino. Convegno (Roma, 16-18  
1360 Febbraio 1972). Accademia Nazionale dei Lincei, Problemi Attuali di Scienza e Cultura, Quaderni  
1361 183, 49-72.
- 1362 ~~[De Falco M, Forte G, Marino E, Massaro L, Santo A \(2023\) UAV and field survey observations on](#)~~  
1363 ~~[the November 26th 2022 Celario flowslide, Ischia Island \(Southern Italy\). Journal of Maps 19,](#)~~  
1364 ~~[2261484.](#)~~
- 1365 de' Michieli Vitturi M, Costa A, Di Vito MA, Sandri L, Doronzo DM ([submitted this issue](#)). Lahar  
1366 events in the last 2,000 years from Vesuvius eruptions. Part 2: Formulation and validation of a  
1367 computational model based on a shallow layer approach.
- 1368 De Simone GF, Perrotta A, Scarpati C (2011) L'eruzione del 472 d.C. ed il suo impatto su alcuni siti  
1369 alle falde del Vesuvio. Rivista Studi Pompeiani 22, 61-71.
- 1370 De Vivo B, Rolandi G, Gans PB, Calvert A, Bohrson WA, Spera FJ, Belkin HE (2001) New  
1371 constraints on the pyroclastic eruptive history of the Campanian volcanic Plain (Italy). Mineralogy  
1372 and Petrology 73, 47-65.
- 1373 Di Crescenzo G and Santo A (2005) Nuovo contributo sul ruolo svolto dai livelli pomicei nelle aree  
1374 di distacco delle frane di colata rapida dei massicci carbonatici campani. Convegno Nazionale La  
1375 mitigazione del rischio da colate di fango a Sarno e negli altri Comuni colpiti dagli eventi del maggio  
1376 1998. Napoli, 2 e 3 maggio 2005 - Sarno 4 e 5 maggio 2005.
- 1377 Di Vito MA, Castaldo N, de Vita S, Bishop J, Vecchio G (2013) Human colonization and volcanic  
1378 activity in the eastern Campania Plain (Italy) between the Eneolithic and Late Roman periods.

1379 Quaternary International 303, 132-141.

1380 Di Vito MA, Sulpizio R., Zanchetta G (1998). I depositi ghiaiosi della valle dei torrenti Clanio e  
1381 Acqualonga (Campania centro-orientale): significato stratigrafico e ricostruzione paleoambientale. Il  
1382 Quaternario Italian Journal of Quaternary Sciences 11, 273-286.

1383 Di Vito MA, Talamo P, de Vita S, Rucco I, Zanchetta G, Cesarano M (2019) Dynamics and effects  
1384 of the Vesuvius Pomice di Avellino Plinian eruption and related phenomena on the Bronze Age  
1385 landscape of Campania region (Southern Italy). Quaternary International 499, 231-244.

1386 Di Vito M, Zanella E, Gurioli L, Lanza R, Sulpizio R, Bishop J, Tema E, Boenzi G, Laforgia E (2009)  
1387 The Afragola settlement near Vesuvius, Italy: The destruction and abandonment of a Bronze Age  
1388 village revealed by archeology, volcanology and rock-magnetism. Earth and Planetary Science  
1389 Letters 277, 408-421.

1390 [Doronzo DM \(2012\) Two new end members of pyroclastic density currents: Forced-convection](#)  
1391 [dominated and inertia-dominated. Journal of Volcanology and Geothermal Research 219-220, 87-91.](#)

1392 Doronzo DM, Martí J, Sulpizio R, Dellino P (2012) Aerodynamics of stratovolcanoes during  
1393 multiphase processes. Journal of Geophysical Research 117, B01207.

1394 Doronzo DM, Dellino P (2013) Hydraulics of subaqueous ash flows as deduced from their deposits:  
1395 2. Water entrainment, sedimentation, and deposition, with implications on pyroclastic density current  
1396 deposit emplacement. Journal of Volcanology and Geothermal Research 258, 176-186.

1397 Doronzo DM (2013) Aeromechanic analysis of pyroclastic density currents past a building. Bulletin  
1398 of Volcanology 75, 684.

1399 Duller RA, Mountney NP, Russell AJ, Cassidy NC (2008) Architectural analysis of a volcanoclastic  
1400 jökulhlaup deposit, southern Iceland: sedimentary evidence for supercritical flow. Sedimentology 55,  
1401 939-964.

1402 Faccenna C, Funiciello R, Bruni A, Mattei M, Sagnotti L (1994) Evolution of a transfer related basin:  
1403 the Ardea basin (Latium, Central Italy). *Basin Resources* 5, 1-11.

1404 Fedi M and Rapolla A (1987) The Campanian Volcanic Area: analysis of the magnetic and  
1405 gravimetric anomalies. *Bollettino della Società Geologica Italiana* 106, 793-805.

1406 Finetti I and Morelli C (1974) Esplorazione di sismica a riflessione nei Golfi di Napoli e Pozzuoli.  
1407 *Bollettino di Geofisica Teorica e Applicata* 16, 62-63.

1408 Fiorillo F and Wilson RC (2004) Rainfall induced debris flows in pyroclastic deposits, Campania  
1409 (southern Italy). *Engineering Geology* 75, 263-289.

1410 Giordano G, Zanella E, Trolese M, Baffioni C, Vona A, Caricchi C, De Benedetti AA, Corrado S,  
1411 Romano C, Sulpizio R, Geshi N (2018) Thermal interactions of the AD79 Vesuvius pyroclastic  
1412 density currents and their deposits at Villa dei Papiri (Herculaneum archaeological site, Italy). *Earth  
1413 and Planetary Science Letters* 490, 180-192.

1414 Girolami L, Roche O, Druitt T, Corpetti T (2010) Velocity fields and depositional processes in  
1415 laboratory ash flows, with implications for the dynamics of dense pyroclastic flows. *Bulletin of  
1416 Volcanology* 72, 747-759.

1417 Gurioli L, Pareschi MT, Zanella E, Lanza R, Deluca E, Bisson M (2005) Interaction of pyroclastic  
1418 density currents with human settlements: Evidence from ancient Pompeii. *Geology* 33, 441-444.

1419 Gurioli L, Sulpizio R, Cioni R, Sbrana A, Santacroce R, Luperini W, Andronico D (2010) Pyroclastic  
1420 flow hazard assessment at Somma-Vesuvius based on the geological record. *Bulletin of Volcanology*  
1421 72, 1021-1038.

1422 Guzman S, Doronzo DM, Martí J, Seggiaro R (2020). Characteristics and emplacement mechanisms  
1423 of the Coranzulí ignimbrites (Central Andes). *Sedimentary Geology* 405, 105699.

- 1424 Ippolito F, Ortolani F, Russo M (1973) Struttura marginale tirrenica dell'Appennino campano:  
1425 reinterpretazioni di dati di antiche ricerche di idrocarburi. *Memorie della Società Geologica Italiana*  
1426 12, 227–250.
- 1427 Iverson RM, Denlinger RP, LaHusen RG, Logan M, (2000) Two-phase debris-flow across 3-D  
1428 terrain: Model predictions, *in* Wieczorek GF and Naeser ND, eds., *Debris-Flow Hazard Mitigation,*  
1429 *Mechanics, Prediction, and Assessment: Taipei, Taiwan, 16-18 August 2000: Rotterdam, Balkema,*  
1430 521-529.
- 1431 Jenkins SF, Phillips JC, Price R, Feloy K, Baxter PJ, Sri Hadmoko D, de Bélizal E (2015) Developing  
1432 building-damage scales for lahars: application to Merapi volcano Indonesia. *Bulletin of Volcanology*  
1433 77, 1-17.
- 1434 Lesti C, Porreca M, Giordano G, Mattei M, Cas R, Wright H, Viramonte J (2011) High temperature  
1435 emplacement of the Cerro Galán and Toconquis Group ignimbrites (Puna plateau, NW Argentina)  
1436 determined by TRM analyses. *Bulletin of Volcanology* 73, 1535-1565.
- 1437 Lowe DR, Williams SN, Leigh H, Connort CB, Gemmell JB, Stoiber RE (1986) Lahars initiated by  
1438 the 13 November 1985 eruption of Nevado del Ruiz, Colombia. *Nature* 324, 51-53.
- 1439 Lowe DR (1988) Suspended-load fallout rate as an independent variable in the analysis of current  
1440 structures. *Sedimentology* 35, 765–776.
- 1441 Lube G, Cronin S, Manville V, Procter J, Cole S, Freundt A (2012) Energy growth in laharcic mass  
1442 flows. *Geology* 40, 475-478.
- 1443 Macedonio G and Pareschi MT (1992) Numerical simulation of some lahars from Mount St. Helens.  
1444 *Journal of Volcanology and Geothermal Research* 54, 65-80.
- 1445 [Manville V, Nemeth K, Kano K \(2009\) Source to sink: A review of three decades of progress in the](#)  
1446 [understanding of volcanoclastic processes, deposits, and hazards. \*Sedimentary Geology\* 220, 136-161.](#)

- 1447 Mariani M and Prato R (1988) I bacini neogenici costieri del margine tirrenico: approccio sismico-  
1448 stratigrafico. *Memorie della Società Geologica Italiana* 41, 519-531.
- 1449 Marotta E., Berrino G., de Vita S., Di Vito M.A., Camacho A.G., 2022. Structural setting of the Ischia  
1450 resurgent caldera (Southern Tyrrhenian Sea, Italy) by integrated 3D gravity inversion and geological  
1451 models. In: Marotta, E., D’Auria, L., Zaniboni, F. and Nave, R. (eds) *Volcanic Island: from Hazard  
1452 Assessment to Risk Mitigation*. Geological Society, London, Special Publications, 519.
- 1453 Martí J, Doronzo DM, Pedrazzi D, Colombo F (2019) Topographical controls on small-volume  
1454 pyroclastic flows. *Sedimentology* 66, 2297-2317.
- 1455 McClelland E, Druitt TH (1989) Paleomagnetic estimates of emplacement temperatures of  
1456 pyroclastic deposits on Santorini, Greece. *Bulletin of Volcanology* 51, 16-27.
- 1457 McClelland E (1996) Theory of CRM acquired by grain growth, and its implications for TRM  
1458 discrimination and paleointensity determination in igneous rocks. *Geophysical Journal International*  
1459 126, 271-280.
- 1460 Newhall CG and Punongbayan R (Eds.) (1996) *Fire and mud: eruptions and lahars of Mount  
1461 Pinatubo, Philippines*. Quezon City: Philippine Institute of Volcanology and Seismology, 1126 pp.
- 1462 Orsi G, de Vita S, Di Vito MA (1996) The restless, resurgent Campi Flegrei Nested Caldera Italy.:  
1463 constraints on its evolution and configuration. *Journal of Volcanology and Geothermal Research* 74,  
1464 179-214.
- 1465 Pareschi MT, Favalli M, Giannini F, Sulpizio R, Zanchetta G, Santacroce R (2000) May 5, 1998,  
1466 Debris flows in circumvesuvian areas (Southern Italy), insights for hazard assessment. *Geology* 28,  
1467 639-642.

- 1468 Pareschi MT, Santacroce R, Sulpizio R, Zanchetta G (2002) The volcanoclastic mass flow hazard  
1469 related to the remobilization of fallout deposits in southern Campania, Italy. Explosive volcanism in  
1470 subduction zones, Mount Pelée, Martinique, 12-16 May 2002, abstract volume.
- 1471 Patacca E and Scandone P (2007) Geology of the Southern Apennines. *Bollettino della Società*  
1472 *Geologica Italiana Special Issue 7*, 75-119.
- 1473 Paterson, GA, Muxworthy AR, Roberts AP, MacNiocaill C (2010). Paleomagnetic determination of  
1474 emplacement temperatures of pyroclastic deposits: an under-utilized tool. *Bulletin of Volcanology*,  
1475 72, 309-330.
- 1476 Peccerillo A (2003) Plio-Quaternary magmatism in Italy. *Episodes* 26, 222-226.
- 1477 Perrotta A, Scarpati C, Luongo G, Aoyagi M (2006) Burial of Emperor Augustus' villa at Somma  
1478 Vesuviana (Italy) by post-79 AD Vesuvius eruptions and reworked (lahars and stream flow) deposits.  
1479 *Journal of Volcanology and Geothermal Research* 158, 445-466.
- 1480 Pierson TC (1985) Initiation and flow behavior of the 1980 Pine Creek and Muddy River lahars, Mt.  
1481 St. Helens, Washington. *Geological Society of America Bulletin* 96, 1056-1069.
- 1482 Piochi M, Pappalardo L, Dea Astis G (2004) Geo-chemical and isotopical variations within the  
1483 Campanian Comagmatic Province: implications on magma source composition, *Annals of*  
1484 *Geophysics* 47, 1485-1499.
- 1485 Pittari A, Cas RAF, Monaghan JJ, Martí J (2007) Instantaneous dynamic pressure effects on the  
1486 behaviour of lithic boulders in pyroclastic flows: the Abrigo Ignimbrite, Tenerife, Canary Island.  
1487 *Bulletin of Volcanology* 69, 265-279.
- 1488 Porreca M, Mattei M, Mac Niocaill C, Giordano G, McClelland E, Funicello R (2007) Paleomagnetic  
1489 evidence for low-temperature emplacement of the phreatomagmatic Peperino Albano ignimbrite  
1490 (Colli Albani volcano, Central Italy). *Bulletin of Volcanology* 70, 877-893.

- 1491 [Roche O \(2012\) Depositional processes and gas pore pressure in pyroclastic flows: an experimental](#)  
1492 [perspective. Bulletin of Volcanology 74, 1807-1820.](#)
- 1493 Roche O, Niño Y, Mangeney A, Brand B, Pollock N, Valentine GA (2013) Dynamic pore-pressure  
1494 variations induce substrate erosion by pyroclastic flows. *Geology* 41, 1107-1110.
- 1495 Roche O (2015) Nature and velocity of pyroclastic density currents inferred from models of  
1496 entrainment of substrate lithic clasts. *Earth and Planetary Science Letters* 418, 115-125.
- 1497 Rodolfo KS (2000) The hazard from lahars and jökulhlaups. In: *Encyclopedia of Volcanoes:*  
1498 *Academic Press, Philadelphia, 973-995.*
- 1499 Rodolfo KS and Arguden AT (1991) Rain-lahar generation and sediment-delivery systems at Mayon  
1500 Volcano, Philippines: Sedimentation in Volcanic Settings, *SEPM Special Publication* 45, 71-87.
- 1501 Rodríguez-Sedano LA, Sarocchi D, Caballero L, Borselli L, Ortiz-Rodríguez AJ, Cerca-Ruiz MF,  
1502 Moreno-Chávez G, Franco Ramos O (2022) Post-eruptive lahars related to the 1913 eruption in La  
1503 Lumbre Ravine, Volcán de Colima, Mexico: The influence of ravine morphometry on flow dynamics.  
1504 *Journal of Volcanology and Geothermal Research* 421, 107423.
- 1505 Rolandi G, Barrella AM, Borrelli A (1993) The 1631 eruption of Vesuvius. *Journal of Volcanology*  
1506 *and Geothermal Research* 58, 183-201.
- 1507 Rolandi G, Munno R, Postiglione I (2004) The A.D. 472 eruption of the Somma volcano. *Journal of*  
1508 *Volcanology and Geothermal Research* 129, 291-319.
- 1509 Rosi M, Principe C, Vecci R (1993) The 1631 Vesuvius eruption. A reconstruction based on historical  
1510 and stratigraphical data. *Journal of Volcanology and Geothermal Research* 58, 151-182.
- 1511 Rosi M and Santacroce R (1983) The A.D. 472 “Pollena” eruption: volcanological and petrological  
1512 data for this poorly-known, Plinian-type event at Vesuvius. *Journal of Volcanology and Geothermal*  
1513 *Research* 17, 249-271.



1514 Russell AJ, Knudsen O (1999) An ice-contact rhythmite (turbidite) succession deposited during the  
1515 November 1996 catastrophic outburst flood (jökulhlaup), Skeidarárjökull, Iceland. *Sedimentary*  
1516 *Geology* 127, 1-10.

1517 Sandri L, de' Michieli Vitturi M, Costa A, Di Vito MA, Rucco I, Doronzo DM, Bisson M, Gianardi  
1518 R, de Vita S, Sulpizio R; ([submitted this issue](#)) Lahar events in the last 2,000 years from Vesuvius  
1519 eruptions. Part 3: Hazard assessment over the Campanian Plain.

1520 Santacroce R, Cioni R, Marianelli P, Sbrana A, Sulpizio R, Zanchetta G, Donahue DJ, Joron JL  
1521 (2008) Age and whole rock-glass compositions of proximal pyroclastics from the major explosive  
1522 eruptions of Somma-Vesuvius: A review as a tool for distal tephrostratigraphy. *Journal of*  
1523 *Volcanology and Geothermal Research* 177, 1-18.

1524 Santacroce R., Sbrana A., Andronico D., Cioni R., Di Vito M., Marianelli P., Sulpizio R., Zanchetta  
1525 G., Arrighi S., Benvenuti E., Gurioli L., Leoni F.M., Luperini W., 2003. Carta Geologica del Vesuvio  
1526 in scala 1:15.000, Santacroce R., Sbrana A., eds. Cartografia derivata dai rilievi geologici in scala  
1527 1:10.000 Regione Campania e dai rilievi in scala 1:25.000 del Progetto CARG., S.EL.C.A., Firenze.

1528 Santangelo N, Romano P, Ascione A, Russo Ermolli E (2017) Quaternary evolution of the Southern  
1529 Apennines coastal plains: A review. *Geologica Carpathica* 68, 43-56.

1530 Scott KM (1989) Magnitude and frequency of lahars and lahar-runout flows in the Toutle-Cowlitz  
1531 River System. U. S. Geological Survey Professional Paper 1447-B, 1–33.

1532 Scott KM, Vallance JW, Pringle PT (1995) Sedimentology, behavior, and hazard of debris flows at  
1533 Mount Rainer, Washington. U. S. Geological Survey Professional Paper 1547, 1-56.

1534 Scott KM, Macias JL, Naranjo JA, Rodriguez S, McGeehin JP (2001) Catastrophic debris flows  
1535 transformed from landslide in volcanic terrains: mobility, hazard assessment and mitigation  
1536 strategies. *US Geol Surv Prof Pap.* 1630, 1-59.

1537 Sheridan MF, Bonnard C, Carrero C, Siebe C, Strauch W, Navarro M, Calero JC, Trujillo NB (1999)  
1538 Report of the 30 October 1998 rock fall/avalanche and breakout flow of Casita Volcano, Nicaragua,  
1539 triggered by Hurricane Mitch. *Landslide News* 12, 2-4.

1540 Siebe C, Schaaf P, Urrutia-Fucugauchi J (1999) Mammoth bones embedded in a late Pleistocene lahar  
1541 from Popocatepetl volcano, near Tocuila, central Mexico. *Geological Society of America Bulletin*  
1542 111, 1550-1567.

1543 [Smith G, Williams R, Rowley PJ, Parsons DR \(2018\) Investigation of variable aeration of](#)  
1544 [monodisperse mixtures: implications for pyroclastic density currents. \*Bulletin of Volcanology\* 80, 67.](#)

1545 Spence RJS, Zuccaro G, Petrazzuoli S, Baxter PJ (2004) Resistance of buildings to pyroclastic flows:  
1546 analytical and experimental studies and their application to Vesuvius. *Natural Hazards Review* 5, 48-  
1547 59.

1548 [Stanzione M, Di Vito MA, Aurino P, Lumaga MRB \(2023\) Sacred plant impressions from Somma-](#)  
1549 [Vesuvius volcanic ash deposits: A medicinal garden in Late Antique Acerra \(Naples, Campania,](#)  
1550 [Italy\)? \*Journal of Archaeological Science: Reports\* 47, 103802.](#)

1551 Sulpizio R, Mele D, Dellino P, La Volpe L (2005) A complex, Subplinian-type eruption from low-  
1552 viscosity, phonolitic to tephri-phonolitic magma: the AD 472 (Pollena) eruption of Somma-Vesuvius,  
1553 Italy. *Bulletin of Volcanology* 67, 743-767.

1554 Sulpizio R, Zanchetta G, Demi F, Di Vito MA, Pareschi MT, Santacroce R (2006) The Holocene  
1555 syneruptive volcanoclastic debris flows in the Vesuvian area: Geological data as a guide for hazard  
1556 assessment. *Geological Society of America Special Paper* 402, 203-221.

1557 [Sulpizio R, Dellino P, Doronzo DM, Sarocchi D \(2014\) Pyroclastic density currents: state of the art](#)  
1558 [and perspectives. \*Journal of Volcanology and Geothermal Research\* 283, 36-65.](#)

1559 Tema E, Zanella E, Pavón-Carrasco FJ, Kondopoulo D, Pavlides S (2015) Palaeomagnetic analysis  
1560 on pottery as indicator for the pyroclastic flows deposit temperature: New data and statistical  
1561 interpretation from the Minoan eruption of Santorini, Greece. *Geophysical International Journal* 203,  
1562 33-47.

1563 Thouret JC, Arapa E, Charbonnier S, Guerrero A, Kelfoun K, Cordoba G, Rodriguez D, Santoni O  
1564 (2022) Modeling tephra fall and sediment-water flows to assess their impact on a vulnerable building  
1565 stock in the City of Arequipa, Peru. *Frontiers in Earth Science* 10, 865989.

1566 Toyos G, Gunasekera R, Zanchetta G, Oppenheimer C, Sulpizio R, Favalli M, Pareschi MT (2008)  
1567 GIS-assisted modelling for debris flow hazard assessment based on the events of May 1998 in the  
1568 area of Sarno, Southern Italy: II. Velocity and dynamic pressure. *Earth Surface Processes and*  
1569 *Landforms* 33, 1693-1708.

1570 Vallance JW and Iverson R (2015) Lahars and their deposits. In: Sigurdsson, H., Houghton, B.F.,  
1571 McNutt, S.R., Rymer, H., Stix, J. (Eds.), *Encyclopedia of Volcanoes*. Academic Press, London, 649-  
1572 664.

1573 Vallance JW and Scott KM (1997) The Osceola mudflow from Mount Rainer: Sedimentology and  
1574 hazards implications of a huge clay-rich debris flow. *Geological Society of America Bulletin* 109,  
1575 143-163.

1576 Vitale S and Ciarcia S (2018) Tectono-stratigraphic setting of the Campania region (southern Italy),  
1577 *Journal of Maps* 14, 9-21.

1578 Voight B (1990) The 1985 Nevado del Ruiz volcano catastrophe: anatomy and retrospection. *Journal*  
1579 *of Volcanology and Geothermal Research* 42, 151-188.

1580 Waitt RB Jr, Pierson TC, MacLeod NS, Janda RJ, Voight B, Holcomb RT (1983) Eruption-  
1581 triggered avalanche, flood, and lahar at Mount St. Helens - Effects of winter snowpack. *Science* 221,  
1582 1394-1397.

1583 [Walsh B, Coviello V, Capra L, Procter J, Marquez-Ramirez V \(2020\) Insights into the internal](#)  
1584 [dynamics of natural lahars from analysis of 3-component broadband seismic signals at Volcan de](#)  
1585 [Colima, Mexico.](#)

1586 Whipple KX, Hancock GS, Anderson RS (2000) River incision into bedrock: Mechanics and relative  
1587 efficacy of plucking, abrasion, and cavitation. Geological Society of America Bulletin 112, 490-503.

1588 White S, García-Ruiz JM, Martí-Bono C, Valero B, Errea MP, Gómez-Villar A (1997) The 1996  
1589 Biescas campsite disaster in the Central Spanish Pyrenees and its spatial and temporal context.  
1590 Hydrological Processes 11, 1797-1812.

1591 [Zanchetta G, Sulpizio R, Pareschi MT, Leoni FM, Santacroce R \(2004a\) Characteristics of May 5-6,](#)  
1592 [1998 volcanoclastic debris flows in the Sarno area \(Campania, southern Italy\): relationships to](#)  
1593 [structural damage and hazard zonation. Journal of Volcanology and Geothermal Research 133, 377-](#)  
1594 [393.](#)

1595 Zanchetta G, Sulpizio R, Di Vito MA (2004b). The role of volcanic activity and climate in alluvial  
1596 fan growth at volcanic areas: an example from southern Campania (Italy). Sedimentary Geology 168,  
1597 249-280.

1598 ~~Zanchetta G, Sulpizio R, Pareschi MT, Leoni FM, Santacroce R (2004a) Characteristics of May 5-6,~~  
1599 ~~1998 volcanoclastic debris flows in the Sarno area (Campania, southern Italy): relationships to~~  
1600 ~~structural damage and hazard zonation. Journal of Volcanology and Geothermal Research 133, 377-~~  
1601 ~~393.~~

1602 Zanella E, Gurioli L, Pareschi MT, Lanza R (2007). Influences of urban fabric on pyroclastic density  
1603 currents at Pompeii (Italy): 2. Temperature of the deposits and hazard implications. Journal of  
1604 Geophysical Research 112, B05214.

1605 Zanella E, Gurioli L, Lanza R, Sulpizio R, Bontempi M (2008). Deposition temperature of the AD  
1606 472 Pollena pyroclastic density current deposits, Somma-Vesuvius, Italy. Bulletin of Volcanology  
1607 70, 1237-1248.

1608 Zanella E, Sulpizio R, Gurioli L, Lanza R (2015). Temperatures of the pyroclastic density currents  
1609 deposits emplaced in the last 22 kyr at Somma-Vesuvius (Italy). Geological Society, London, Special  
1610 Publication, The Use of Palaeomagnetism and Rock Magnetism to Understand Volcanic Processes  
1611 396.

1612 [Zaragoza G, Caballero-Garcia L, Capra L, Nieto-Torres A \(2020\) Lahares secundarios en el volcan](#)  
1613 [Popocatepetl: El lahar Nexpayantla del 4 de febrero, 2010. Revista Mexicana de Ciencias Geologicas](#)  
1614 [37, 121-134.](#)

1615 Zuccaro G, De Gregorio D (2013) Time and space dependency in impact damage evaluation of a sub-  
1616 Plinian eruption at Mount Vesuvius. Natural Hazards 68, 1399-1423.